UNIVERSITÀ DEGLI STUDI DI MILANO

PhD in Integrative Biomedical Research
Department of Biomedical sciences for health
Morphological curriculum/ XXIX cycle

JNK signalling pathway and its implication in RTT syndrome: study on synaptic plasticity and morphological profile in human and in mouse model.

ANNA MARIA CASTALDO
(R10475)

TUTOR: Prof. Rumio Cristiano
CO-TUTOR: Prof. Borsello Tiziana
PhD coordinator course: Prof. Sforza Chiarella

PhD thesis reviewers:

Prof. Tommaso Pizzorusso

Professore associato
Dipartimento di Neuroscienze,
Area del Farmaco e Salute del Bambino (NEUROFARBA)
Sezione di Psicologia - Padiglione 26
Via di San Salvi, 26
50135 FIRENZE, Italy
Email: tommaso.pizzorusso@unifi.it

Dr. Ilaria Meloni

Unità Operativa di Genetica Medica
Dipartimento di Biologia Molecolare
Policlinico Le Scotte
Viale Bracci 22
53100 Siena, Italy
e-mail: meloni2@unisi.it

Prof. Maurizio Giustetto

Ricercatore Università Degli Studi di Torino
Dipartimento di Neuroscienze
C.so M. D'Azeglio 52
10126 Torino - ITALY
Email: maurizio.giustetto@unito.it

Index

ABSTRACT ***6***

INTRODUCTION ***8***

1. Rett syndrome: an overview *8*

1.1 Forms and phases of Rett syndrome *9*

1.2 Rett variants *10*

1.3 Localization, structure and function of Mecp2 protein *12*

1.3.1 Localization *12*

1.3.2 Gene structure and protein function *13*

1.4 MECP2 modification led to the syndrome phenotype *16*

1.5 The Rett syndrome and mouse model *17*

2. Synapses and spine plasticity ***20***

2.1 Synaptopathology *22*

2.2 Role of the major scaffold proteins: PSD95 and SHANK3 *24*

2.3 Rett syndrome as an example of synaptic dysfunction *26*

3. ***Synaptopathy and Mapks*** ***29***

3.1 C-Jun N terminal kinase (JNK) *30*

3.2 Physiological and pathological functions of JNK *31*

3.3 Regulation of JNK *33*

3.4 C-Jun: the main JNK target *35*

4. Cell permeable peptide ***38***

4.1 JNK inhibitors 39

5. AIM OF THE WORK ***41***

6. MATHERIALS AND METHODS ***43***

6.1 Animal breeding *43*

6.2 PCR genotyping *43*

6.3 Body weight and survival *44*

6.4 Behavioural tests *45*

6.4.1 Rotarod *45*

6.4.2 Open field test (OF) *46*

6.5 Subcellular fractionation (TIF) *47*

6.6 Western blot *47*

6.7 Analysis of gene expression *48*

6.8 Immunohistochemistry *49*

6.9 IPSCs from Rett patients *50*

6.10 LDH assay *51*

6.11 Statistical analysis *51*

7. RESULTS ***52***

7.1 Characterization of MeCP2 mouse model *52*

7.2 MeCP2 -/y metabolic profile characterization *55*

7.3 Evaluation of motor impairment *56*

7.4 Characterization of intracellular stress pathway in MeCP2 mouse model *60*

7.5 Immunohistochemical characterization of MeCP2 mouse model *64*

7.6 A new strategy to prevent Rett Syndrome: the cell permeable JNK inhibitor peptide (D-JNKI1) treatment in MeCP2 mouse model *65*

7.7 Effect of D-JNKI1 treatment on well-being of MeCP2 mouse model *66*

7.8 Effect of D-JNKI1 treatment on behavioural performance of MeCP2 mouse model *68*

7.9 Biochemical evaluation of D-JNKI1 treatment on MECP2 mice *72*

7.10 JNK signalling and activation *73*

7.11 JNK's role at the dendritic spine *75*

7.12 D-JNKI1 in MeCP2 mouse model: immunohistochemical analyses *77*

7.13 Biochemical evaluation of D-JNKI1 effect on inflammation in MeCP2 mouse model. *79*

7. 14 JNK pathway in a translational model of IPSCS from RETT HUMAN girl deriving from fibroblasts *81*

8. DISCUSSION.....83

9. CONCLUSIONS and future prospective 95

10. Bibliography.....96

ABSTRACT

Rett syndrome (RTT) is a rare progressive neurodevelopmental disorder that occurs in 1:10,000-15,000 females. Normal early growth is followed by, above all, motor and cognitive regression. RTT is caused by mutations of the MECP2 gene, located on an X-chromosome and subject to random inactivation, that generates a very variable phenotype. Methyl-CpG-binding protein-2 (MeCP2) is a transcriptional factor involved in brain connectivity, neural circuits and – importantly - in synaptic plasticity and deficits. However, the molecular mechanisms related with these defects are largely unknown.

We previously showed that c-Jun N-terminal protein kinase (JNK), a stress-activated kinase, was closely involved in synaptic dysfunction related to neurodegenerative disease (Alzheimer's disease and ischemic stroke) and its specific inhibition, using the cell-permeable D-JNKI1 peptide, led to recovery of dendritic spine structure and restoration of function, with rescue of cognitive deficits. We here show for the first time that JNK signalling is powerfully activated in RTT mice and acts as a key modulator of synaptic dysfunctions.

We used MeCP2 tm 1.1 Bird male mice (referred as Mecp2 -/y) for our investigation because although they do not present mosaicism they have an early-onset, most severe phenotype within a homogeneous genetic background. D-JNKI1 (22 mg/kg) was injected intraperitoneally for the first time at the third week of age then repeated after three weeks. Well-being and behavioural studies were done, with weekly recordings of food and water intake, weight and locomotor abilities. At seven weeks, mice were killed and tissues were processed for biochemical analysis. In the brain JNK's preferential target, c-Jun, a nuclear transcription factor, was strongly activated. Repeated D-JNKI1 doses improved the mice's general wellbeing. Treated mice had a rescue of motor deficits and improved motor coordination, as seen in Rotarod and Open Field behavioural tests. Since RTT

causes locomotor impairment, we checked synaptic dysfunction in the cerebellum. Isolating the post-synaptic region, we found that D-JNKI1 treatment rescued the levels of AMPA and NMDA receptors. D-JNKI1 treatment showed to bring again level of PSD95 and Shank3 protein. In our studies focused on the inflammatory pathway triggered by JNK and we found activation of astrogliosis and microgliosis, completely rescued by D-JNKI1.

We then moved to translational medicine to further clarify JNK's pivotal role in RTT, using human RTT iPSCs (induced pluripotent stem cells). The mutant neuronal-IPSc presented JNK activation while isogenic control neuronal-IPSc did not. D-JNKI1 inhibited JNK activity and the rescue of its activation on a human model increase the clinical relevance of the proposed treatment.

RTT is a rare and incurable progressive postnatal female neurodegenerative disorder and manipulation of the JNK pathway may offer an innovative strategy to tackle the syndrome. JNK plays a key role in mice and human mutated neuronal iPSC and consequently it is important in clinical studies. We now need to better characterize D-JNKI1's effect in a female mosaicist model, closer to the human phenotype.

INTRODUCTION

1. Rett syndrome: an overview

The Rett syndrome (RTT) is a rare neurodevelopmental disorder that occurs with an incidence of 1:10,000 children. RTT syndrome was originally described as a clinical entity by Dr. Andreas Rett, an Austrian paediatrician, that in 1966 observed two little patients in his waiting room with similar stereotyped hand movement[1,2]. After a long period of silence, Hagberg and colleagues increased awareness of the syndrome with a further description of the disorder in a group of 35 girls[3]. The earliest hypothesis on the inheritance of RTT was funded on the seemingly exclusive appearance of the disorder in females. These observations suggested an X-linked dominant inheritance with male lethality. In 1999, it was firstly demonstrated that RTT is caused by mutations of the gene encoding the methyl-CpG binding protein 2 (Mecp2), located in Xq28[4]. This gene encodes a protein that is expressed in many mammalian tissues and, binding specifically methylated DNA, acts as a repressor of transcription. The MECP2 mutations are found in about 95% of classic RTT patients and in a lower percentage of variants cases. In some rare cases, Rett can occur without known mutated gene, possibly due to changes in MECP2 that are not still identified. Moreover, mutations in other genes may result in clinical similarities overlapping with these seen in the RTT[5,6], such as in CDKL5 (cyclin dependent kinase like 5) and in FOXG1 (forkhead box G1). RTT syndrome is caused by a *de novo* mutation not depending from the parents. Mutations can also be inherited from phenotypically normal mothers who have a germline mutation in the MECP2 gene[4]. In these cases, inheritance follows an X-linked dominant pattern and it is seen almost exclusively in females, while most males die in utero or shortly after birth[7,8]

1.1.Clinical stages of Rett syndrome

MECP2 loss-of-function is associated with RTT. This syndrome is characterized by a high rate of phenotypic variability in age of onset, severity of impairments and profile of clinical course. To date, it has been hypothesized that this heterogeneity could be due to differences in MECP2 gene mutations or to the random X-chromosome inactivation. However, these studies have yielded conflicting results and have left unresolved the issue of genotype-phenotype correlations, suggesting that additional modifier genetic factors can be involved[9].

After a period of apparently normal early infancy, affected children show first signs of decline around the 6^{th}-18^{th} month. Typical features of the syndrome are hand stereotypies movements development, microcephaly, growth delay and seizures. Despite of symptoms variability Rett syndrome progresses though 4 stages, described below.

The *stage I* is called early onset and typically begins between 6 and 18 months of age. Early symptoms are often very vague and nonspecific. The infant may begin to show less eye contact and have reduced interest in toys. There may be delays in gross motor skills such as sitting or crawling. Hand-wringing and decreasing head growth may occur, but not enough to draw attention. This stage usually lasts for a few months but can continue for more than a year.

The *Stage II*, or the rapid deterioration or regression stage, usually begins between the 1^{st} and 4^{th} year of child's life and may last for weeks or months. Its onset may be rapid or gradual; the child loses purposeful hand skills and spoken language. Breathing irregularities such as episodes of apnoea and hyperventilation may occur, although breathing usually improves during sleep. Some girls also display autistic-like symptoms such as loss of social interaction and communication. Walking may be unsteady and starting motor movements can be difficult.

The *Stage III*, or the plateau or pseudo-stationary stage, usually begins between ages 2 and 10 and can last for years. Apraxia, motor problems, and seizures are prominent during this stage. However, there may be improvement in behaviour, with less irritability, in hand use and communication skills. Despite improvement, mental impairment and hand stereotypies continue. Girls are often affected by rigidity, bruxism, motor dysfunction and seizures. Episodes of hyperventilation or breath holding may continue. Many girls remain in this stage for most of their lives.

The *stage IV*, or the late motor deterioration stage, can last for years or decades. Prominent features include reduced mobility, scoliosis and muscle weakness, rigidity, spasticity, and increased muscle tone with abnormal posturing of arms, legs, or top part of the body. Girls who were previously able to walk may stop walking. Cognition, communication, or hand skills generally do not decline in *stage IV*. Repetitive hand movements may decrease and eye gaze usually improves[10].

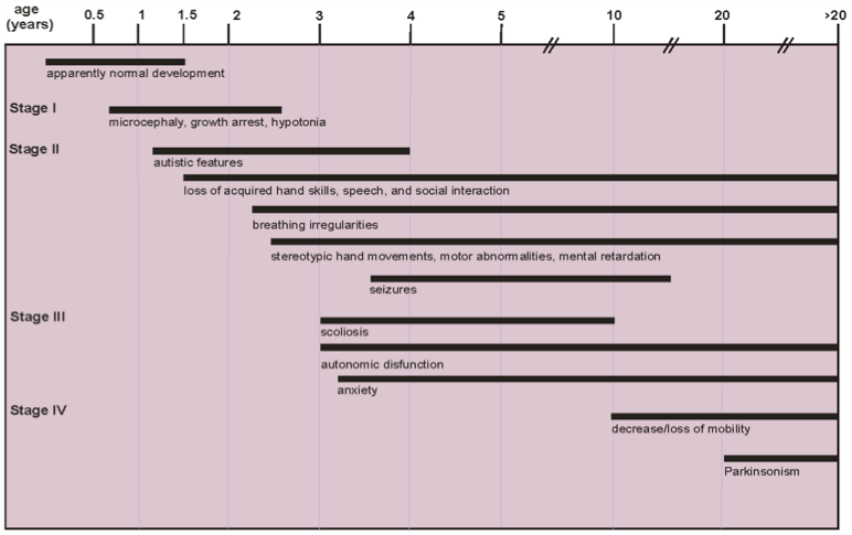

Figure 1- four stages of clinical pathogenesis of Rett symptoms in human. *At 6-18 months, children start to develop first signs of mental retardation that increase during the second stage, until 2,5 years. The third stage is characterized by a stationarity of condition that can get worse in the fourth stage, until they die*[10].

Patients with Rett syndrome often survive to adulthood, however, their life expectancy is lower than the rest of the healthy population. The percentage of annual death for Rett

syndrome is estimated to be 1.2%. Approximately 25% of these deaths are due to peripheral nervous system disorders or to heart abnormalities[11,12].

1.2. Rett syndrome variants

In 95% of patients are affected by classic Rett syndrome [13]. In addition, five atypical variants at least were described, with a different degree of severity based on the phenotypic variability associated with MECP2 different mutations[14,15]. These include:

a. The *"forme fruste"* shows delayed onset of symptoms than the classic form. Regression begins between the first and third year of life. The use of the hands is preserved and the characteristic stereotyped movements are less intense[16,17].

b. The Zappella variant or "preserved speech variant" (PSV) is characterized by the ability to formulate sentences; patients show the ability to use hands and head circumference is normal. They are generally overweight compared to patients with the classic form[18].

c. The congenital form does not follow a normal period of development, but symptoms appear already from the first day of life and regression occurs within the first month of life. most cases of congenital variant are related to mutations in the gene FOXG1[19].

d. The Hanefeld variant is characterized by early onset compared to the classical form. Symptoms occur within the 6th month of life accompanied by seizures of varying severity[20] and is often caused by mutations in the gene CDKL5[21].

e. The late regression variant is observed rarely and is characterized by a medium mental retardation, followed by a regression with the appearance of the classic symptoms[22].

1.3. Localization, structure and function of MeCP2 protein

1.3.1. Localization

Classic Rett is a syndrome characterized by MECP2 gene mutation, that codifies for MeCP2 protein (Methyl-binding CpG protein-2), expressed widely throughout the body, in particular in mature nerve cells of the grey matter in the central nervous system[23,24], specifically in post-mitotic neurons. The clinical course of RTT has provided clues as to the role of MeCP2 in the maturation of the nervous system. RTT-associated neuronal dysfunction firstly manifests itself in early postnatal life, when sensory experience is required for the refinement of developing neuronal circuits[25].

MeCP2 was well characterized as a transcription factor involved in regulating gene expression, but it is also involved in neuronal morphological changes[26], in excitatory-inhibitory transmission imbalance[27–30] and in short-term plasticity[31] during the development. This observation suggests that MeCP2 might mediate some of the effects on synapse and neural circuit development, and that the absence of activity-dependent regulation of MeCP2 in RTT contributes to the ethology of this disorder[25].

The reversibility of the RTT-like phenotype upon restoration of MeCP2 and the catastrophic consequences of MeCP2 removal in adult mice argue that MeCP2 is not solely a neurodevelopmental regulator[32]. Moreover, removal of MeCP2 from specific brain regions and neuronal subtypes compromises the function of that brain region. For example, deletion of the *MECP2* gene exclusively in the forebrain causes behavioural abnormalities[33] — including limb clasping, impaired motor coordination, increased anxiety and abnormal social behaviour — but does not affect locomotor activity or context-dependent fear conditioning. Similarly, loss of MeCP2 from all inhibitory GABA-releasing neurons leads to a severe RTT-like phenotype, whereas a smaller subset of MeCP2-negative neurons has much milder consequences[34].

The MeCP2 function is therefore not restricted to neuronal cells. Deletion of MeCP2 from glial cells has mild phenotypic consequences, which is consistent with the idea that its primary function is in neurons[35]. However, co-culture experiments have revealed that MeCP2 in glia has a non-cell-autonomous role in supporting the normal dendritic morphology of neurons. Furthermore, re-expression of MeCP2 in astrocytes completely rescues the breathing abnormalities observed in *Mecp2*-null male mice, leading to greatly increased survival rates[36]. Interestingly, wild-type microglia introduced by transplantation of bone marrow were reported to ameliorate some of the deficits observed in *Mecp2*-null mice[37] even if involves destruction of blood brain barrier.

1.3.2. Gene structure and protein function

The MECP2 gene spans 76 kb in Xq28 and is composed of 4 exons; it is considered an housekeeping gene because it has a CpG island associated with 5'-end and is ubiquitously expressed. It is widely expressed in embryonic and adult tissues although expression is at low levels early in development.

MECP2 has two main splice variants MeCP2_e1 and MeCP2_e2, which encode proteins with a different N-termini[38,39] and expressed in a tissue-specific way. Moreover, MeCP2 has a long conserved 3'UTR with multiple poly-adenylation sites, which can additionally generate four different transcripts (with different length, between 7,5 and 10 kb). MeCP2_e1 is 498 amino acids long and has a translational start site in exon 1 excluding exon 2 from the final protein, and is ten times more abundant in the brain. It was found almost in hypothalamus[38,40,41]. Whereas, isoform MeCP2_e2 excludes the exon 1, is 486 amino acid long and was detected mostly in the dorsal thalamus and layer 5 of cortex[40].

The possible specific role of MeCP2_e1 in the brain is already unclear, but pathogenic mutation have been discovered in exon 1 of this isoform in RTT patients, while such

mutations have been not seen for exon 2[41]. However, studies shown that exon 1 mutations may be associated with a reduction of e2 protein levels[42].

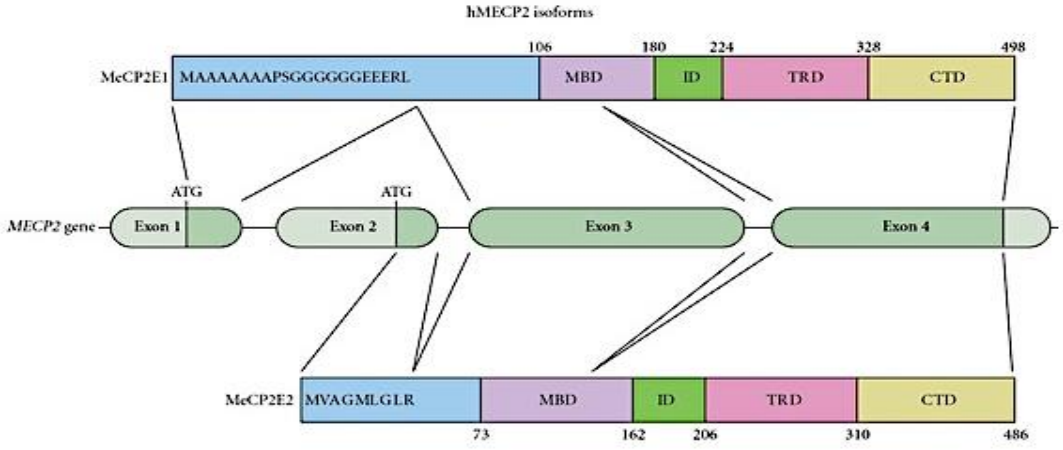

Figure 2- structure of MECP2 gene and of mecp2 proteins[43]***.*** *On the top is shown Mecp2_e1 isoform; below is shown Mecp2_e2. The two isoforms are derived from a different splicing of MECP2 gene, in the centre of the image: e1 starts with exon 1 and does not contain exon 2; e2 starts with exon2 and does not contain exon 1. Both proteins have the same function and the same functional domain, MBD, TRD and CTD as described in the text.*

Despite from different included exons, as shown in figure 3, the two MeCP2 isoforms show the same amino acidic sequence and domains including:

- three functional domains (MBD, methyl-binding domain; TRD transcriptional repressor domain and CTD, carboxyl-terminal domain)
- two NLS, signals for nuclear localization.

The methyl-binding domain (MBD) consists of 85 amino acids at the end of protein and is essential for binding of Mecp2 to heterochromatin[44] as well as to DNA four way junctions[45]. MBD has been localized in a region within exons 3 and 4 and require A/T-rich motifs to bind the symmetrically methylated CpG dinucleotides. Even if it requires only a single methylated CpG for binding DNA, MeCP2 preferentially associates with whole blocks of methylated CpGs[46].

The transcriptional repression domain (TRD) was described by Nan et al. and is located among amino acids 207-310. Its involvement in transcriptional repression occurs through

several mechanisms. For example, it seems to reacts with Sin3 and to recruit the histone deacetylase complex. The MeCP2 may also make direct contacts with the basal transcription machinery, such as TFIIB, leading to a deacetylase-independent repression. The original model of MeCP2 protein function involves deacetylation of core histones resulting in the compaction of the chromatin and making it inaccessible to components of the transcriptional machinery[47,48]. Surprisingly, interactions between TRD and various cofactors demonstrate that MeCP2 protein can read methylated CpGs differently and, depending on the context, mediate multiple downstream responses. It will be interesting to know what region of the protein are involved in recruitment of co-repressor in some instance and of co-activators in others. Moreover, one of two identified nuclear localization signals (NLS) is embedded within the TRD. The other NLS, located in HMGD2, between the MBD and TRD[49], identified an RG (arginine-glycine) repeated region in HMGD2, which are known to mediate RNA-protein interactions, and MeCP2 was shown to bind to mRNA and double-stranded siRNA independent of its MBD, suggesting that MeCP2 may have activity as part of a selective RNA–protein complex.

The C-terminal domain, CTD-α and CTD-β are other chromatin binding domains. The CTD-α recognize methylated DNA in chromatin, while the CTD-β contains conserved poly-proline motifs that can bind to group II WW domain splicing factors[50] (see fig. 3).

Recent studies suggest that MeCP2 is also implicated in alternative splicing as part of an RNA-protein complex[51] using YB1, which is an RNA-binding protein and influences splice site. The precise mechanisms by which MeCP2 protein directed and regulated various functions and interactions, remain to be elucidated.

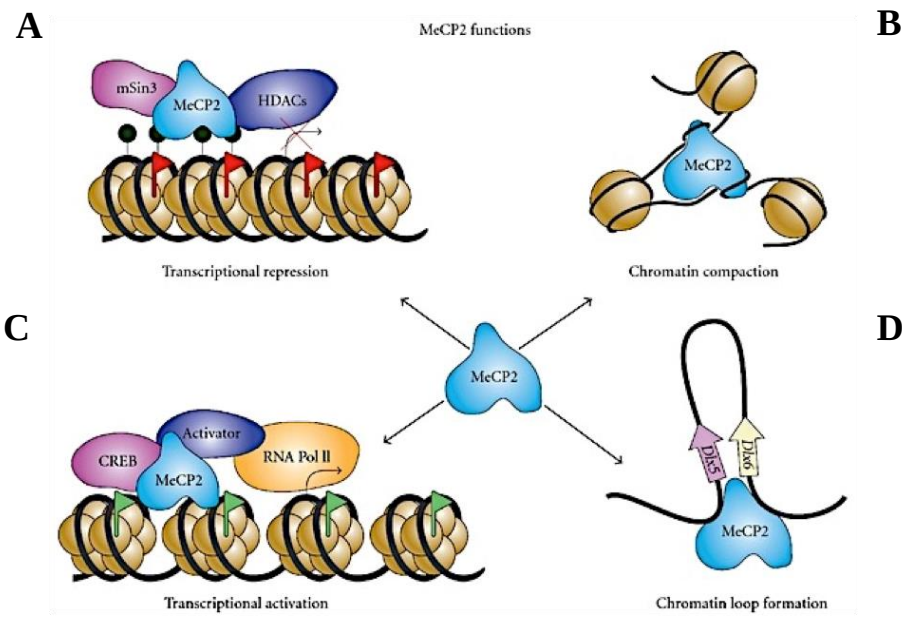

Figure 3- The functions of MeCP2 protein. *MeCP2 was firstly discovered as a transcriptional repression protein(A) by interacting with DNA in complex with Sin3A and recruiting HDACs, it showed an involvement in chromatin accessibility, remodelling structure by association with histone H3 Lys9 methyltransferase and with the Dnmt1(B) or by loop formation (D). Recently has emerged a role in transcriptional activation(C) binding RNA pol II complex.*

1.4. MECP2 modification led to the syndrome phenotype

MECP2 mutations have been identified in 75-90% of sporadic cases and approximately in 50% of familial cases. Interestingly, even though almost mutations are *de novo*, there are 8 common point mutations resulting from C >T transitions in CpG island[15]. There are also cases of small deletion in correspondence of a pentanucleotide repeated (CCACC) at exon 4. More than 60 distinct mutations have been identified, the majority are nonsense or frameshift mutations that occur throughout the gene. For example, one mutation (Q19X) introduces an extremely early stop codon, which is likely to be a null allele. Additional nonsense mutations have been found in the MBD (Y141X), between the MBD and TRD (R168X, Q170X, and R198X), and within the TRD (R255X, K256X, R270X, and R294X). A partial loss of MeCP2 function cannot be excluded, however, because premature stop codons within the last exon may not lead to nonsense mediated mRNA decay. Therefore, the possibility that premature stop codons within exon 4 may produce

a truncated form of the protein that retains partial function, still exists. A truncated protein that retains the MBD, for instance, may still be able to bind to methyl-CpG nucleotides and may, by solely binding upstream of potential promoter regions, at least partially interfere with transcription. Whether the Rett syndrome is caused by both null and hypomorphic alleles remains an interesting question. Missense mutations have been identified in regions of the gene encoding the MBD, TRD, and C-terminus of the protein. Three of the mutations within the MBD (R106W, R133C, and F155S) have been shown to reduce binding to methylated DNA by more than 100- fold. It remains to be shown whether missense mutations in the TRD reduce interactions with the Sin3A complex and whether mutations in the C-terminus, which enhances the binding of MeCP2 to nucleosomal DNA[52,53], decrease interactions with components of the nucleosome.

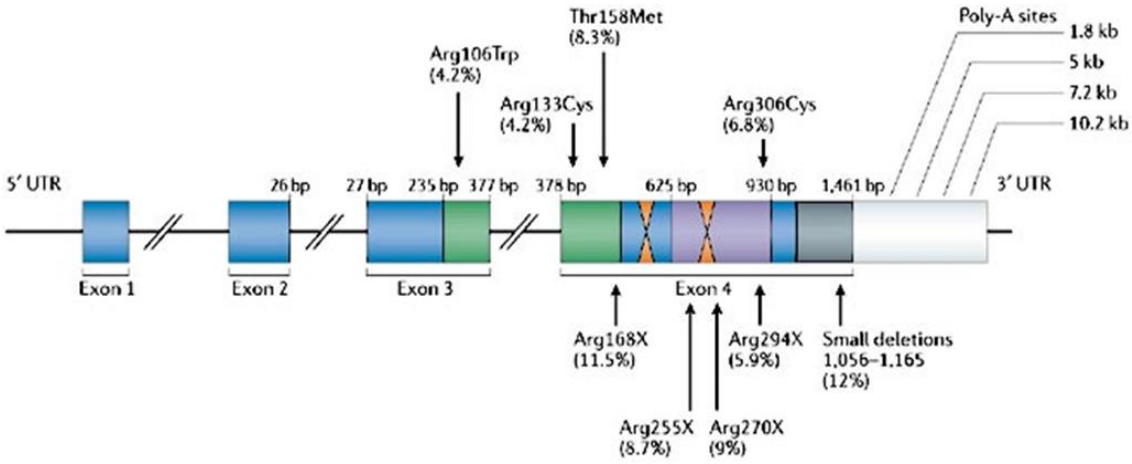

Figure 4- MECP2 gene and most common kind of mutation that led to a Rett syndrome phenotype like. *MECP2 (methyl-CpG-binding protein 2) gene structure. The positions and frequencies of the most common mutations that are associated with Rett syndrome in females are indicated. Image taken by Bienvenu et al. Nature Reviews Genetics 7, 415–426 (June 2006) | doi:10.1038/nrg1878*

1.5.MeCP2 mouse model

Rett syndrome is mainly due to a partial loss of MeCP2 function, which is particularly expressed in brain. More than irreversible damage, its lack seems to cause a functional disturbance of neuronal circuits[54].

The study of RTT arouses increasing attention, but the necessity of post-mortem human brain made it difficult for the availability of the material and for sample quality. Moreover, today is not available a cure or a treatment for RTT and, even if there is a long history of failure in translating findings from preclinical to clinical, it is necessary to have a model reproducing most of the symptoms of human disease. Experimental and transgenic animal models of Rett syndrome have been developed for elucidating the RTT onset and progression. Mouse models represent a good tool to study RTT, showing validity of construct (that led to analogue molecular mechanism with humans), reproducibility, robustness of findings and similarity with anatomical, physiological and behavioural phenotype. In addition, mouse models allow validating potential treatment strategy for human Rett.

Mice used at this purpose have three kind of mutated allele, classifiable in this three groups reported below:

a) Null alleles, with a large deletion detectable in 10% of patience ($Mecp2^{tm1.1Bird}$, $Mecp2^{tm1.1Jae}$, $Mecp2^{tm1.1Pplt}$). These mice showed no signs of Mecp2 protein expression and developed a postnatal behavioural phenotype that resembles RTT synptoms[55,56].

b) Truncation or single nucleotide mutation (codon-308-C-terminal truncation). These mice express a truncated protein with the MBD and a portion of the TRD elements still intact, suggesting residual protein function[56–58], they could be considered mutant mice. The introduction of a premature STOP codon in the mouse *Mecp2* gene led to the expression of a protein truncated at the amino acid 308 ($Mecp2^{308}$)[59], as thought to be the case in some RTT patients presenting milder disease feature.

c) Point mutation. These mice show missense or nonsense *MECP2* mutations, including R106W, R133C, T158M, R168X, R255X, R270X, R294X, and R306C, account for

more than half of the RTT cases[60]. Thus, mice carrying a single nucleotide change in *Mecp2* would represent the closest experimental model of patients with RTT.

Mouse model	**Phenotype**			**Take-home message**
	Onset	**Survival**	**Symptoms**	
Mecp2 deletion	6 weeks (−/y) and (−/−)	10 weeks	Ataxia, reduced motor activity, tremors, hind limb clasping	Lack of MeCP2 causes RTT-like phenotypes in mice; disease onset in females depends upon time, not developmental stage
	6 months (+/−)	Normal lifespan	Milder, variable phenotypes	
MeCP2 truncation	4 months ($MeCP2^{308}$/y)	90% 10 months	Progressive motor and activity dysfunction. Abnormal social interaction. Forepaw movements	Truncated protein found in many RTT cases also produces RTT-like phenotypes in mice
	10 months ($MeCP2^{308}$/MeCP2)	Normal lifespan	Milder, variable phenotypes	
MeECP2 point mutation	6- 8 months	Normal lifespan	Small size, arrhythmia, increased breathing rate. Anxiety, motor and learning impairment.	Point mutations not representative, but are characteristic of only a small part

Table 1: Mice models of Rett syndrome.

In addition to mutated mice, conditional knockout mice have also been generated and characterized, and the inactivation of MeCP2 in single brain areas or neuronal subtype generally leads to subset of typical Rett[61]. While numerous transgenic mice have been created modelling on common mutations in MeCP2, the behavioural phenotype and the biochemical analysis of many of these male and female is not well characterized[62].

2. *Synapses and spine plasticity*

Synapses are connections between neurons and, because of their key role in neuronal transmission, in learning and in memory consolidation mechanisms, they are studied with increasing interest. Synapses have gradually revealed an involvement in neurodegenerative and psychiatric disorders, such as autism[63], intellectual disability, schizophrenia [64], depression [65], Huntington's disease [66,67], Amyotrophic Lateral Sclerosis[68], Parkinson's disease, epilepsy, Alzheimer's disease [69]and neurodevelopment disorder as Rett syndrome[70].

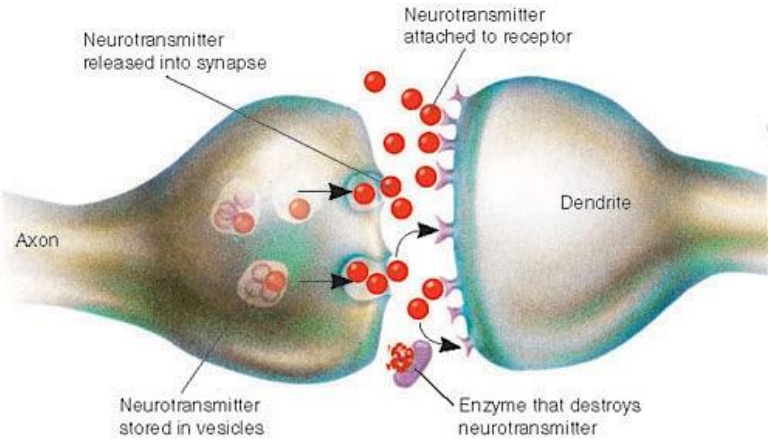

Figure 5- Representation of a synapse. *On the left side is showed pre-synaptic element of a neuron, releasing neurotransmitters stored in the vesicles. Neurotransmitters bind specific receptors located on post-synaptic element, in the right part of the figure, and transform chemical in electrical signals. Once completed their function, neurotransmitters were re-uptake or degraded by enzymes, while the electrical signal is transmitted to other neurons.*

Excitatory synapses are being well characterized in literature during years, as composed by a definite structure, situated on dendritic spine head. Glutamate mediates most of excitatory neurotransmission in the brain, acting mainly on three different receptor classes: NMDA (N-Methyl-D-aspartate), AMPA (α-amino-3-hydroxy-5-methyl-4-isoxazolepropionic acid) and $mGluR_{1-8}$ metabotropic receptors.

Release of glutamate from pre-synaptic terminal allows the opening of AMPAr with increment of Na^+ e K^+ currents. A short burst of high frequency is enough for generating

a phenomenon called long-term potentiation (LTP) often associated with long-term memory. This strong depolarization determinate a strengthening of excitatory synapses for a prolonged period and influences neuronal plasticity. The excitatory post-synaptic potential (EPSP) generates detachment of Mg^{2+} ion from NMDA receptors and their opening, which in turn, determinates entrance of calcium influx. Calcium currents modify the shape of the spine, the number of receptors located on the synapses and consequentially spine plasticity[71]. mGluRs mediates slow post-synaptic response to decrease neuron excitability.

The synaptic plasticity determinates an high variability of dendritic spine morphology, strictly correlated with biochemical and electrical features of the compartment[72].

The variable spine shape and volume is thought to be correlated with the strength and maturity of each spine and many studies have shown that there is a *continuum* among spine shapes (fig. 6)

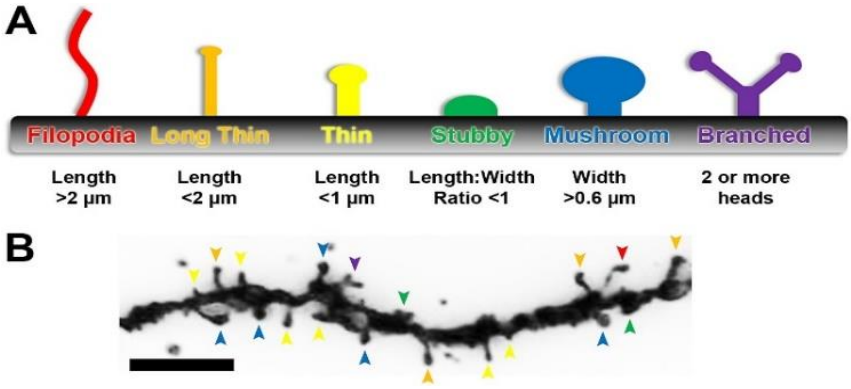

Figure 6- Dendritic spine classification. *In the higher part (A) the different kind of spine and a general classification are shown. In the lower part (B) a dendritic Golgi stained neuron highlights the different kind of spines. To make easier the correspondence, each spine is correlated with a colour, the same used in A.*

Large spines, named also "memory spines," are stable, persistent for longer periods of time, and are the postsynaptic side of strong excitatory synapses[73,74]. Mushroom spines have a large head connected to the parent dendrite through a narrow neck. Stubby spines do not have a noticeable neck and are formed usually during postnatal development[75,76].

Conversely, thin spines have a thin, long neck, and a small bulbous head, they are highly mobile, unstable, and often short-lived, usually representing weak or silent synapses[76]. Because thin spines are more plastic than large ones and have the potential to become stable spines, they have been dubbed "learning spines" [73,74,77,78]. It should be noted that thin protrusions longer than thin spines and without a notable head are called dendritic filopodia, and are more numerous than spines in developing neurons. The dendritic filopodia are transient and highly motile protrusions that can develop synaptic input into mature spines, thus initiating synaptogenesis[72,79].

Usually, an incoming stimulus provokes reversible modification of spine plasticity, with related arrangement of shape, length and functionality; in some pathological instance the stimulus can persist, determining a complete loss of function followed by a total spine retraction, with related biochemical and structure loss. The irreversible perturbation of the synaptic function is known as synaptopathy.

2.1. Synaptopathology

Many neurodevelopment disorders, such as RTT, Angelman or Down syndrome are characterized by abnormal density and morphology of dendritic spines, synapses loss and aberrant synaptic signalling and plasticity[80], hallmarks of synaptic pathology.

Synaptopathology, defined as the dysfunction of synapses, can be generated by a gene mutation of synaptic proteins such as ion channel, neurotransmitter receptor, or protein involved in neurotransmitter release. It can also arise as a result of an autoimmune response, in which antibody bind a synaptic protein.

Synaptic dysfunction is one of the first signs that occurs in neurodegenerative pathology. Morphological changes correlate often with alteration of functions in this area and affect

communication among neurons. A complete loss of synaptic function is strictly related to cognitive deficits, hallmarks of brain disorders.

Many studies have shown that the dynamic process leading to spine loss is associated with a decrease in glutamate receptors [81–84] and normally occurs in 3 steps. In fact, spines have a stable conformation as long as a stimulus, such as Aβ oligomers, leads to the first step of synaptic dysfunction, characterized by internalization or desensitization of NMDA and AMPA receptors and by a slight reduction of scaffold protein such as PSD-95 protein. Moreover, direct postsynaptic activation of α7 nicotinic acetylcholine receptor (α7-nAChR) was proposed and then, the activation of extrasynaptic NMDA receptors, {Merging Citations} particularly NR2B-mediated NMDA currents, was shown. Numerous intracellular signalling pathways like calcineurin/STEP/cofilin, p38 MAPK, and GSK-3β could be activated. this reversible step is followed by, a major decrease of PSD-95 occurs inducing an atrophy of the post-synaptic element that generate synaptic loss and eventually neuronal death[85,86]

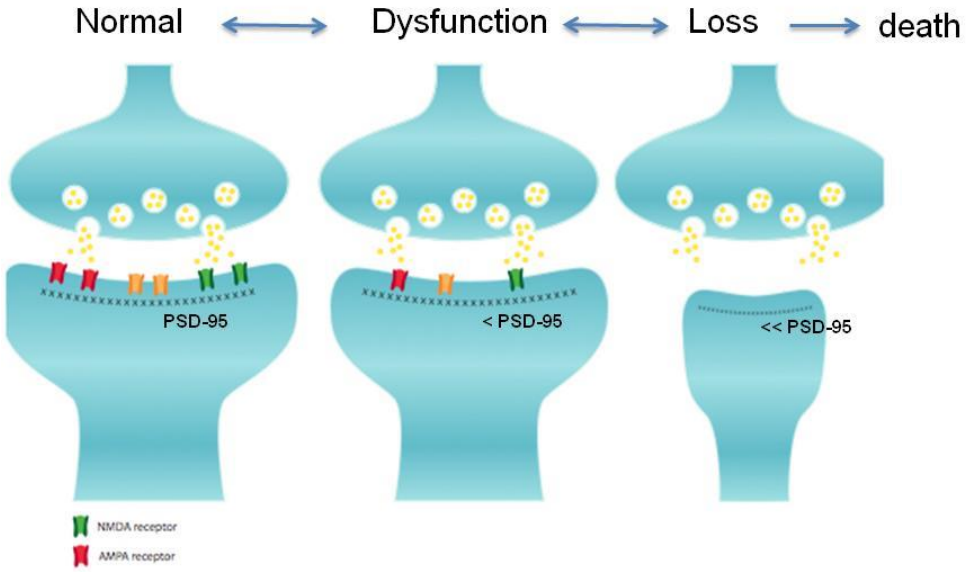

Figure 7- Pathological mechanism of synaptic dysfunction. *The post-synaptic region show a specialized cell membrane structure called the postsynaptic density region (PSD). This zone contains many scaffolding, like PSD-95 and Shank3, which plays an important role in AMPA (red channels) and NMDA (green channel) receptors localization. Slight perturbations of the spine architecture lead to spine dysfunction and subsequently loss.*

2.2. Role of the major scaffold proteins: PSD95 and SHANK3

The efficient regulation of synaptic signal transduction of the excitatory synapses is provided and supported by the postsynaptic density (PSD), that is an electron-dense structure attached to the cytoplasmic surface[87,88]. The PSD consists of hundreds of proteins with a molecular architecture not yet fully understood. A well characterized family of protein belong to the MAGUK family (membrane-associated guanylate kinase). This protein network plays a role in the regulation of the short- and long-term changes that affect the synaptic transmission during the lifetime of a mature neuronal circuit, in synaptic plasticity helping to regulate scaffold proteins located in the post-synaptic density region (PSD)[89].

Among MAGUKs, the PSD95 is the most abundant scaffold protein of the excitatory postsynaptic density[90] and is involved in the regulation of AMPA receptors upon induction of LTP[91,92], which presumably underlies its essential role in learning and memory. Moreover, PSD-95 have shown an important influence in localization and organization of receptors, ion channels, kinases, phosphatases and signalling molecules[93,94]. PSD-95 structure and its important interactions are shown in the figure 8. The protein consists of three PDZ domains followed by a src homology 3 (SH3) domain and a guanylate kinase-like (GK) domain[95]. PDZ domains 1 and 2 of PSD-95 bind to various membrane proteins including the NMDA receptor subunits[96], whereas the third

PDZ domain of PSD-95 (PDZ3) preferentially binds the C termini of a different set of proteins, including, for example, the synaptic protein CRIPT[97].

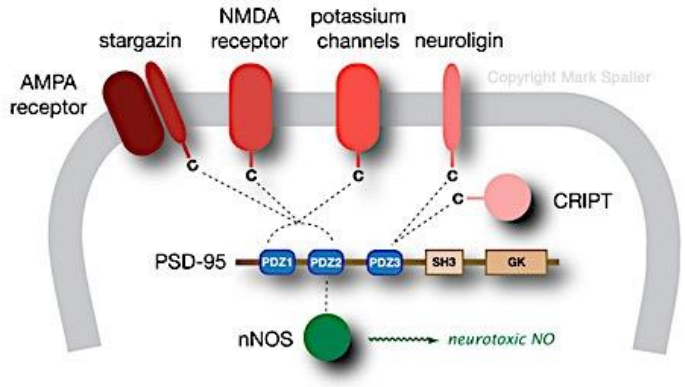

***Figure 8*- PSD95 structure, location and interaction**. *PSD95 protein belongs to the MAGUK family and thanks to its specific domains (PDZ, SH3 and GK) allows interaction with different kind of proteins involved in modulation of cellular pathway in the dendritic spines.*

PSD-95 is thought to determine the size and strength of synapses and to be involved in spine stability. Many studies reported that modifications of the protein, as well as phosphorylation of PSD-95, are related to a remodelling of proteins and receptors of dendritic spines and molecules were re-located, leading to a disruption of spine morphology.

Shank family (Shank1, Shank2, Shank3) is made up of scaffold proteins interacting with a variety of cytoplasmic and membrane protein[98], for example are the most abundant binding partners of Homer protein in the PSD[90]. Shank contains an amino-terminal ankyrin repeat domain, an SH3 (Src homology 3) domain, a PDZ (PSD-95/Discs large/zona occludens-1) domain, a long proline rich sequence containing binding sites for Homer and cortactin, and a carboxy-terminal SAM (Sterile alpha motif) domain[99,100].

In a similar way to PSD95, through these domains, Shank directly interacts with AMPA and NMDA receptors[101] and many other signalling and scaffolding molecules in the PSD region. *De novo* mutation of Shank3 was found in a patience with a RTT-syndrome like phenotype[102]. Overexpression of Shank in neurons results in enlargement of dendritic spines, and the effect is significantly enhanced by co-expression of the long form of Homer [103].

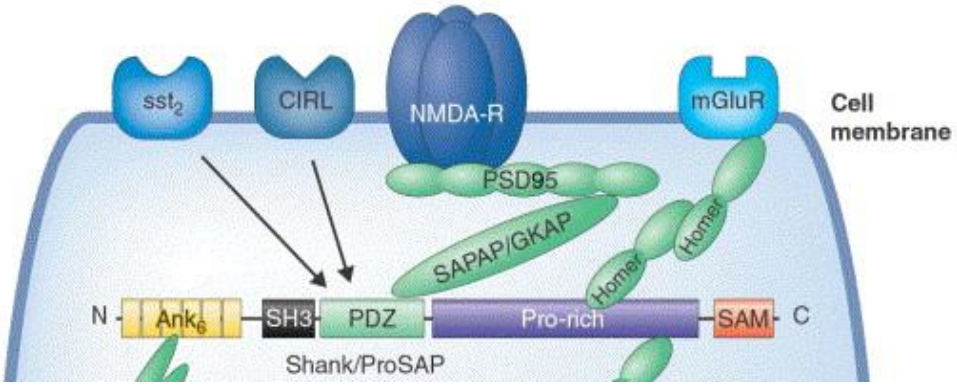

Figure 9- Structure and function of SHANK3 scaffold protein.

2.3. Rett syndrome as an example of synaptic dysfunction

RTT patients are affected by a dendritic spine dysgenesis which includes not only lower spine density, but also atypical morphology, resulting in a decreased proportion of mushroom spine in cortex and hippocampus[104–106]. The brain of RTT patience is characterized by typical hallmarks, including reduced neuronal size and increased neuronal density in several brain regions[107,108], as well as reduced dendritic arborisation[104] and spine dysmorphogenesis[105,106,109]. Similarly, mouse models of RTT are widely used and recapitulate many of the behavioural and anatomical abnormalities associated with the human disorder [110,111] the alteration in density[30,112–114], size and shape [115,116] ; moreover they are affected by an important impairments in both LTP and LTD[32,117,118]. The so-called spine dysgenesis phenotype[119] is recapitulated not only by *MECP2*-null mice but also by mice with only a region-specific deletion of *MECP2*[55,57]. Interestingly, pyramidal

neurons of the hippocampus of *Mecp2* KO have fewer dendritic spines only before postnatal day 15, suggesting that MeCP2 is necessary for dendritic spine formation during early postnatal development, but a compensatory mechanism takes place after this period in *Mecp2* KOs[62,106].

The same dendritic spine phenotype is delayed in female heterozygous mice, and it seemed more severe in Mecp2-expressing neurons than in Mecp2-lacking neurons, suggesting both cell autonomous and non-cell autonomous consequences of *Mecp2* deletion[120]. In addition to similar lower spine densities, the intensity of immunolabeling for PSD-95 was lower in layer V pyramidal neurons of motor cortex of Jaenisch *Mecp2* mutant mice[30].

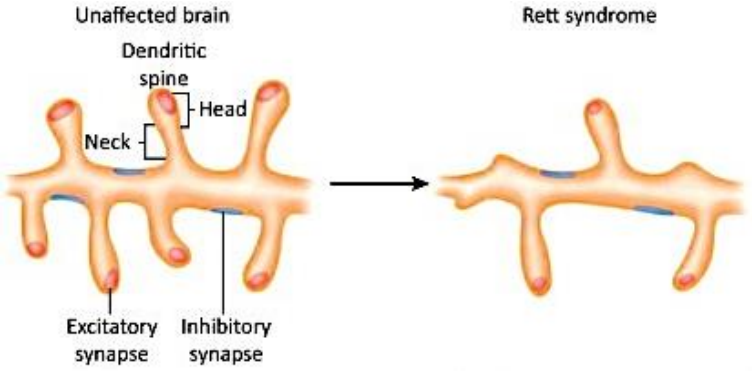

Figure 10- Healthy and pathologic RTT dendritic spine.

Synaptic dysfunction seems to be localized in particular region of the brain. In RTT patients, cortical networks are weakened and hypo-active. Dendritic spine density is lower in pyramidal neurons of layers V-VI of motor cortex from male hemizygous and female heterozygous Bird *Mecp2* knockout mice[120].

Mouse models showed a significant volumetric reductions of cortex and cerebellum, and decreased ratios of the thickness of motor cortex to cerebrum and corpus callosum to cerebrum[121]. While cortical lamination was normal, the thickness of somatosensory and motor cortices was significantly reduced in comparison to wt males[116,121,122]. Cerebellum

appear to be normal, but analysing cerebellar vermian lobules or the corpus callosum of RTT pateints, they showed significantly decrement. Cerebellar atrophy may contribute to the deterioration of the motor system seen in older patients with Rett syndrome[123]

Pyramidal neurons in the cortex[115] and hippocampal CA3 region, as well as granule cells of the dentate gyrus show reduced dendritic complexity[36] and have lower spine densities compared to wildtype controls[116]. Furthermore, pyramidal neurons in CA1 region of the hippocampus from Bird *Mecp2* knockout mice also show lower spine densities, in addition to dendritic swelling, reduced diameter of dendritic spine heads and elongation of their necks[120]. Intriguingly, this study described significant different consequences between a deletion[55] and expression of a truncated Mecp2 protein[57].

Moreover, degeneration and loss of spinal ganglion nerve cells, in addition to gliosis of both the white and grey matter of the spinal cord, were evident. The number of motor neurons appeared to be reduced and axonal changes suggestive of degeneration were observed in both the ascending and descending tracts[124].

.

3. SYNAPTOPATHY AND MAPKS

Synaptic plasticity is regulated by different intracellular signalling pathways. Among them, mitogen-activated protein kinases (MAPKs) have shown to have a role in controlling neuronal synaptic function phosphorylating many targets at the spine level.
In mammals, three main classes of MAPKs have been characterized: JNK, p38 and extracellular signal-regulated kinase (ERK)[125]. It is assumed that ERK1/2 mediates preferentially proliferation and differentiation, being activated by growth factors, while p38 and JNK respond to stress stimuli to induce mainly apoptosis.

The molecular mechanisms underlying the synaptic adaptability to injury remain almost unclear, but there are increasing evidences of the involvement of mitogen-activated protein kinases (MAPKs). JNKs are a family of kinase protein, found to be involved in dendritic spine plasticity and stability. In our previous works, we showed that in neurodegenerative disease, such as Alzheimer's disease, Aβ oligomers caused a strong activation of the JNK pathway in the synaptic compartment, indicating a key role in this first neurodegenerative event. This activation occurs prior to the onset of the cognitive impairment[126] and it is correlated with spine density reduction, decrement of postsynaptic markers (AMPAR and NMDAR subunits, PSD95 and drebrin) and activation of caspase-3 in the postsynaptic compartment.

To confirm the involvement of JNK in synaptic degeneration mechanisms induced by Aß oligomers, we used the specific cell permeable JNK inhibitor peptide, D-JNKI1. Treatment with D-JNKI1 reverted the synaptic degeneration, preventing the loss of dendritic spines and the reduction of AMPA-r and NMDA-r subunits, PSD95 and drebrin from the postsynaptic membrane[127]. Moreover, D-JNKI1 treatment was able to reduce excitatory synapses retraction, reverting their dysfunction, revealing that JNK is a key

signalling pathway in synaptic injury and that its specific inhibition offers an innovative therapeutic strategy to prevent spine degeneration[126].

Rett syndrome is a neurodevelopmental disorder different from AD, but in the same way is characterized by a strong synaptic dysfunction with an aberrant synaptic plasticity, so we investigated JNK activation and its role in this pathology.

C-Jun N terminal kinase (JNK)

JNK proteins are a family of evolutionarily conserved serine/threonine kinases. They have first been discovered in a c-Jun binding assay[128] where JNKs were shown to bind the activation domain of c-Jun [128,129] and phosphorylate it at Ser63 and Ser73 residues located in the N-terminus[130]. In mammalian genomes three genes (JNK1, JNK2 and JNK3) encode a family of three JNK isoforms (Jnk1, Jnk2, and Jnk3 also termed SAPK-γ, SAPK-α and SAPK-β, respectively) with a total of ten splice variants. Jnk1 and Jnk2 are widely expressed in a variety of tissues, while expression of Jnk3 is mainly located into brain, heart and testis[131,132]. The structure of the different Jnk isoforms is essentially the same, since they share an 80% sequence identity. They all possess three relevant domains for JNK function, that are: the activation loop, the active site, and the peptide binding site.

The activation loop or phosphorylation lip is the region containing the JNK regulatory phosphorylation. It is composed by a tripeptide, Thr-X-Tyr, where X is a proline, a glutamate and a glycine in the sequence of JNK, ERK and p38, respectively. The activation loop is adjacent to the active site.

The active site is composed by a glycine-rich phosphate anchor loop with a role in the ATP binding. The adenine base of ATP is bound in the back of the domain interface and

forms non polar interactions with amino acids of the glycine loop[132]. The conserved Asp189 and Asp207 residues are thought to be essential for protein kinase activity.

At least, the substrate binding site lies in the C-terminal domain and is formed by a loop contiguous with the phosphorylation lip. Changes in conformation in this region allow substrate binding to the active form of JNK, explaining how phosphorylation at the activation loop may play a role in the activation of JNK.

A huge number of studies demonstrated that JNK has a central role in development and in many different diseases. In particular, JNK pathway is involved in pathogenesis of a great variety of CNS diseases, i.e. in cerebral ischemia[133,134], in Parkinson disease (PD)[135], in AD[136], and recently in X-fragile syndrome[137], very similar to RTT.

3.2 Physiological and pathological functions of JNKs

The JNK basal activity is higher in the brain than in other tissue where it is involved in both physiological than pathological processes. Concerning physiological functions, JNK has shown a role in regulation of homeostatic processes in development and in the adult brain[138]. During development, JNK is involved in regulation of neuronal death[138], in modulation of microtubule dynamics[139], in dendritic formation and elongation as well as in branching and sprouting[140], in neuronal polarity and in axonogenesis[89,141,142]. The role of JNKs in the regulation of the neuronal cytoskeleton was initially supposed by their localization within cytoskeleton associated structures such as synapses, growth cones, and cell membranes in primary hippocampal neurons. This hypothesis was then confirmed by the observation that deletion of JNK1 induces progressive degeneration of long nerve fibres, substantial reduction of dendrite length as well as atrophy in dendritic spines[143,144]. Additionally, cytoplasmic JNK substrates such as doublecortin (DCX) and SCG10 are involved in promoting neurite extension and stability[144]. In the adult brain,

JNKs are important in various aspect of plasticity, learning and memory formation[140], although their role is partially unexplored. Noteworthy, JNKs are implicated in membrane receptor mobility and in particular in AMPA receptor trafficking following changes in neuronal activity[145,146]. JNKs have shown an involvement in learning and cognitive processes, by the way, the exact molecular mechanisms by which contribute to learning processes are far from being understood. Nonetheless potential downstream candidates regulated by JNKs may be proteins like: synaptotagmin-4[147], cytoskeletal proteins such as MAPs[148], AMPA receptors [145,146] and transcription factors, including c-Jun, ATF-2, calcium/cAMP response element binding protein (CREB) and Elk-1[132]. Such substrates are good candidates in JNK mediated pathways during learning since they are involved in memory processes.

Whereas, the importance of JNKs in pathological conditions lies on the fact that they are activated by a variety of stress signals, including UV irradiation[149], pro-inflammatory cytokine, oxidative stress[150,151], excitotoxicity [133,152], hypoxia and glucose deprivation[153,154] as well as cerebral ischemia[133] and have a well-established role in apoptosis, necrosis and autophagic cell death[155–157]. In fact deletion or inhibition of JNKs prevents neuronal programmed death [158], in particular, JNK3, and not JNK1 or JNK2, is required for the apoptosis of hippocampal neurons induced by glutamate receptor agonist kainic acid, clearly establishing that JNK3 is essential for mediating the apoptotic response of neurons to stress[138]. Finally JNK is a key player in Alzheimer disease as discussed before[126,127,159].

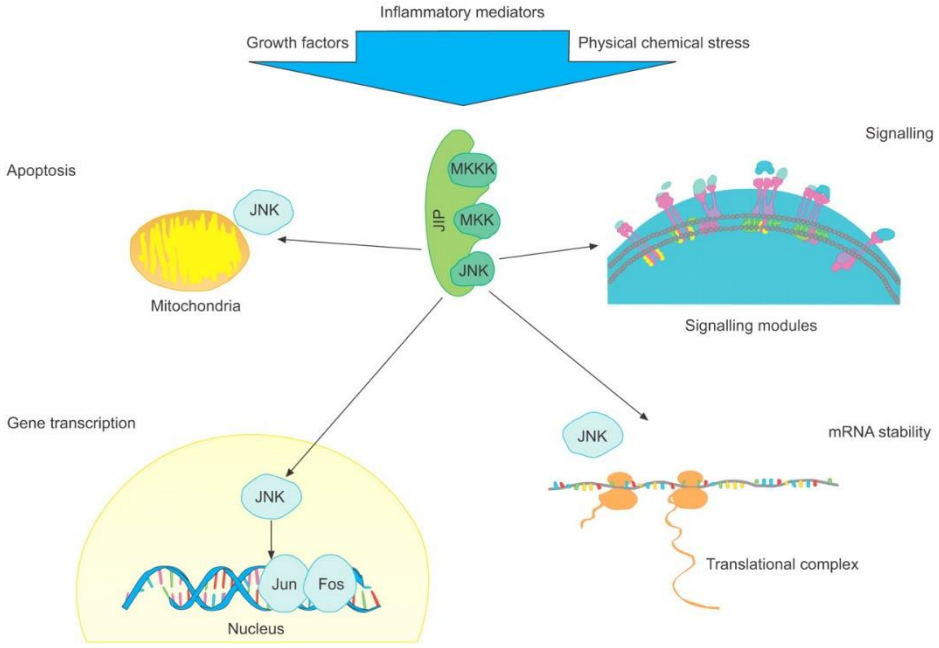

Figure 11- JNK activation and function. *As discussed previously, JNK is activated by many stimuli and is implicated in apoptosis, gene transcription, mRNA stability and in signalling in the post-synaptic region. Image taken by c-Jun N-terminal kinase-dependent mechanisms in respiratory disease of B. L. Bennett- European Respiratory Journal 2006 28: 651-661; DOI: 10.1183/09031936.06.00012106*

3.3 Regulation of JNK

Analogous to other MAPKs, JNKs are activated by dual phosphorylation on Thr and Tyr residues within the Thr-Pro-Tyr motif in the phosphorylation lip. These phosphorylations are mediated by two MAP kinase kinase (MAPKK), which are in turn activated by multiple MAP kinase kinase kinase (MAPKKK)[160]. Two MAPKKs have been identified for JNKs: MKK4 and MKK7. While MKK7 is a specific activator of JNK and phosphorylates predominantly the Thr residue, MKK4 can also activate p38 and phosphorylates predominantly the Tyr residue[131,161,162]. This specificity suggests that JNK can be activated by MKK4 and MKK7 depending by some circumstances[131]. The fact that is sufficient a mono phosphorylation of JNK on Thr residues to increase JNK activity, indicated that MKK7 is important to trigger JNK activity whereas the additional phosphorylation of the Tyr by MKK4 ensures optimal JNK activation[162].

MKK4 and MKK7 protein kinases are activated in turn by a dual phosphorylation of MAPKKKs. Several MAPKKKs have been reported to activate the JNK signalling pathway. These include members of the MEKK group (MEKK1-4), the mixed-lineage protein kinase group (MLK1, MLK2, MLK3, DLK, and LZK), the ASK group (ASK1-2), TAK1, and TPL2[131]. Some of these MAPKKK can activate MAPKK without distinction, others bind specifically to one MAPKK. For instance, MLK3, MEKK1 and TAK1 can interact with both MKK7 and MKK4[163–165], while MEKK4 specifically bind to MKK4[166], and DLK to MKK7[167].The specific transmission of signals from the upstream kinase to the MAPKs is ensured by interaction between the components of the cascade either directly or via scaffold proteins[149,168]. Both mechanisms may operate in parallel to allow differential responses of the same MAPK signalling pathway to different stimuli[169]. Scaffold proteins, such as JIP1, interact with several enzymes of the JNK cascade, creating multi-enzyme complexes[131]. These multimerized complexes organize the pathway and facilitate interactions with proteins, accelerating the activation cascade and localizing the signal in a specific cellular compartment or a restricted region of the cell[131,170,171].

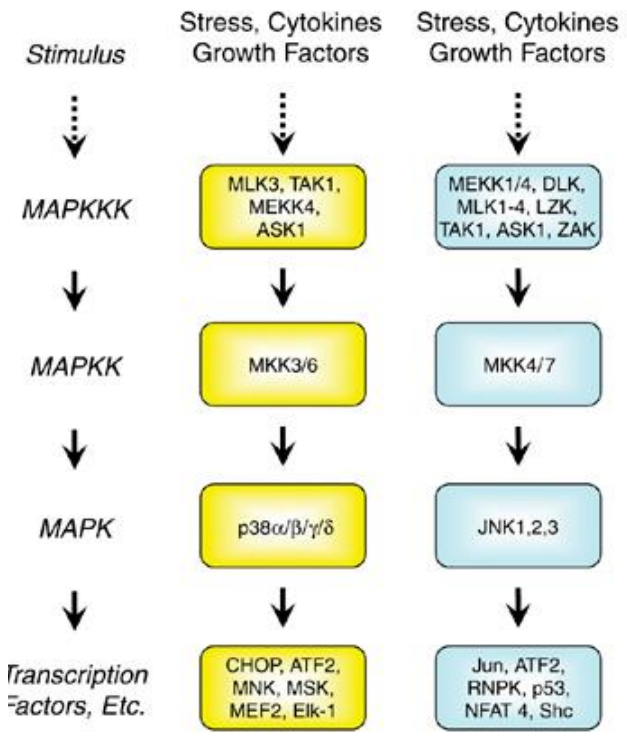

Figure 12- MAPK signalling pathway. *On the left side it is a schematic representation of MAPK activation that occur thanks to successive phosphorylation, generated by a stimulus. On the central and on the right side are shown the pathway involving respectively, activation of p38 and JNK.*

C-Jun: the main JNK target

Physiological and pathological stimuli induce activation of the transcription factor c-Jun, involved in neurodegenerative functions[172]. Together with Fos, ATF, and Maf subfamilies, c-Jun is the major component of the AP-1 complex, involved in cellular processes regulation, including differentiation, proliferation, and apoptosis[173].The variety of dimeric complexes and the dual roles of AP-1 as a transcriptional activator and repressor of genes may explain how c-Jun regulates so many different, and sometimes opposing, cellular processes[174].

The c-Jun promoter region contains several regulatory elements, including TRE (tetradecanoyl phorbol acetate response element)[175,176], that binds dimers of c-Jun and ATF factors regulating its own expression.

The transcriptional activities of c-Jun is regulated upon phosphorylation by various protein kinases, including the mitogen-activated protein kinases (MAPK), mainly by JNK

with a rapid, large, and transient stimulation[177,178].In fact, c-Jun can bind DNA target sequence motifs after a double phosphorylation by the Jun N-terminal kinases (JNKs) at serines 63 and 73[179]. This modification increase Jun's activity (AP-1 activity) and gene target transcription in stress-induced apoptosis and cellular proliferation[180]. Basal expression is detected in various compartments including dentate gyrus, motoneurons, peripheral neurons and nuclei of the autonomic nervous system following excitotoxicity stimulation and destruction of the neuron-target-axis including withdrawal of trophic molecules.

The c-Jun/JNK-axis is involved in neuronal plasticity and in memory formation: taken together, they participate in cytoskeletal alterations, in neuronal differentiation, in neurite extension and maturation of neural cells, and finally, initiate long-lasting genetic alterations by activation of TFs such as c-Jun, Jun-D or ATF-2[132,181]. Moreover, c-Jun appears to be essential for hippocampus-dependent learning behaviour and amygdala-dependent fear-conditioning responses. However, c-Jun proteins also regulate degeneration, apoptosis in the CNS and upregulation of harmful programs in non-neuronal cells (e.g. microglia and astrocytes) with release of neurodegenerative molecules.

The apoptosis-realizing target genes of c-Jun/AP-1 are not well defined. Fas ligand[182,183], TNFa[184], cyclin D1[185,186], p53[187] may be c-Jun effectors, even if they are independently regulated by c-Jun/JNK or are not involved in neuronal apoptosis [188,189].

Beyond direct transcriptional activation of endogenous neuronal killer proteins as it is likely for the kainic-acid induced hippocampal[180,190], pro-degenerative effects of c-Jun can be exerted by transcription of genes which enhance the pathological stress. Inhibition of c-Jun/JNK axis may be useful to contrast neurodegeneration.

4. CELL PERMEABLE PEPTIDES

Cell penetrating peptide (CPP) are short peptides that facilitate cellular intake/uptake of various molecular equipment (from nano-size particles to small chemical molecules and large fragments of DNA). The typical structure of a CPP is composed of a CARGO peptide linked to an effector-peptide. The cargo is associated with the peptides either through chemical linkage via covalent bonds or through non-covalent interactions.

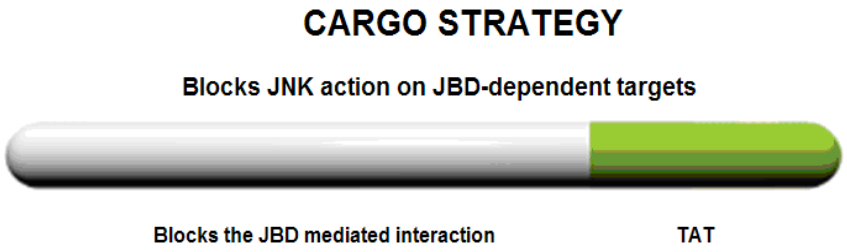

Figure 13- *Schematic representation of the CPP compose of a CARGO sequence (tat in green) and an active effector (in white).*

The cargo is transported into cells usually by unfolding the bilayer of the biological membrane. The cellular up-take is possible thanks to positively charged amino acids, such as lysine or arginine. The CPPs may be synthetically designed and allow a non-invasive import of different cargos. This technology shows numerous advantages that include: high and rapid output, relatively low costs for synthesis, versatility (few scaffold cores can be used to generate several compounds able to act at different levels from kinases inhibitors to secretase-like molecules), stability (when synthesized in D-amino acids), low catabolism, and low toxicity. Last but not least CPPs can be active in a range of nanomolar concentrations[170]. Consequently, CPPs are attractive drug delivery tools being capable of targeting intracellular signalling pathways as well as interfering with intracellular protein-protein complexes to rebalance a perturbed cellular function[170].

The cell permeable inhibitor of JNK, D-JNKI1[191], produces an allosteric modulation of JNK by blocking the access of the kinase to some of its targets, preventing protein-protein interactions, without interfering with its activation. The JIP-1 scaffold protein and c-Jun, the main target of JNK, share a similar JNK binding domain (JBD). However, JNK binding affinity to JIP-1 is about 100-fold higher than to c-Jun, for this reason the inhibitor peptide is able to block the access of JNK to its preferential substrate. D-JNKI1 peptide has been engineered by linking the 20 amino acids of JIP1 to 10 amino acids of the TAT-sequence of the human immunodeficient virus (HIV)[191]. Between the TAT and the JBD_{20} sequence, two proline-residues were inserted as spacer to allow for maximal flexibility. Thanks to those polycationic residues, D-JNKI1 can cross biological membranes via an energy-independent cellular process. Moreover, D-JNKI1 sequence has been synthesised with D-aa and in a retro-inverse form. These modifications lead to a significant increase of peptide stability, since D-aa are not recognized by endogenous proteases, and to a reduction in the immunogenic response.

The inhibitory action of D-JNKI1 peptide is fundamentally different from that of classical small chemical inhibitors[133,191,192]. D-JNKI1 does not inhibit JNK enzymatic activity, but selectively blocks access to many of its substrates by a competitive mechanism[192,193].

To determine the specificity of the peptide in blocking JNK action, the effects of the peptide on the activity of 40 different kinases towards their respective substrates in a cell free system was characterized[193,194]. D-JNKI1 did not interfere with the activities of other kinases, proving its exceptional selectivity for JNK, if compared to chemical inhibitors.

D-JNKI1 peptide completely inhibits excitotoxicity in primary culture and strongly prevents neuronal loss against two different models, transient and permanent, of middle cerebral artery occlusion (MCAo)[133,195]. Additionally, other authors demonstrated powerful protection by D-JNKI1 in different models of CNS injury: D-JNKI1 protects

against toxic drug and acoustic trauma induced auditory hair cell death[196] as well as against retinal ganglion cells death following optic nerve crush[197]. Moreover, we found that inhibition of JNK pathway was usefully in rescuing cognitive and synaptic deficit in AD[159] and in rescuing function and locomotor ability after spinal cord injury[198]. This cell permeable peptide inhibitor thus offers interesting possibilities for therapeutic application.

4.1. JNK inhibitors

Because of JNK role in a variety of pathologies, several research laboratories have proposed JNK inhibitors (Figure 14) to find effective drugs for their treatment.

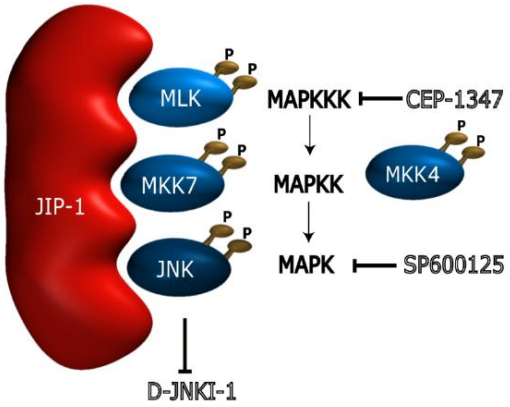

Figure 14- JNK inhibitors and their targets.*CEP-1347 inhibits the MLK group of MAPKKK, while SP600125 and D-JNKI1 block JNK.*

Inhibitors could be divided mainly in two classes: chemical compounds and cell permeable peptides (CPPs) inhibitors. Chemical compounds are small organic competitive inhibitors of the ATP-binding site of the kinase. At contrary, cell permeable peptide (CPPs) are short and positive peptides composed of lysine or arginine residues (20 to about 50 amino acids) which can cross the cellular plasma membrane[199] delivering biological active proteins to all tissues, including the brain. Among all, two chemical inhibitor compounds, CEP-1347 and SP600125, have been developed and tested. However, the published information on their efficacy in clinical trials remains limited.

CEP-1347 is a semi-synthetic inhibitor of the upstream component of the JNK pathway, blocking MLK group of MAPKKK as shown in Figure 16 [200]. CEP-1347 promotes survival of a variety of primary neurons in cell culture after either trophic factor withdrawal, DNA damage, or oxidative stress[200,201]. Moreover, *in vivo* it demonstrated to prevent neuronal cell death in models of AD, PD and cochlear hair cell death[196].

SP600125, developed by Celgene, is an ATP competitive inhibitor of JNK which inhibits all three JNK isoforms as well as c-Jun phosphorylation in a dose-dependent manner. However, it is not selective for JNK, since it also inhibits MKK4 and MKK7 activity as well as other MAPKs, such as ERK and p38, at higher doses[202].

In vivo, this compound protects dopaminergic neurons in the MPTP model of PD [196] and it was used to attenuate apoptosis in a model of AD neurotoxicity [203].

5. AIM OF THE WORK

Rett is a rare neurodevelopmental disorder that affects usually female in the first decade of life. Children affected by this pathology loss gradually their abilities to speech, to walk and develop autism features, epilepsy and breathing problems that get worst with time. Since RTT a genetic disease, today there is no cure for this disease, neither there are effective pharmacological treatments to reduce the locomotor and cognitive damage associated with this pathology.

c-Jun N-terminal protein kinase (JNK), is a stress-activated protein kinase, which plays an important role on synaptic functionality. It showed an involvement in synaptopathology related with Alzheimer's disease, spinal cord injury and ischemic stroke; its inhibitions revealed a real rescue of synaptic receptors levels, accompanied by an amelioration of cognitive and locomotor deficits. With those evidences in hand, we started to be interested in JNK's role in RTT. Its inhibition may represent an innovative strategy to tackle the syndrome. The main aim of this work was to characterize the JNK's role in the syndrome, analysing the D-JNKI1 effect (a cell permeable peptide JNK inhibitor) by behavioural, biochemical, and immunohistochemical studies in a mouse model of RTT. We choose a model with the most aggressive phenotype in order to evaluate the potentiality in preventing symptoms. To achieve this purpose, we performed:

* MeCP2 mouse model characterization;
* D-JNKI1 treatment evaluation on behaviour of MeCP2 mice;
* Biochemical evaluation of D-JNKI1 treatment on MeCP2 mice;
* Immunohistochemical evaluation of D-JNKI1 treatment on MeCP2 mice;
* Morphological evaluation of D-JNKI1 treatment on MeCP2 mice;
* D-JNKI1 treatment evaluation on neuroinflammation associated to MECP2 mice.

Furthermore, to evaluate the effectiveness of D-JNKI treatment, and to translate it to human patients, we decided to test the peptide action in IPSCs derived from RTT patients. We strongly believe that such approach will allow us to create a translational model from animal to human aimed to demonstrate the beneficial effect of D-JNKI1. D-JNKI1 treatment trying to translate from mouse to human model, evaluating its effect on IPSCs obtained from RTT patients (on going experiments).

This work will evaluate efficiency and safety of our approach and if successful, it provides a proof of principle for a novel therapeutic RTT modality that will be further advanced for clinical development. Last but not least, D-JNKI1 peptide is already in phase III clinical trials, consequently reducing the timing of reaching the actual availability of the peptide.

6. MATERIALS AND METHODS

6.1 Animal breeding

All animals used in experimental procedures are housed in according with European procedures. Mice were purchased from Jackson Laboratory, and bred at IRCCS Mario Negri Institute of Pharmacological Research in a specific pathogen free (SPF) facility with a regular 12:12 h light/dark cycle (lights 07:00 a.m- 7:00 p.m.), at a constant room temperature of 22 ± 2°C, and relative humidity approximately 55 ± 10%. Animals were housed (3-4 per group) in standard mouse cages, all with hard wood shavings as bedding material, ad libitum food (Global Diet 2018S, Harlan Italy) and water.

For our experiments, as largely discussed in the introduction, we used Mecp2 $^{tm1.1Bird}$ animals[61], that present a deletion in exon 3 and 4 and consequentially no detectable MeCP2 protein level in homozygous (male mice) indicated as Mecp2-/y and 50% of protein in heterozygous mice (female) Mecp2+/-. Moreover, females are affected by X-chromosome random inactivation and presents a very variable phenotype, depending from cells lacking the protein. The 21th day after birth, the animals were weaned and genotyped by PCR to identify the different genetic mutation.

Male mice, used for treatment, were weaned at the 19-20th days; the day after they were intraperitoneally injected with a D-JNKI1 (AURIS MEDICAL) 2mM solution (22mg/kg) at the 21st day and at the 42nd day. Mice were weighted before and after treatment and every time they were used for behavioural tests; when they reached 7 weeks of age, mice were sacrificed by decapitation and used for the biochemical, immunohistochemical and mRNA expression evaluations.

6.2 Polymerase chain reaction (PCR) for genotyping

To obtain mutated mice, we mated two heterozygous females with a wild-type male. We analised DNA from puppies' ears or tails pieces. DNA was extracted with a solution of NaOH (Sigma Aldrich) 50 mM for 1 hour at 99°C. After complete digestion, samples were adjusted of TRIS-HCl solution 80 mM and were stored at 4°C till use. DNA amplification was conducted with a commercial kit buy from Promega (GoTaq® G2 Flexi DNA Polymerase) and primers (Sigma-Aldrich) with the sequences reported on the Jackson Laboratories web site, which are:

COMMON: 5'-AAA TTG GGT TAC ACC GCT GA-3'

MUTANT REVERSE: 5'-CCA CCT AGC CTG CCT GTA CT-3'

WILD TYPE REVERSE: 5'-CTG TAT CCT TGG GTC AAG CTG-3'

Amplification cycles were performed with the BioRad S1000^{TM} thermal-cycler, following the instruction reported by Jackson Laboratory who provided us mice (94°C for 2min; 10 cycles at 94°C for 20 sec, 65°C for 15 sec, 68°C for 10 sec; then 28 cycles at 94°C for 15 sec, 50°C for 15 sec, 72°C for 10 sec; at the end 72°C for 2 min and 4°C). to visualize reaction product, we performed an electrophoretic run on agarose gel (1,5%) at 100V for almost 20 minutes.

6.3 Body weight and survival

Animals were monitored daily for well-being and welfare-related disease symptoms. Their body weights were recorded weekly. Body weight loss more than 15% in two consecutive weeks (>15% + >15%) was considered the humanitarian end-point of the study and the animals were euthanized. The trial was stopped 7 weeks after starting the study because of higher mortality in the KO groups.

6.4 Behavioural tests

6.4.1 Rotarod

Rotarod test was performed using the accelerating Rotarod apparatus (Ugo Basile 7650 model, in fig.15)[204]. The apparatus has a rotating bar subdivided in 5 slots to test in the same time 5 animals. Once the animals were positioned on the bar, time was started and the rod was accelerated at a constant rate of 0.3 rpm/s from 3 rpm to 30 rpm for a maximum of 5 min. The latency to fall was scored in seconds at which the animal fell from the bar.

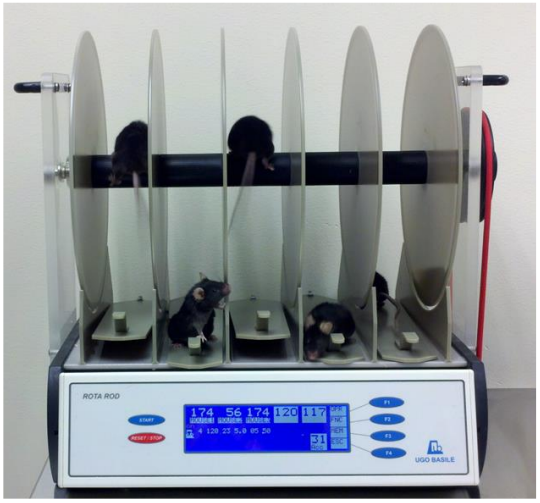

Figure 15- Rotarod apparatus. *One mice in one slot could be individually evaluated. When mice falls down, the Rotarod registered time of latency automatically.*

Motor coordination was tested by considering this latency time in every trials that mice performed[205,206]. Test was performed once a week, starting from the 3rd week to 7th week of life; tree trials were given to each animal and all times performed were recorded. we used ten animals for each experimental group.

6.4.2 Open field (OF) test

The OF test is used to examine general locomotive behaviour, as well as exploration and consequent level of anxiety, by exposing mice to a novel, open space[207,208]. We used a grey Perspex OF box (40 × 40 × 40 cm) with the floor divided into 25 (8 × 8 cm) squares (Fig. 17). Mice were placed in the centre of the floor defined as a 'starting point' and their behaviour was video-recorded.

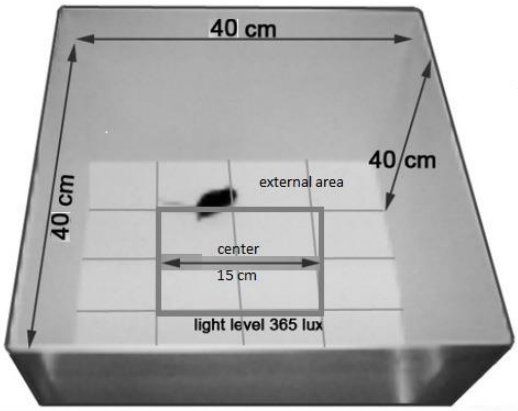

Figure 16- Open field apparatus

The mice behaviour was analysed for 5 min to measures spontaneous locomotor activity, exploratory activity and state of anxiety. At this purpose, we considered as parameters:

- time of locomotion divided into the number of internal (the 9 central squares) and external (the 16 peripheral squares) squares crossed,
- time spent in the central and outer area of the open field,
- mean of velocity gain from mice in the arena;
- time in which mice is immobile for more than 5% of pixel movement
- number and duration of rearing (standing on the hind paws),
- number and duration of self-grooming (rubbing the body with paws or mouth and rubbing the head with paws)[209]

For the OF at 7 weeks of age we used ten animals for each experimental group.

6.5 Subcellular fractionation (TIF)

After performing behavioural tests at 7 weeks, mice were sacrificed by decapitation and used for biochemical evaluations. After dissecting, subcellular fractionation was performed as reported in the literature with minor modifications both for cortex and cerebellum from hemizygous mice[210]. Briefly, tissue was homogenized with a glass-glass potter in 0.32 M ice-cold sucrose buffer containing the following (in mM) concentrations: 1 HEPES, 1 MgCl2, 1 EDTA, 1 NaHCO3, and 0.1 PMSF, at pH 7.4, in the presence of a complete set of protease inhibitors (Complete; Roche Diagnostics, Basel, Switzerland) and phosphatases inhibitors (Sigma, St. Louis, MO). A part of this homogenate was stored at -80°C to be used as whole extract. Samples were centrifuged at 1000 × *g* for 10 min. The resulting supernatant (S1) was centrifuged at 3000 × *g* for 15 min to obtain a crude membrane fraction (P2 fraction). The pellet was dissolved in buffer containing 75 mM KCl, 1 mM HEPES and 1% Triton X-100 plus protease and phosphatases inhibitors and ultracentrifuged at 47,000 × *rpm* for 1 h. The supernatant was stored and referred to as TSF, triton soluble fraction (S4). The final pellet (P4) referred to as TIF, triton insoluble fraction that was resuspended with sonication (BANDELIN sonicator, 20 of power, 5 cycles, 1 minutes each) in a 20 mM HEPES solution with a complete set of protease and phosphatases inhibitors and stored at − 80 °C until been used for further investigation.

6.6 Western blot

Protein concentrations were quantified using the Bradford Assay (Bio-Rad Protein Assay 500-0006, Munchen, Germany). 10 μg of TIF (triton insoluble fraction) extracted proteins or 20 μg of total extract were separated by 10% SDS polyacrylamide gel electrophoresis. PVDF membranes were blocked in 5% no fat milk in Tris-buffered saline solution 0.1% Tween20 for 1 h at room temperature. Primary antibodies were diluted in the same buffer

(incubation overnight, 4 °C) using: anti NR2A and anti NR2B (1:2000, a kind gift of Alomone Lab), anti GluA1 (1:1000, Millipore), anti GluA2 (1:1000, Millipore), anti PSD-95 (1:2000, Cayman), anti Drebrin (1:1000, Enzo), GFAP (1:5000, Millipore), anti P-c-Jun (1:1000 cell signalling), anti c-Jun (1:1000 cell signalling), anti IBA-1 (1:1000 WAKO). Anti.Actin (1:5000, Millipore) was used as housekeeping protein and at least six independent experiments were performed. Blots were developed using horseradish peroxidase-conjugated secondary antibodies (anti-Rabbit and anti-Mouse, as reported by datasheets from Santa Cruz Biotechnology) and the ECL chemiluminescence system (Promega). Western blots bands were quantified by densitometry using ImageJ software.

6.7 Analysis of gene expression

RNA was extracted from cerebellum of mice at 7th weeks of age. All samples were suspended in TRIzol reagent (Invitrogen, Milan, Italy), and RNA was isolated according to the manufacturer's instructions. One microgram of RNA was used for cDNA preparation with Moloney murine leukemia virus reverse transcriptase (Promega, Milan, Italy), as previously described[7]. Control reactions without the addition of the enzyme were performed for each sample. A 1:4 cDNA dilution was amplified using SYBR green chemistry. The PCR was carried out in triplicate or duplicate on a 96-well plate using GoTaq®qPCR Master Mix technology (Promega) according to the manufacturer's protocol using a 7900HT fast real time PCR system (Applied Biosystems, Life Technologies) with the following thermal profile: 2 min at 95 °C; 40 cycles, 15 s at 95 °C, 1 min at 60 °C. Gene expression of target genes was assessed for Gfap (Gfap FW: 5'-AGGGCGAAGAAAACCGCAT-3';Gfap REV: 5'-GGTGAGCCTGTATTGGGACA-3'), Shank3 (Shank3 FW: 5'-CGGAGAAGAAAAGGGGAGAAGTT-3'; Shank3 REV: 5'-CAATGTCCGGCCTCAGTGTC-3'), Iba-1 (Iba1 FW: 5'-

ACCCAGCGGACAGACTGCCA-3'; Iba 1 REV: 5'-TTTCCTCCCTGCAAATCCCTGCT-3'), C1qa (C1qa FW: 5'-GACCACGGAGGCAGGGACAC-3', C1qa REV: 5'-CTTCCCGTTGGGTGCTCGGC-3'). Data were analysed using the $2^{-\Delta\Delta Ct}$ method[59] using *36b4* as the housekeeping gene (forward primer, 5′-GGCGACCTGGAAGTCCAACT-3′; reverse primer, 5′-CCATCAGCACCACGGCCTTC-3′).

6.8 Immunohistochemistry

Mice were deeply anesthetized with ketamine (100 mg/kg intraperitoneally, i.p.) and xylazine (10 mg/kg i.p.), and perfused through the ascending aorta with 50 mM cold phosphate-buffered saline (PBS, pH 7.4) followed by chilled 4% PAF in PBS. The brains were post-fixed at 4 °C overnight, and then transferred to 30% sucrose in PBS 0,01 M at 4 °C for enough 24 h. Then, the brains were immersed in − 50 °C isopentane for 3 min and stored at − 80 °C until assayed.

Serial coronal sections (20 μm) were cut from 0 to − 6.6 mm from bregma and were collected in 100 mM PBS. We prepared 6 series of 4 sections that were stained for GFAP (1:300, Millipore), CD11B (1:500, not-commercial, a kind gift of Veglianese's group), NeuN (1:500, chemical MAB IgG1) and for P-c-Jun (1:50, cell signalling).

Coronal cryosections (15 μm; Leica CM3050 S) from the total hemisphere were stored at −20°C. All sections were post–fixed with 4% formaldehyde (PFA) for 5 minutes, pretreated with 80% formic acid for 2 minutes and 2% H2O2 for 7 minutes. After washing with 10 mM phosphate buffered saline (PBS), pre - incubation solution (10% normal goat serum (NGS), 1% bovine serum albumin (BSA), 0.5% Triton X-100 in 10 mM PBS) was applied to the sections for 30 minutes at room temperature. Afterwards, the sections were

incubated with specific polyclonal primary antibody (Millipore) diluted following manufacter's instructions in primary antibody solution (3% NGS, 1% BSA, 0.5% Triton X-100 in 10 mM PBS) at 4°C overnight. The antisera were generated and evaluated for specificity as described in datasheet. After washing steps, the sections were incubated for 1 hour with a biotinylated secondary antibody (BA-1000, Vector Laboratories, CA, USA) diluted at 1∶300 in 3% NGS, 1% BSA, 0.5% Triton X-100 in 10 mM PBS, washed in 10 mM PBS, and afterwards, incubated 1 hour at room temperature with streptavidin-biotinylated horseradish peroxidase complex diluted at 1∶100 in 0.5% Triton X-100 in 10 mM PBS. After washing with 10 mM PBS, all sections were incubated with 3,3′-diaminobenzidine tetrahydrochloride (Sigma, MO, USA) for 5 minutes, before 0.1% H2O2 was added to 10 ml DAB solution and applied on the sections until proper labelling was achieved (3 minutes). The sections were briefly rinsed in water, mounted and stored at room temperature.

6.9 IPSCs from Rett patients

Fibroblasts were isolated from skin RTT patients and controls and cultured according to standard protocols were used for reprogramming following the procedure by Takahashi et al. (2007). Briefly, the IPSc were first re-programmed and then differentiated in neurons for 60 days. The neuronal-IPSc will be first analysed in order to identify dendritic spine and subsequently JNK activation will be measured as P-c-jun/jun ratio in neuronal-IPSc of Rett patients versus control.

Finally, neuronal-IPS cells were treated with D-JNKI 2 µM and 4 µM to value the effect of peptide on the synaptophaty associated to RTT syndrome. We lysed cell cultures in 0.32 M ice-cold sucrose buffer containing the following (in mM) concentrations: 1 HEPES, 1 MgCl2, 1 EDTA, 1 NaHCO3, and 0.1 PMSF, at pH 7.4, in the presence of a

complete set of protease inhibitors (Complete; Roche Diagnostics, Basel, Switzerland) and phosphatases inhibitors (Sigma, St. Louis, MO), the same used for mouse tissues.

6.10 LDH assay

Ldh assay is a test to evaluate level of the enzyme lactate dehydrogenase released by death cells in their medium culture. Medium was collected from cells before and after D-JNKI1 treatment and stored at -20°C. We followed instruction reported by the commercial test (PROMEGA, ldh assay) and read the adsorbance at 495 nm with TECAN spectrophotometer.

6.11 Statistical analysis

Statistical analysis was done using Graph Pad Prism 6 program. Two groups data were analysed using unpaired t-Test, whereas when we have four conditions we used the two-way ANOVA, followed by Bonferroni's *post hoc* test. All data were expressed as mean ± SEM with statistical significance given at $P< 0.05$.

7. RESULTS

7.1 Characterization of MeCP2 mouse model

Rett syndrome (RTT) is caused by mutations of the MECP2 gene, which encodes for a transcriptional regulator with many functions carried out mainly in the brain. The disease is characterized by an onset not easily diagnosed, and highly variable phenotype. The high variability makes difficult to replicate motor and cognitive deficits of patients in a unique animal model. Among Rett mouse models, we used the MeCP2 Bird tm1.1 mouse model that replicates especially locomotives deficit and, to a lesser extent, cognitive ones[55].

The mice MeCP2tm1.1Bird, as amply described in the literature, have a deletion at the level of exons 3 and 4 of the MECP2 gene on chromosome X. Mutated male mice, defined knock-out (KO) or Mecp2 -/y, are hemizygous for the mutation and do not present detectable protein levels. Females are heterozygous for the mutation, defined Mecp2 +/-, are affected by mosaicism due to random inactivation of the X chromosome, a condition closer to human. Females Mecp2 +/- are fertile and have a high breeding index and to expand the colony two heterozygous females were crossed with a male wild type. During the breeding period, MeCP2 +/- female showed problems in nursing and caregiving to pups. To expand the mouse colony, the MeCP2 +/- were replaced post-partum with CD1 mice nurses, to reduce the pups' mortality and cannibalism episodes. Despite the nurse, many puppies were not able to feed themselves and to survive and we registered a death rate of 17%, as shown in Fig 17.

In addition to the high mortality observed during the expansion of the colony, we found among survivor mice, a low percentage of hemizygous and heterozygous genotypes (23% for hemizygote $MeCP2^{tm1.1\ Bird}$ -/y and 15% for heterozygotes $MeCP2^{tm1.1\ Bird}$ +/-)

compared to the wild-type genotype, equal to 45%. Consequently, it was necessary time to expand the colony and to get Mecp2tm1.1bird -/y males used for our evaluation.

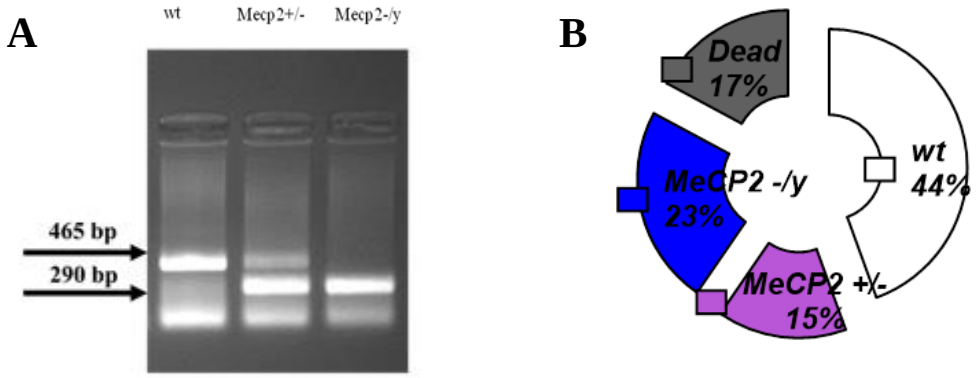

Figure 17- Genotyping of MeCP2$^{tm1.1\ Bird}$ mice. *A) PCR analysis shows the different genetic background among wt (single line), MeCP2 +/- heterozygous mice (double line) and MeCP2 -/y hemizygous mice (single line down). B) Percentage of the different genetic background showed that 23% of total are MeCP2 -/y (hemizygous, in blue) mice, 15% are MeCP2 +/- (heterozygous, in violet) mice, 44% are wild type mice (in white) and in grey are shown mice found dead in cage after birth corresponding to 17%.*

For our experiments, we chose male MeCP2 hemizygous mice model, because they show a rapid onset (at 3-4 weeks), see fig. 18A and a more aggressive pathological phenotype that bring them to have a high state of suffering and mortality around the 8th – 10th week of life as reported also by Guy in 2001. Despite heterozygous female are affected by mosaicism, they show a delayed onset (at 16-20 weeks, see fig 18B) and a milder phenotype.

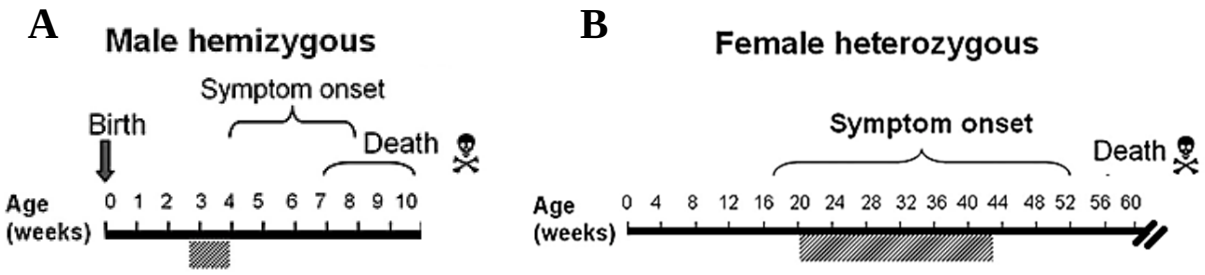

Figure 18- The differences between MeCP2 y/- and MeCP2 +/- mice concerning onset and progression of the pathology*. Male hemizygous(A) shown a rapid onset, around the 3rd-4th week of life. The pathology is more severe and led to death in a very early stage of life, at maximum 10 weeks. Whereas, female (B) have symptom onset around the 16th week of life, but pathology is not progressive.*

Moreover, male present a more homogeneous genetic background which reduces the individual variability typical of heterozygous female mice (affected by mosaicism), and this results in a simpler design of our study as well as interpretation of the results obtained. A summary of the major features of MeCP2 -/y mice is shown in table 2.

Mouse models: Male Mecp2 $^{tm1.1\ Bird}$					
Phenotypes	Body Weight	Grooming/Fur Quality	Tremor, Forelimb Movement or Hindlimb Clasp	Kyphosis	Survival
General Health	On B6 background, Underweighted from 4 weeks, sometimes at weaning; Robust and Reproducible	"Ragged" Look is common by ~PND60; Robust, some variability in severity	Tremor phenotype reproducibly present late in symptomatic progression. Hindlimb clasp reproducibly observed	Apparent later in symptomatic progression	Lifespan significantly reduced. Approximately 90% of male Mecp2tm1.1Bird mice die before 12-14 weeks of age. minimal genetic background influence
Phenotypes	Open Field or Running Wheel Tests	Rotorod	Grip Strength		
Behavioral & Motor Properties	Increased Immobility, Decreased Rearing, Decreased Ambulation. Phenotype is Robust and Reproducible between labs. Phenotypic onset before 5 week of ages.	Impaired performance. Decreased latency to fall on accelerating rod. Phenotypic onset by 6 weeks of age. Robust phenotype that is reproducible between labs.	Diminished grip strength from 6 weeks of age		

Table 2. *Summary of the general health, lifespan, behavioural and motor properties of MeCP2 tm1.1 Bird male mice.*

MeCP2 -/y mice are characterized by locomotor and cognitive impairments and a high rate of suffering with a dramatic decrease of body weight (15%) in MeCP2 -/y in the last stage of pathology. For these reasons, we decided to study the pathology in this mouse model from day 0 to 42 (corresponding to 7 weeks of age).

7.2 MeCP2 -/y metabolic profile characterization

In order to characterize MeCP2 -/y animal model, we analysed the metabolic profile by evaluating the growth curves and the consumption of water and food during the entire experiment As shown in fig. 19, we found a highly significant effect of genotype (two-way ANOVA, genotype effect #### p <0.0001) in males hemizygous Mecp2 -/y compared to wild type mice (wt), with a weight reduction of 60%.

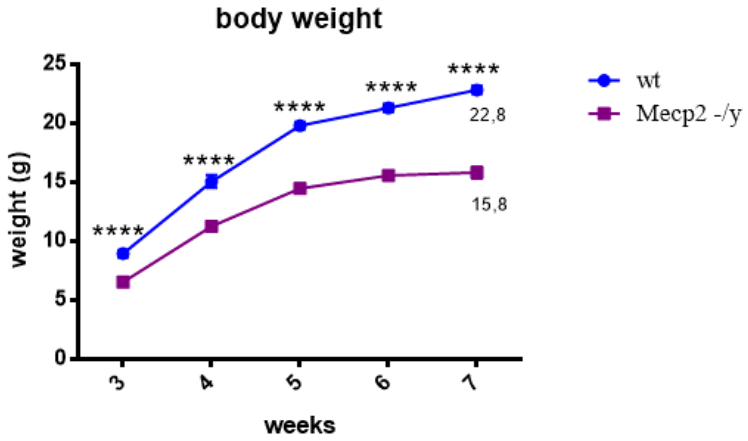

Figure 19 - Body weight of MeCP2 -/y or ko mice. *Significant reduction of body weight in male MeCP2 compared to wt mice analysed starting from 3rd week to the 7th week (n=10 for each group). Statistical analysis: two-way ANOVA genotype effect #### P<0,0001, post-hoc test Bonferroni's multiple comparisons test**** p>0.0001 MeCP2 -/y compared to wt mice. Data were shown as mean ± SEM.*

To understand if the decrement of body weight was related to a reduced consumption of water and food, we analysed these parameters since their weaning (3 weeks of age) until the end of the experiment (7 weeks of age). As shown in Fig. 20A, Mecp2 -/y mice showed no statistical significant differences in food consumption, meanwhile they shown a significant reduction in water consumption (two-way ANOVA, genotype effect #### p <0.0001; Fig. B) compared to wild type animals.

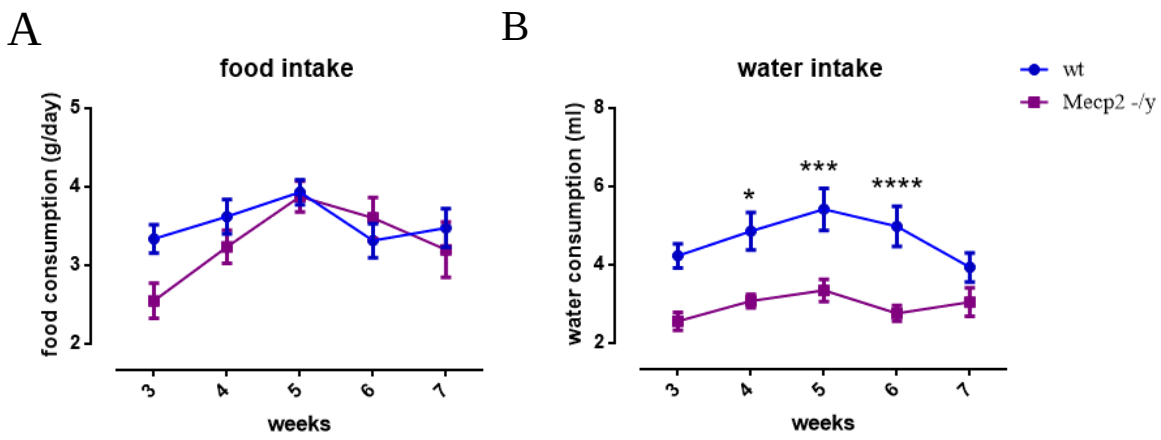

Figure 20 - Food and water consumption in MeCP2 -/y ko mice. A)*No significant difference in food consumption of male MeCP2 -/y compared to wt mice in the time windows analysed (n=5 for each group).* ***B)*** *Significant reduction of water consumption in male MeCP2 -/y compared to wt mice in the time windows analysed (n=5 for each group). Statistical analysis: two-way ANOVA genotype effect #### P<0,0001, post-hoc test Bonferroni's multiple comparisons test * P<0,05, *** P<0.001 **** P>0.0001 compared to wt mice. Data were shown as mean ± SEM.*

7.3 Evaluation of motor impairment in MeCP2 mice.

A progressive deterioration of well-being was identified during the 7 weeks in MeCP2 -/$y^{tm1.1\ Bird}$ mice, related to an increasing reduction in body weight and food and water consumption. Then we decided to analyse the possible behavioural deficits associated with Rett syndrome. In order to evaluate the physical disabilities, similar to those of girls suffering from RTT, we administered $Mecp2^{tm1.1Bird}$ mice to specific tests widely used in science to assess locomotor deficits such as Rotarod and the Open Field Test (previously described in materials and methods).

As shown in fig.21, results obtained with the Rotarod test (performed every 7 days from 3rd to 7th week of life) showed a significant and progressive motor deficit in mice MeCP2 -/y. In fact, the ability of MeCP2 -/y to perform on the rotating bar (measured with the latency time of each animal on the bar) was significantly lower (two-way ANOVA, genotype effect #### p<0.0001) when compared with wild type animals. Moreover, the deficit is progressive: the motor performance of MeCP2 males - /y at 3 weeks had a mean

of 177 seconds and, after a partial recovery until the 6th week of age with an average value of 229 seconds, there is a final reduction of the latency time equal to 164 seconds corresponding to the terminal stage of the disease.

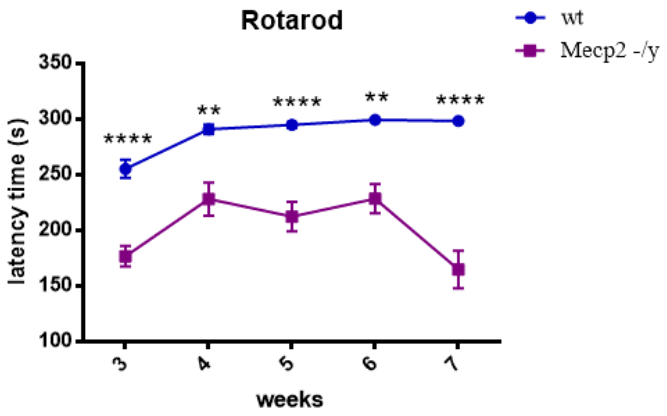

Figure 21-Evaluation of locomotor activity in MeCP2 mice by Rotarod test. *Details of test are largely discussed in the text. We found a significant reduction of latency time in male MeCP2 -/y compared to wt mice in each point analysed (n=10 for each group). Statistical analysis: two-way ANOVA genotype effect #### P<0,0001, post-hoc Bonferroni's multiple comparisons test ** P<0,01, **** P<0.0001 compared to wt mice. Data were shown as mean ± SEM.*

To confirm and well-characterize locomotor deficits, we decided to test animals with the Open Field Test, which analyse not only related locomotor activity parameters (such as the total distance travelled, speed of movements and the time of immobility), but also exploratory related parameters (as the time spent in the central and peripheral arena, the number of crossings in these areas) and parameters related to an anxiety-like behaviour (as rearing and grooming). In fig.22A we can observe a significant reduction in the average distance travelled by MeCP2 -/y mice compared to wild type animals (two-way ANOVA, genotype effect #### p<0.0001). Consequently, MeCP2 -/y mice showed a reduced average in speed of movements (Fig. 22B; two-way ANOVA, genotype effect #### p <0.0001) and an increase of immobility (Fig. 22C; two-way ANOVA, genotype effect ### p <0.001) compared to wild type mice. Those evidences confirm the locomotor deficits and the progressive symptoms worsening in animals affected by RTT. In fact, the results obtained show a correlation between a reduced ability to move, a decrease speed

of movement and an increase state of immobility, highlighting how the animals MeCP2 -/y spent progressively more time in a stage of immobility.

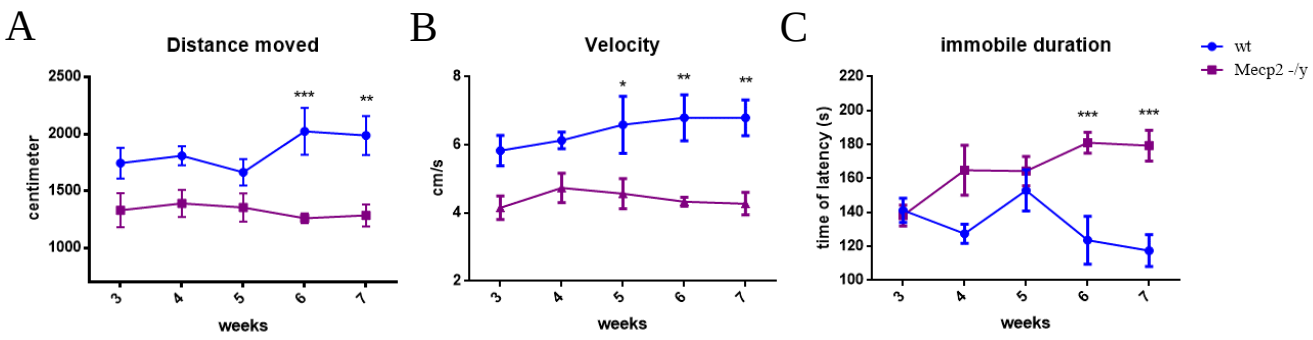

Figure 22- Evaluation of locomotor activity in MeCP2 mice using Open field test. *Analysing the distance moved (**A**), the velocity of crossing (**B**) in MeCP2 -/y and wt mice, we found a significant decrease in male MeCP2 -/y compared to wt mice in the time windows analysed. Valuating the immobile duration (**C**), we observed a significant increase in male MeCP2 -/y compared to wt mice (n=5 for each group). Significant relative to wt mice * p<0.05, ** p<0.001. Data were shown as mean ± SEM*

For whom it concerns parameters related to the exploration activities, we measured time in exploring the inner area and the outside area of Mecp2-/y mice, observing a tendency in spending more time in the outside zone and lesser in the inner zone (Fig. 22 A-C). We considered also the number of crossings from area to area, founding a significant reduction of this parameter in mice Mecp2-/y compared to wild type animals (Fig. 22 B-D; two-way ANOVA, from centre to external zone genotype effect ## p <0.01, from external to centre zone genotype effect ### p <0.001). The results highlighted an exploratory locomotor deficits in line with the obtained data, because the animals Mecp2-/y spend time in a stage of immobility, carrying only 8 crossings in 200 seconds in the outdoor area and 4 crossings in 6 seconds in the inner.

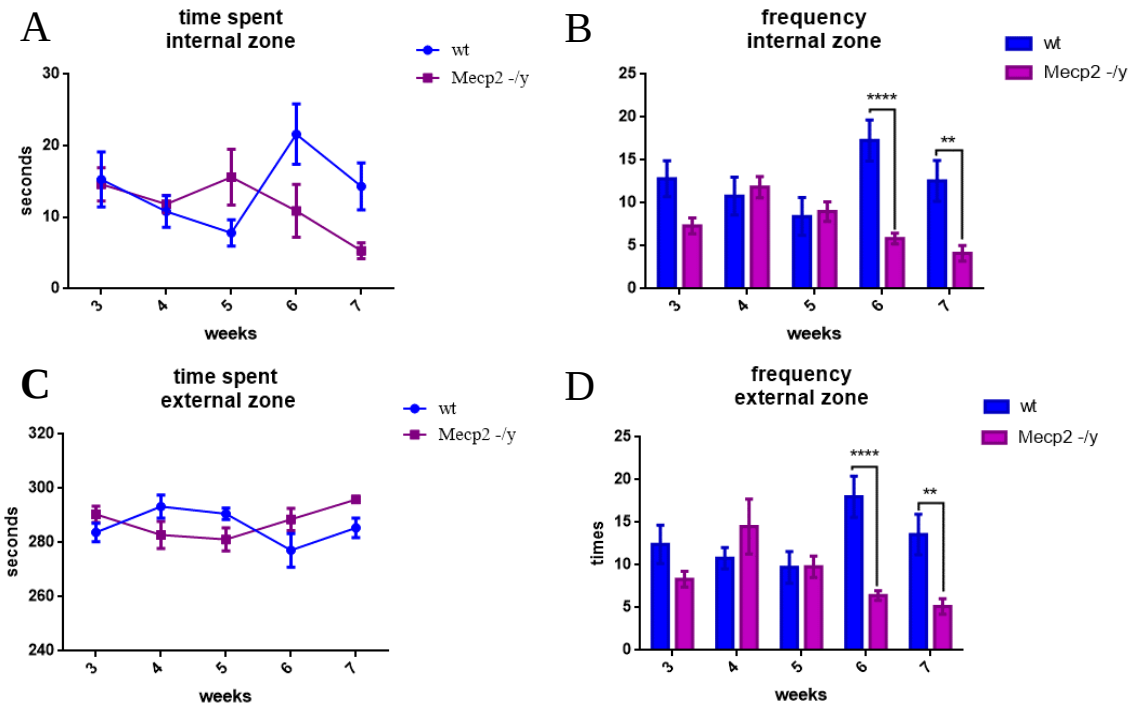

F***igure 23-Evaluation of exploratory activity in MeCP2 mice using Open field test. A-C)*** *Analysing the exploratory activity in MeCP2 -/y and wt mice, we did not find any significant difference in the time spent in external and internal zone between two experimental groups, but we observed in the frequency of crossing a significant decrease in male MeCP2 -/y compared to wt mice in the time windows analysed (n=5 for each group). Significant relative to wt mice * p<0.05. Data were shown as mean ± SEM.*

Rett syndrome is classified as an autism spectrum disorders, so we decided to evaluate if our mouse model replicates the typical anxiety-like behaviour of these diseases. At this purpose, we have evaluated two parameters: rearing, that is the attitude of the animals to stay balanced on the hind limbs, and grooming. Mecp2 -/y mice showed a significant reduction both in time (two-way ANOVA, genotype effect ### p <0.001, Fig. 24 A) and in frequency of rearing compared to wild type animals (fig. 24 B).

Moreover, Mecp2 -/y mice presented a tendency in increment of grooming time (p = 0.06 Fig. 24C) and a significant decrease in frequency (two-way ANOVA, genotype effect #### p <0.0001, Fig 24D) compared to wild type.

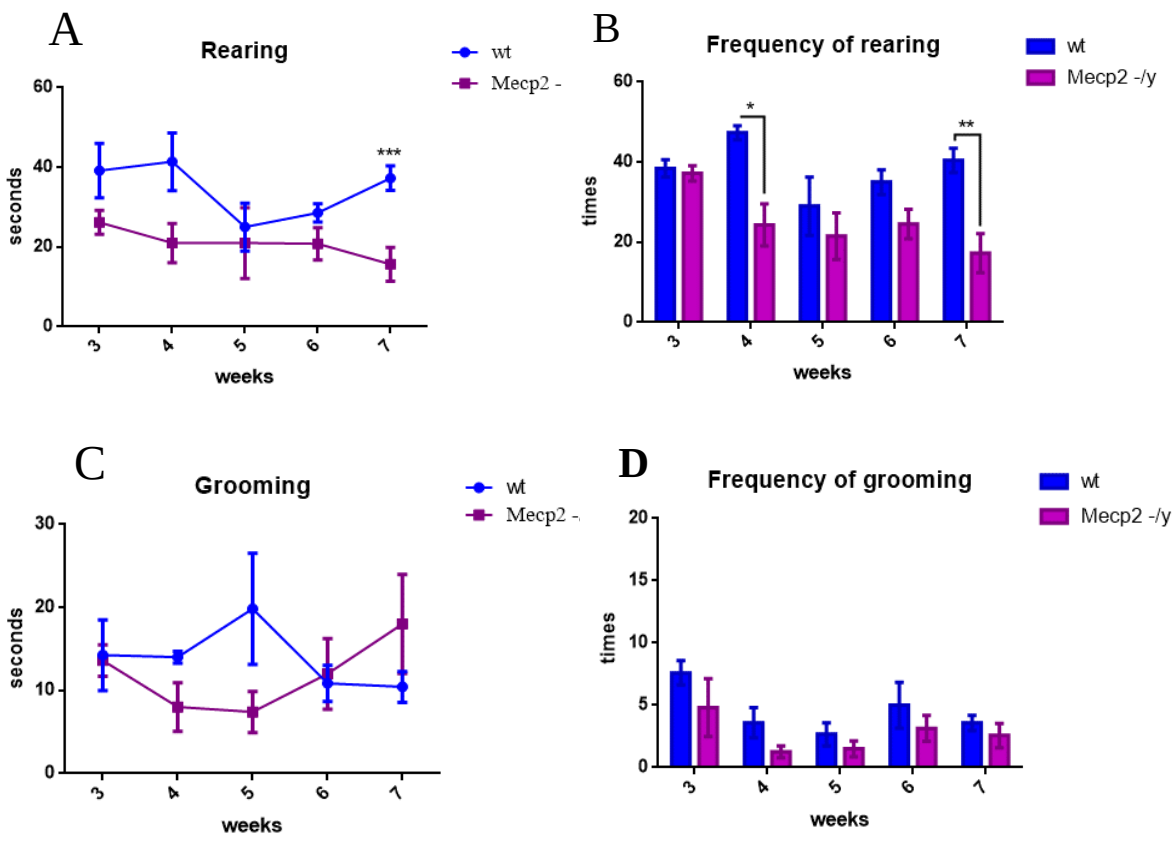

Figure 23-Evaluation of anxiety-like behaviour in MeCP2 mice using Open field test. *Analysing different parameters in open field test as time and frequency spent for rearing (A-B) and time and frequency spent for grooming (C-D), we found a significant decrease of time spent for rearing and a tendency to an increase of time spent for grooming in male MeCP2 -/y compared to wt mice. (n=5 for each group). For the others parameters analysed (panel **B-D**) we did not find any significant difference between two experimental groups. Significant relative to wt mice § $p < 0.05$. Data were shown as mean ± SEM.*

7.3 Characterization of intracellular stress pathway in MeCP2 mouse model.

The most involved brain areas in locomotor activity are the cerebellum and the prefrontal cortex. Cerebellum is profoundly involved in motor learning and behaviour, tasks strictly connected with synaptic plasticity. The loss of neuronal plasticity and the impairment of spines in this structure, can cause extensive damage in motor and cognitive processes. Behavioural tests showed in Mecp2 -/y mice showed also an inability to learn and memorize the execution of the part of test.

To investigate the synaptic damage underlying these deficits in RTT syndrome, we decided to study neuronal post-synaptic compartment using the TIF fractionation[211] of

cerebellum of our animal model. We analysed markers associated with post synaptic density, especially subunits of NMDA and AMPA receptors, and the two main scaffold proteins of excitatory synapses, PSD-95 and SHANK3.

We observed a significant increase of NR2A and NR2B subunits levels (t-test, * $p < 0.05$, ** $p < 0.01$ Fig.) and the same tendency for GluR1 and GluR2 subunits levels of ($p = 0.06$, Fig. 25) in mice Mecp2- / y compared to wild type control. In addition, as a further confirmation of the presence of a synaptic damage in the cerebellum, we found a significant decrease of the two scaffold proteins of excitatory synapses, PSD-95 and Shank 3 (t-test, * $p < 0.05$, ** $p < 0.01$ Fig. 24) in knockout mice compared to their respective controls.

Several evidences in literature have shown a correlation between the synaptic dysfunction and the activation of the MAP kinase JNK[126,194]. Supporting those evidences, our laboratory has been extensively studied and characterized JNK and its role in neurodegenerative diseases as a key player in synaptic damages. We decided to assess the role of MAP kinases JNK in dendritic spine level even in neurodevelopmental diseases such as Rett syndrome.

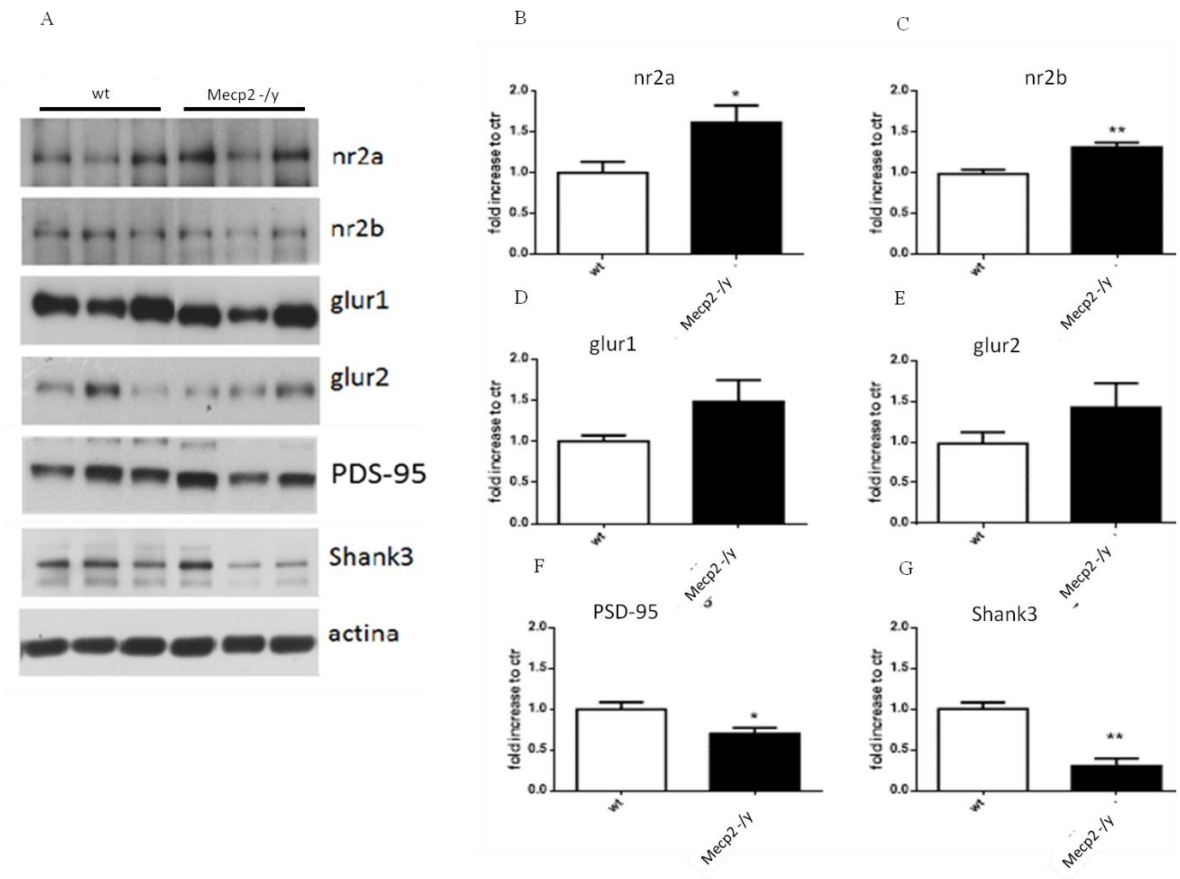

Figure 24- Analysis of main post-synaptic receptors in MeCP2 -/y mice vs wt *A-B) Western blot analysis of NMDA receptors nr2a and nr2b, revealed a significant increase of level of both in male MeCP2 -/y compared to wt mice (n=4 for each group). C-D) Western blot analysis of AMPA receptors glur1 and glur2, revealed a tendency in increasing. E-F) Psd95 and Shank3 levels are reduced in MeCP2 -/y mice compared to wt. Statistical analysis: t-test. Significant relative to wt mice *p< 0.05, ** p<0.01, *** P<0,001. Data were shown as mean ± SEM.*

Biochemical analysis of the cerebellar post-synaptic area highlighted an increment of JNK phosphorylation in dendritic spines (t-Student, * p <0.05, Fig A) in Mecp2 -/y compared to wild-type.

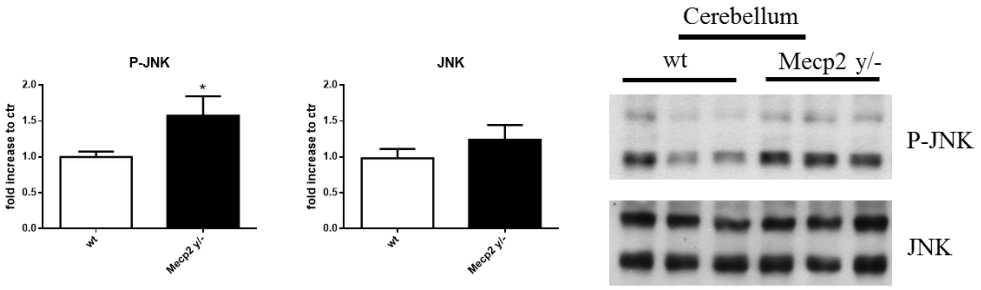

Figure 25- Analysis of activation of JNK pathway in MeCP2 -/y mice vs wt A-B) *Western blot analysis cerebellum revealed a significant increase of JNK phosphorylation, express as P-JNK/JNK in male MeCP2 -/y compared to wt mice (n=4 for each group). Statistical analysis: t-test, significant relative to wt mice *p< 0.05. Data were shown as mean ± SEM.*

As widely characterized, activated kinases act with a cascade mechanism on their targets. The elective target of JNK is the nuclear transcription factor, c-Jun. When activated through phosphorylation, c-Jun determinates transcription of target genes involved in various stress cellular response such as inflammation and neuronal death. We then performed Western blot analysis to assess the activation of c-Jun, checking its phosphorylated form, P-c-Jun, which was found to increase significantly in mice Mecp2-/y compared to the wild type control (t-test * $p < 0.05$, Fig.).

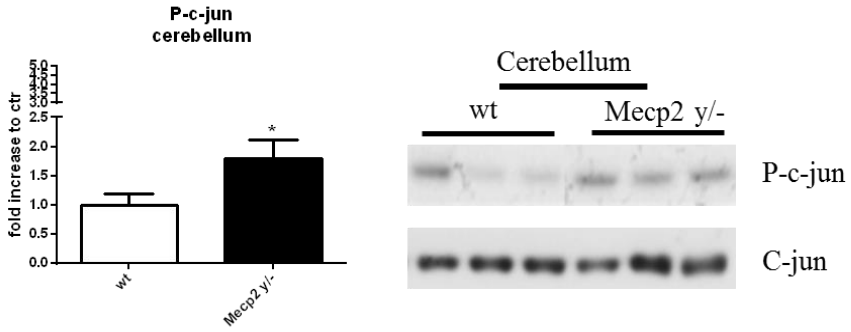

Figure 26 -Analysis of JNK pathway in MeCP2 -/y mice vs wt. *Western blot analysis of and cerebellum revealed a significant increase of P-c-Jun/c-Jun ratio in male MeCP2 -/y compared to wt mice (n=4 for each group). Significant relative to wt mice *p< 0.05, *** p<0.001. Data were shown as mean ± SEM.*

7.4 *Immunohistochemical characterization of MeCP2 mouse model*

In addition to our biochemical analysis, that shown clearly JNK activation in dendritic spine and its related pathway, we performed immunohistochemical analysis to make our results more consistent. MeCP2 -/y mice cerebellum exhibited activation of the JNK signalling with the strong immunoreactivity of its elective target c-Jun (P-c-Jun positive staining, panel G-H), confirming biochemical experiments. Due to the strictly correlation between c-Jun phosphorylation and inflammation status[212], as well as for the inflammatory status reported in RTT disorder[213,214] we here also examined the astroglial and microglial activation in MeCP2 -/y mice vs wt.

We reported an advanced state of inflammation, with overexpression of GFAP, a marker of astrogliosys (positive staining in panel A-B-I), as well as the hyperactivation of microglia (CD11β positive staining, panel C-D-L), importantly without a reduction of neuronal population (NeuN positive staining, panel E-F-M).

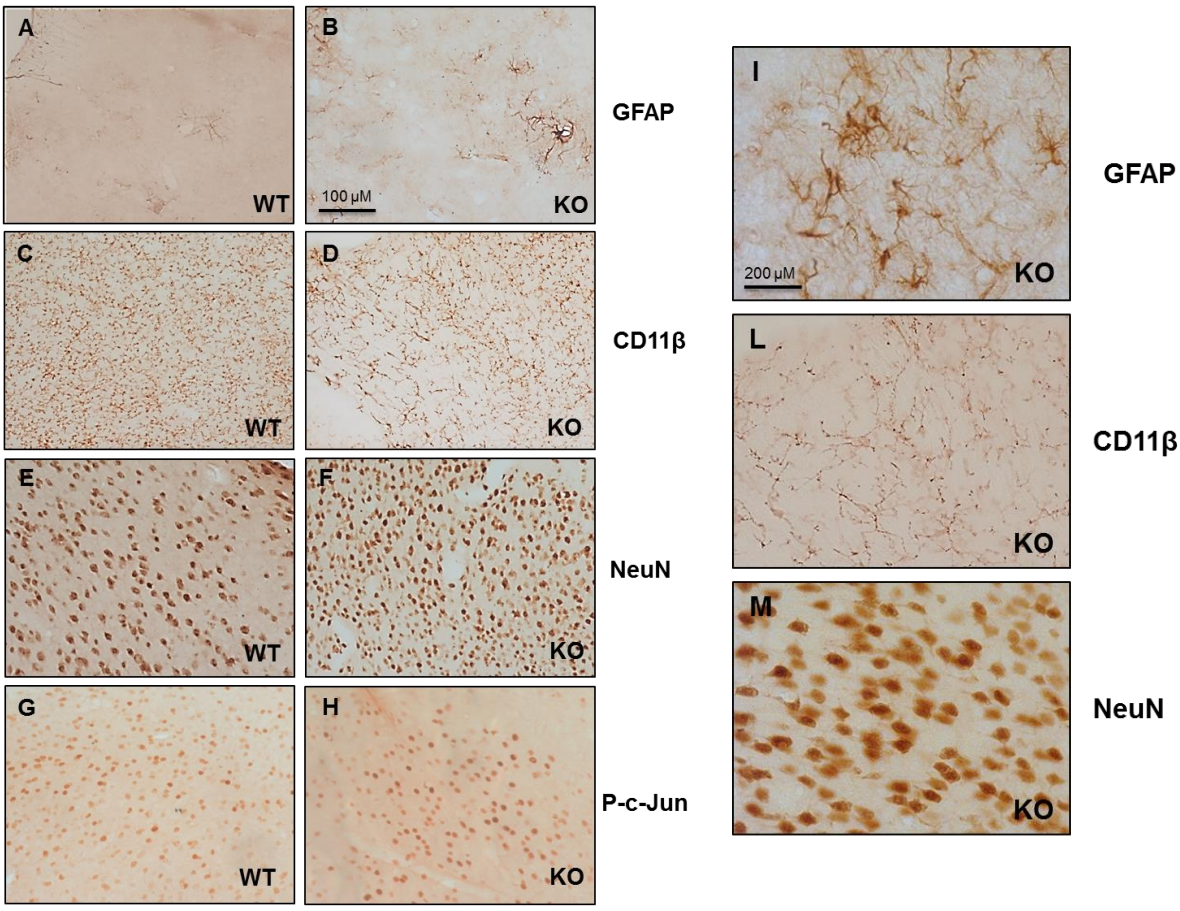

Figure 27--Immunohistochemical analysis of cerebellum of MeCP2 -/y compared with wt mice and related magnification (40X)*. A-B) GFAP staining revealed an advanced state of inflammation in ko compared to wt mice C-D) CD11β staining revealed a microglia activation in ko compared to wt mice. E-F) NeuN staining didn't reveal a reduction of neuronal population in ko compared to wt mice. G-H) P-c-Jun staining revealed an increase of c-Jun phosphorylation in ko compared to wt mice.* ***I)*** *GFAP magnification staining revealed an increment of inflammation state MeCP2 -/y mice with a characteristic astrocyte morphology.* ***L)*** *CD11β staining highlighted microglia activation state in MeCP2 -/y mice.* ***M)*** *NeuN staining revealed vitality of MeCP2 -/y mice. Representative sections are shown of 4 animals used per each group. Scale bar: 100 µm (A-H); 200 µm (I-L-M).*

7.5 A new strategy to prevent Rett Syndrome: the cell permeable JNK inhibitor peptide (D-JNKI1) treatment in MeCP2 mouse model.

From previous studies conducted in our laboratory, we proved that the inhibition of the MAP kinase JNK may contribute to synaptic dysfunction recovery[126,215] cognitive and motor damage related with neurological diseases [159,216], while the inflammation reduction associated with these diseases[217,218].

The cell-permeable peptide D-JNKI1 is able to prevent JNK action on the JBD dependent targets, this results in a potent neuroprotection in both acute and chronic injury of the CNS. To prove that JNK stress kinase plays a key role in Rett Syndrome, we perform a treatment with the cell permeable inhibitor peptide, D-JNKI1, in MeCP2 $^{tm1.1\ Bird}$ mouse model.

The summary of the treatment can be seen in fig.32. The mice were intraperitoneally injected with D-JNKI1 (22 mg/kg) at the 3rd and 6th week of life, and weekly evaluated for well-being parameters (body weight, food and water intake), behavioural tests (rotarod and open field test) and finally sacrificed to perform biochemical and immunohistochemical analysis at 7 weeks.

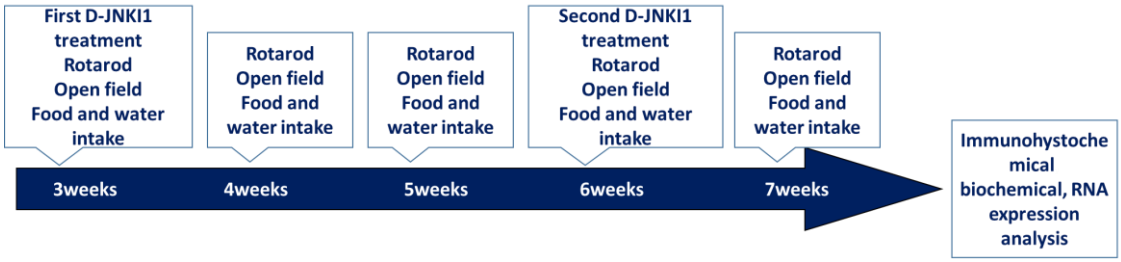

Figure 28-Treatment schedule of D-JNKI1 in MeCP2 mice

According to our previous pharmacokinetic studies[153,193,219] the D-JNKI1 administration was effectuated with intraperitoneal injection[215] (i.p.) every 3 weeks. The peptide is stabile for 3 weeks, this long stability is due to its D-amino acidic configuration, the D-amino acidic are more difficult to degrade by the proteases.

7.6 Effect of D-JNKI1 treatment on well-being of MeCP2 mouse model.

To evaluate the D-JNKI1 effect on this animal model, we analysed the metabolic profile by evaluating the growth curves and the consumption of water and food during the entire experimental phase. As shown in Fig. 29, we found a significant effect between Mecp2 -/y males treated and not with the peptide (ANOVA, § p <0.05), with a recovery of body weight equal to 10% in treated ko compared to ko and equal 8% in treated wild type compared to wild-type, emphasizing the improvement of the health conditions of both animals MeCP2- /y that wild type treated with D-JNKI1. (two-way ANOVA, §§ treatment effect p< 0.01, Fig.30).

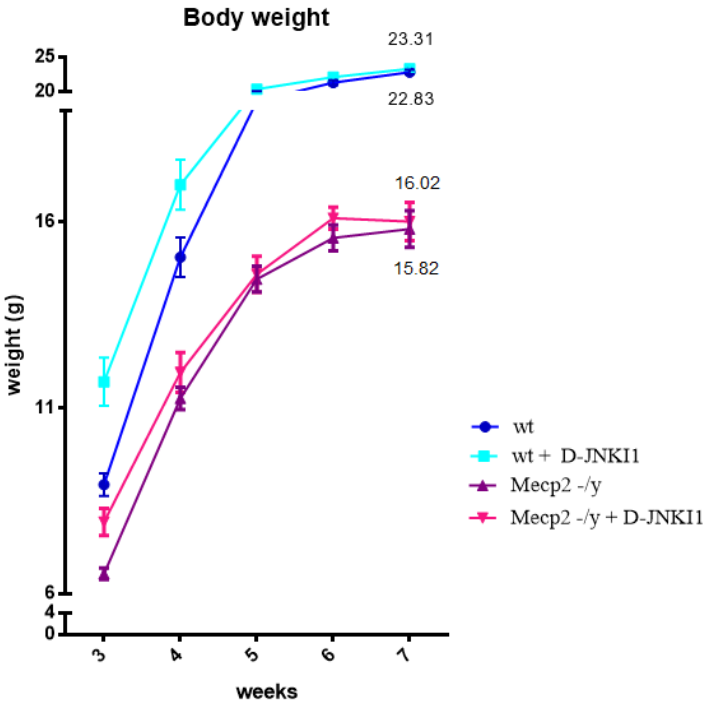

Figure 29 – Summary and overview of the D-JNKI effect on body weight of MeCP2 mice. *D-JNKI1 administration led to a significant increase of body weight in treated wild type compared to wild type and in MeCP2 -/y compared to untreated MeCP2 -/y mice. Statistical analysis: two-way ANOVA, (n=10 for each group), treatment effect comparing treated and not treated Mecp2 § P<0,01; genotype effect #### P<0,0001).*

To understand whether the recovery of body weight due to the treatment with D-JNKI1 could influence the consumption of water and food, we investigated these parameters from the first treatment (at 3 weeks of age) until the end of the experiment (7 weeks of age). As shown in Fig. 30, MeCP2 -/y treated mice tend to consume more food than the untreated (ANOVA, * p <0.05; Fig. 30A), while no differences were found for water consumption (Fig. 30B) between the two groups. The obtained data confirm the absence of toxic effects due to the treatment, because the peptide treatment determinated a recovery of the body weight and the consumption of water and food comparable (ANOVA, p §§§§ < 0.0001)

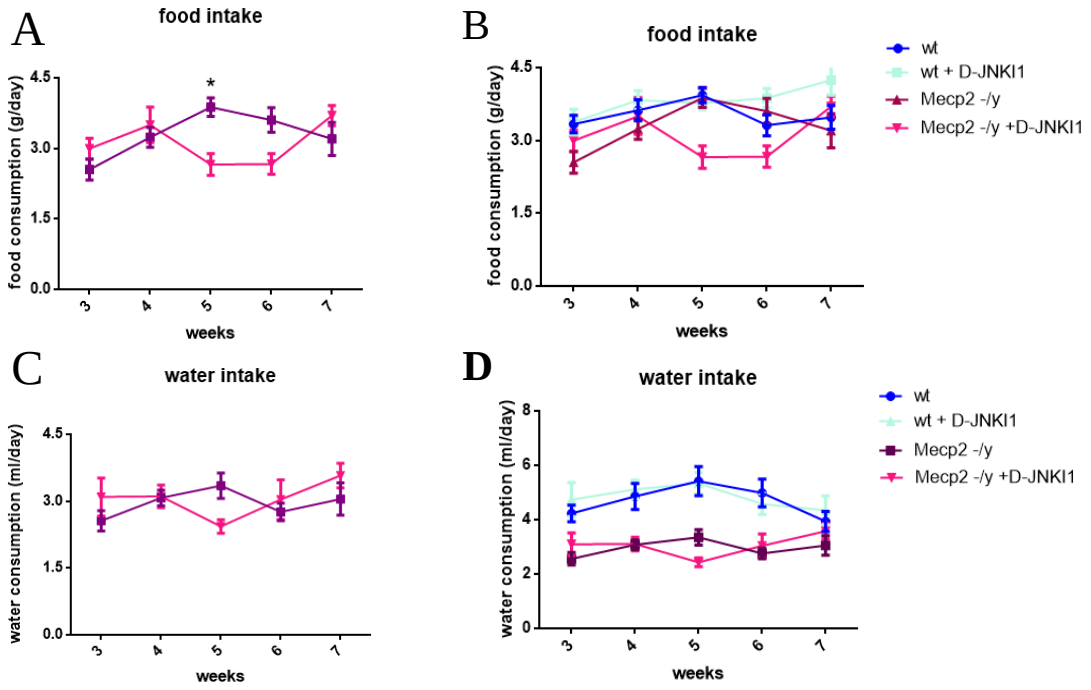

Figure 30- Evaluation of food (g) and water (ml) intake pro die. *In fig. 30A is show the consumption of food for treated MeCP2-/y and untreated ko. We found a similar consumption for both treated and untreated mice (n=5 each group). Statistical analysis effectuated: two-way ANOVA. (B) summary for consumption recorded for every group in our experiment. (C) water consumption shows a general decrement in water consumption by treated and untreated MeCP2 -/y mice, with a general genotype effect. (n=5 each group) Statistical analysis effectuated: two-way ANOVA §§§§ P<0,0001 Data were shown as mean ± SEM*

7.7 Effect of D-JNKI1 treatment on behavioural performance of MeCP2 mouse model

The MeCP2 mouse model is mostly characterized by a motor impairment. The progressive improvement of well-being during the treatment of Mecp2tm1.1Bird mice treated with D-JNKI1 and especially no toxic effect resulting from administration of the peptide, we decided to analyse the effect of D-JNKI1 on behavioural deficits associated with Rett syndrome. We tested treated and untreated knockout and wild type animals with behavioural tests like Rotarod and Open Field Test to evaluate a possible recovery of locomotor deficits, explorative and anxious-like behaviours.

Fig. 31, showed results obtained with the Rotarod tests. Treated Mecp2 -/y mice had a significant and progressive recovery of motor skills in compared to Mecp2 -/y mice. In fact, the ability to move on the rotating bar is significantly increased at 7 weeks (two-way ANOVA treatment effect §§§§ p <0.0001), corresponding to the worse disability in RTT of the knockout mice.

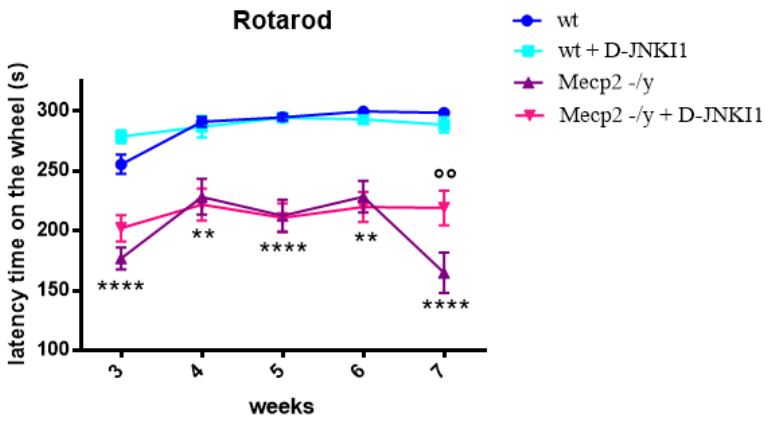

Figure 31 - Evaluation of D-JNKI1 effect on locomotor activity in MeCP2 mice with Rotarod test. *MeCP2 -/y mice were found with a significant motor deficit, that was ameliorated by D-JNKI1 administration: treated Mecp2 -/y performed better than untreated MeCP2 -/y. The increment of latency time on the wheel is appreciable 7 weeks of age (n=10 for each group). Statistical analysis: two-way ANOVA, genotype effect #### p<0.0001. post-hoc test: Bonferroni's multiple comparison, mecp2 -/y vs wt ** p<0.05, **** p<0.0005, Mecp2 -/y vs D-JNKI1 treated Mecp2 -/y °° p<0.05. Data were shown as mean ± SEM.*

To confirm the improvement of locomotor deficits, we decided to test the animals with the Open Field Test, analysing the parameters related to locomotor, exploratory activity and to anxiety-like behaviour.

Regarding the locomotor activity, in Fig. 32A we can see a significant increase in the average distance travelled by treated Mecp2-/y mice compared to that covered by ko untreated animals (two-way ANOVA, §§§§ p <0.0001). We recorded in treated Mecp2-/y mice an increase of speed (Fig. B; two-way ANOVA, §§§ p <0.001) and, in line with the results previously obtained, a decrease in the immobility time (Fig. C; two-way ANOVA, §§§ p <0.001) compared to untreated mice, confirming that the locomotor deficit and progressive worsening of symptoms in animals with RTT is almost completely reverted by the administration of the peptide. In fact, the results obtained show an overall improvement in motor performance of the animal treated. This improvement persists for the duration of the experimental treatment and goes increasing in time.

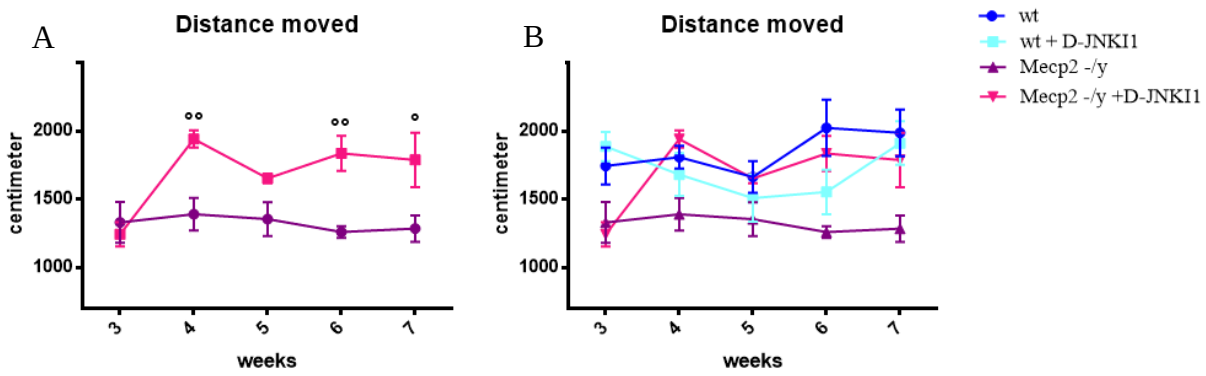

Figure 32 -Evaluation of D-JNKI1 effect on *the distance moved* ***in MeCP2 mice using the Open field test.*** *we observed (**A**) for treated (pink) versus untreated Mecp2 -/y mice (violet), a significant increase in D-JNKI1 treated (n=5 for each group). Statistical analysis: two-way ANOVA treatment effect §§§§ p<0.0001. Post-hoc test: Bonferroni's multiple comparison relative to D-JNKI1 MeCP2 -/y mice vs untreated MeCP2 mice, °° p<0.01. ° p<0.05.* ***(B) Summary*** *of distance moved by all considered groups Data were shown as mean ± SEM.*

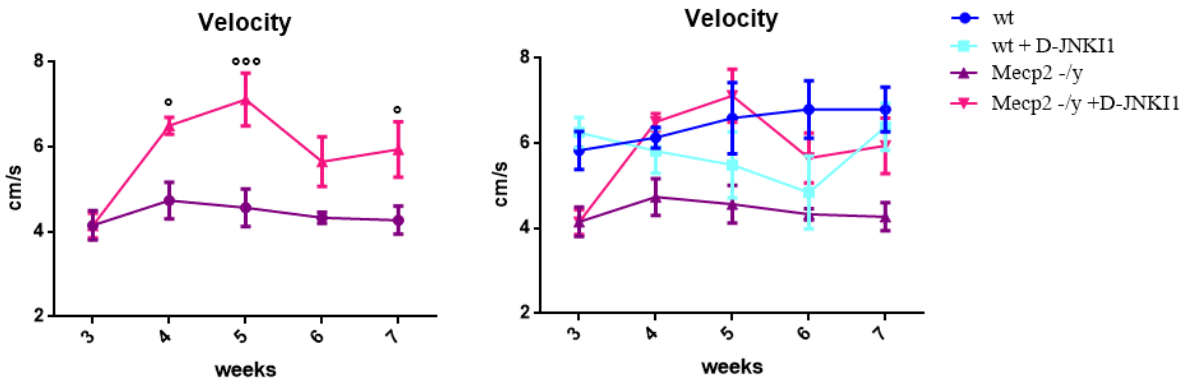

***Figure 33-Evaluation of D-JNKI1 effect on** the velocity **in MeCP2 mice using the Open field test.** We observed **(A)** for treated (pink) versus untreated Mecp2 -/y mice (violet), a significant ncrease in D-JNKI1 treated (n=5 for each group). Statistical analysis: two-way ANOVA treatment effect §§§§ p<0.0001. Post-hoc test: Bonferroni's multiple comparison relative to D-JNKI1 MeCP2 -/y mice vs untreated MeCP2 mice, °°° p<0.001. ° p<0.05. **(B) Summary** of distance moved by all considered groups. Data were shown as mean ± SEM.*

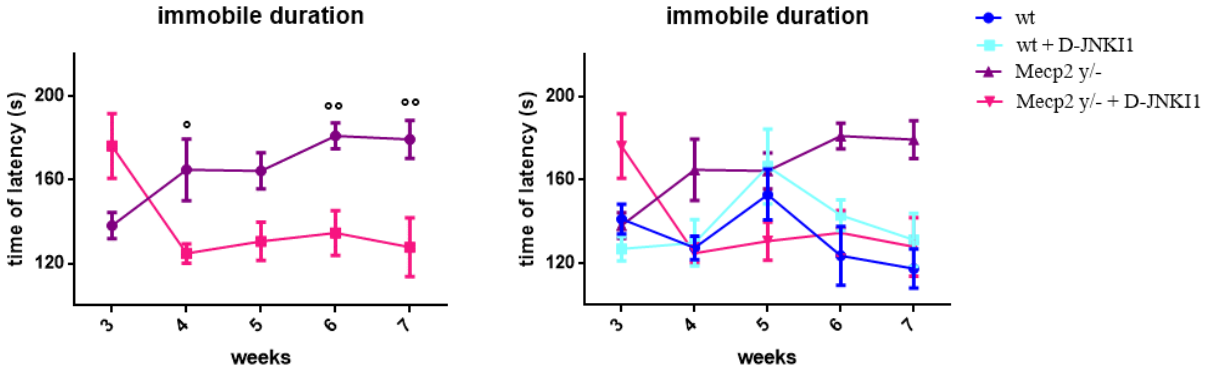

***Figure 34 -Evaluation of D-JNKI1 effect on** the immobile time duration **in MeCP2 mice using the Open field test.** We observed **(A)** for treated (pink) versus untreated Mecp2 -/y mice (violet), a significant increase in D-JNKI1 treated (n=5 for each group). Statistical analysis: two-way ANOVA treatment effect §§§§ p<0.0001. Post-hoc test: Bonferroni's multiple comparison relative to D-JNKI1 MeCP2 -/y mice vs untreated MeCP2 mice, °°° p<0.001. ° p<0.05. **(B) Summary** of distance moved by all considered groups. Data were shown as mean ± SEM.*

In the evaluation of the exploratory performance, we considered the time spent in the external and in the internal zone, and the frequency with whom mice crossed the arena. D-JNKI1 treated compared to untreated MeCP2 -/y mice showed a significant reduction in exploration activities, with an increment in the frequency of crossing from the internal to external zone (Fig. 35C-D). meanwhile they spent less time in internal zone and showed a reduction in the opposite crossing (Fig. 34A-B) in D (ANOVA, p< 0.05).

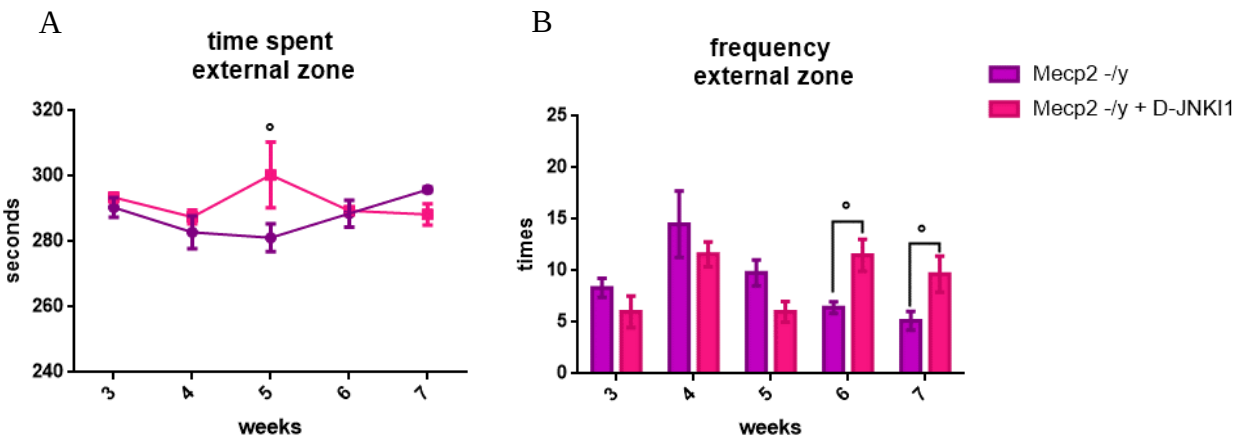

Figure 35-Evaluation of D-JNKI1 effect on exploratory activity in MeCP2 mice using Open field test. *Evaluating the time spent in external zone (**A-B**) in D-JNKI1 treated and untreated MeCP2 -/y mice, we found any significant difference between experimental groups in the time windows analysed (n=4 for each group). Whereas, the frequency of crossing toward the external zone is affected by a significant difference due to the genotype effect (**C-D**). The statistical analysis: two-way ANOVA § p<0.05. Data were shown as mean ± SEM*

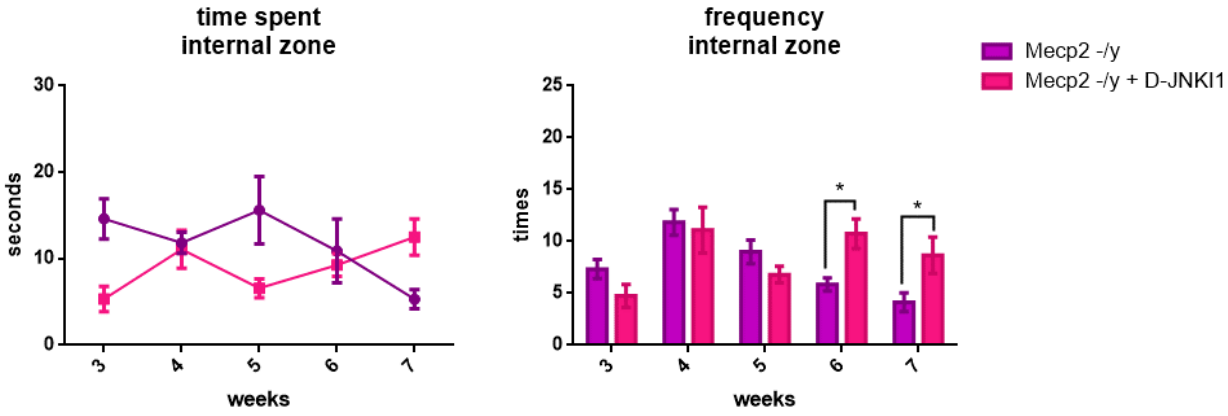

Figure 36-Evaluation of D-JNKI1 effect on exploratory activity in MeCP2 mice using Open field test. *Analysing the D-JNKI1 effect on frequency of entering in internal zone (**A-B**), we observed a significant increase of frequency in D-JNKI1 treated vs untreated MeCP2 -/y mice. Valuating the time spent in internal zone (**C-D**) in D-JNKI1 treated and untreated MeCP2 -/y mice, we found any significant difference between experimental groups in the time windows analysed (n=5 for each group). Significant relative to wt mice * p<0.05, D-JNKI1 MeCP2 mice vs untreated MeCP2 mice § p<0.05. Data were shown as mean ± SEM.*

Concerning the D-JNKI1 effect on anxiety-like behaviour we recorded rearing and grooming parameters for MeCP2 -/y mice and D-JNKI1 treated MeCP2 -/y. We observe a significant increase in the time spent for rearing (two-way ANOVA, §§ p <0.01, Fig. 36A) and a significant increase in the frequency at the 4th week in the treated Mecp2 -/y compared to the untreated (Sidak's multiple comparison * p <0.05). We also observed in

treated animals a reduction of grooming time (p = 0.06 Fig. C) and frequency (ANOVA, §§ p <0.01; fig. BD).

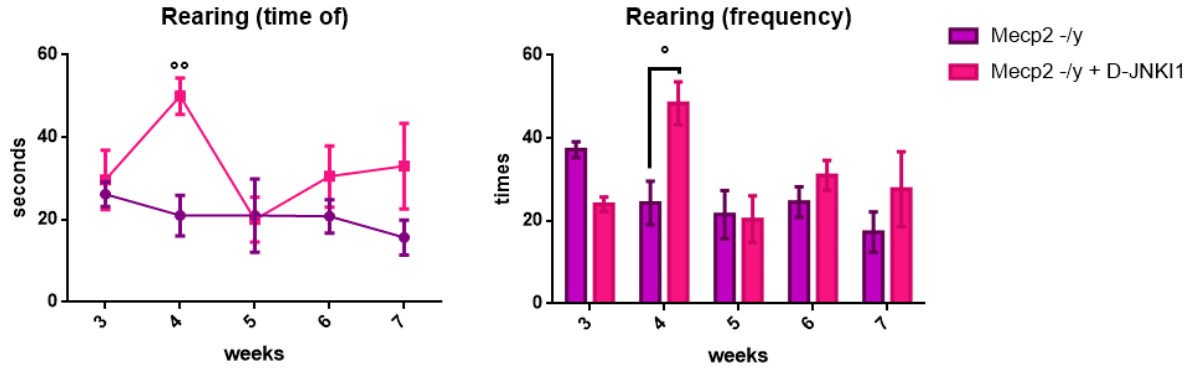

Figure 37 -Evaluation of D-JNKI1 effect on anxiety-like behaviour in MeCP2 mice using Open field test. *D-JNKI1 effect on time spent for and on frequency of rearing. (**A**), We observed a significant increase of time spent in D-JNKI1 treated vs untreated MeCP2 -/y mice (Statistical analysis:two-way ANOVA genotype effect §§ p<0.01; post-hoc test: Sidak's multiple comparison °°p<0.01). Valuating the frequency of rearing (**C-D**) in D-JNKI1 treated and untreated MeCP2 -/y mice, we found a significant difference at 4th week between experimental groups(n=4 for each group). Significant relative toMeCP2 -/y mice (post-hoc test: Sidak's multiple comparison °°p<0.01). Data were shown as mean ± SEM.*

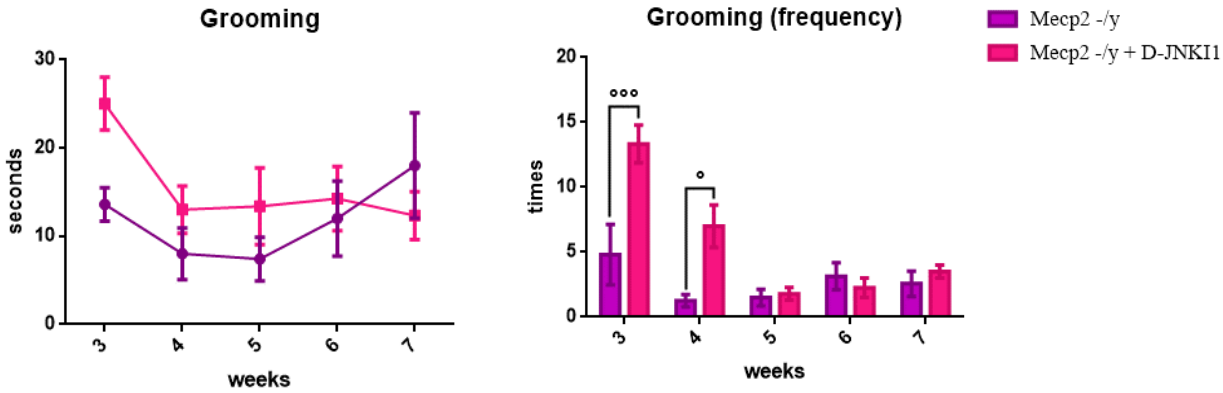

Figure 38 -Evaluation of D-JNKI1 effect on anxiety-like behaviour in MeCP2 mice using Open field test. *Analysing the D-JNKI1 effect on time spent for grooming (**A**), we found any significant difference between experimental groups. Valuating the frequency of grooming (**B**) in D-JNKI1 treated and untreated MeCP2 -/y mice, we observed a significant increase of time spent in treated MeCP2 -/y mice. in the time windows analysed (Statistical analysis: two-way ANOVA genotype effect §§ p<0.01; post-hoc test: Sidak's multiple comparison °p<0.05, °°° p<0.001, n=4 for each group). Data are shown as mean ± SEM.*

7.8 Biochemical evaluation of D-JNKI1 treatment on MeCP2 mice

The D-JNKI1 treatment determined an improved metabolic and behavioural profile in MeCP2 -/y mice, we here look for a correlation between the peptide effect on JNK

signalling and synaptic plasticity focusing on the cerebellum, the area most involved in locomotor ability and in synaptic plasticity.

The D-JNKI1 effect has been investigated with western blot analysing and TIF fractionation.

7.9 JNK *signalling and activation.*

As shown before, JNK is activated in post-synaptic density and may have a role in neurodevelopmental disorders as a key player in synaptic dysfunction. We checked the D-JNKI1 effect on JNK protein of dendritic spine. Biochemical analysis of the cerebellar post-synaptic area highlighted a decrement of JNK phosphorylation in treated MeCP2 -/y compared to MeCP2 -/y. Then we evaluated P-c-Jun/c-Jun ratio (fig. 26), the major target of JNK that was significantly increased in cerebellum of MeCP2 -/y compared to wt mice (t-test, $p< 0.01$), indicating a powerful activation of JNK signalling we checked if D-JNKI1 treatment prevent JNK action as expected. The D-JNKI1 treatment inhibits c-Jun phosphorylation in treated MeCP2 -/y compared to untreated MeCP2 -/y mice (two-way ANOVA, cerebellum: $p< 0.01$; fig. 39), the peptide reduces the P-c-Jun/c-Jun ration, bringing levels to the control conditions, comparable with wild-type. The JNK signalling pathway is powerfully activated in cerebellum and was rescued by D-JNKI1 peptide treatment.

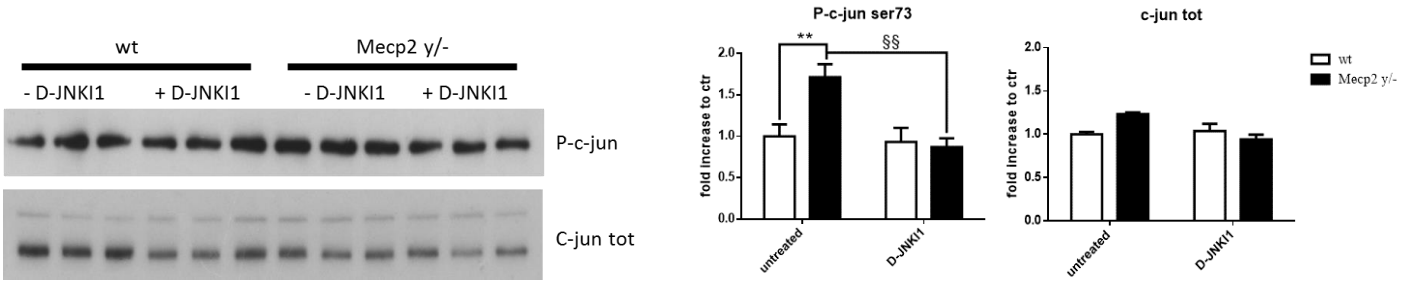

Figure 39 -Analysis of D-JNKI1 effect on JNK pathway in MeCP2 mice A-B) *The densitometry analysis of western blot of whole extract from cerebellum.* ***(A)*** *P-c-Jun/c-Jun ratio revealed a significant decrease of c-Jun phosphorylation in D-JNKI1 treated MeCP2 -/y compared to untreated (n=5 for each group). Statistical analysis: two-way ANOVA. Post-hoc test: Bonferroni's multiple comparison, genotype effect* ***p< 0.01, treatment effect §§ p< 0.01. Data were shown as mean ± SEM.*

To deeper investigate the JNK signalling we investigated also the protein directly involved in upstream JNK activation: the MAP kinase kinase MKK4 and MKK7. The MKK7 activation was not increased in MeCP2 -/y versus wild type mice. While MKK4 activation was strong higher, the p-MKK4/MKK4 ratio was significantly increased in MeCP2 -/y compared to wt. Importantly this activation was prevented by the D-JNKI1 treatment, as expected [194], see fig 37. JNK activation is exclusively mediated by MKK4 and not by MKK7 in treated MeCP2 -/y (Fig. 40 A-B). The D-JNKI1 treatment significant decrease levels of P-MKK4 in treated MeCP2 -/y compared to untreated MeCP2 -/y mice (ANOVA, cerebellum: $p < 0.001$, fig. 38C) as expected by the treatment[194].

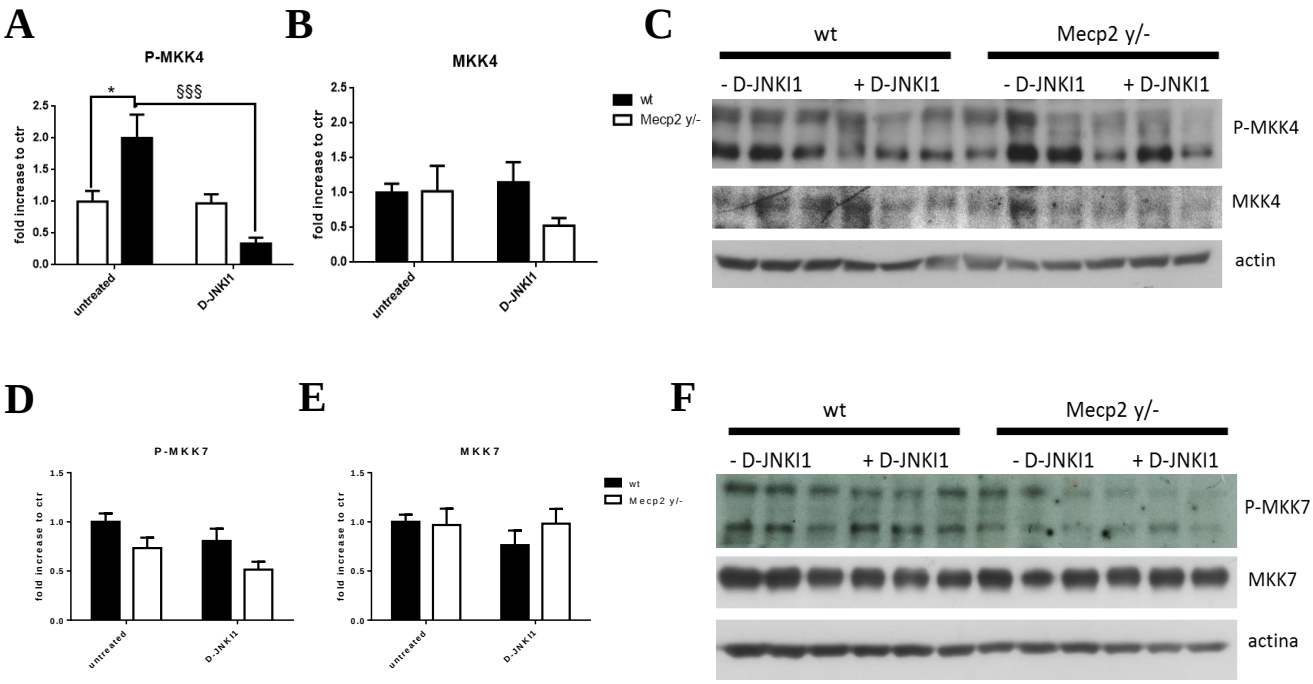

Figure 40 -Analysis of MKK4 and MKK7 signalling and D-JNKKI1 effect in MeCP2 mice. A-B) *Western blot and relative quantification performed on the total homogenate of male MeCP2 ko and wt mice D-JNKI1 treated vs untreated. MeCP2 -/y mice showed a significant increase of P-MKK4/MKK4 ratio (A) if compared with age-matched wt mice. D-JNKI1 treatment induced a significant reduction of P-MKK4/MKK4 ratio, while MKK4 total levels are similar between groups (**B**) (n=5 for each group). Evaluating the ratio of P-MKK7/MKK7, (D), levels of P-MKK4 (E) and MKK7 (F), we didn't find any significant D-JNKI1 effect. Significant relative to wt mice *p< 0.05.D-JNKI1 MeCP2 mice vs untreated MeCP2 mice §§§ p< 0.001. Data were shown as mean ± SEM*

7.10 JNK's role at dendritic spine.

MeCP2 -/y mice showed a great activation of JNK in the postsynaptic region (As shown in fig. 25), we verified the effect of D-JNKI1 treatment at this cellular level. To investigate the effect of JNK inhibition in excitatory synapses of MeCP2 mice we analysed the biochemical marker of the PSD region.

In MeCP2 -/y mice spine presented a decrement of PSD-95 and Shank3 together with an increment of AMPA and NMDA receptors.

The D-JNKI1 treatment bring the NMDA receptors of treated MeCP2 -/y to a normal level of wild-type (two-way ANOVA, cerebellum: $p < 0.0001$; fig. 41A-B), while for AMPA receptor subunits levels (GluR1 and GluR2) are not significantly changed by the treatment (fig. 41C-D).

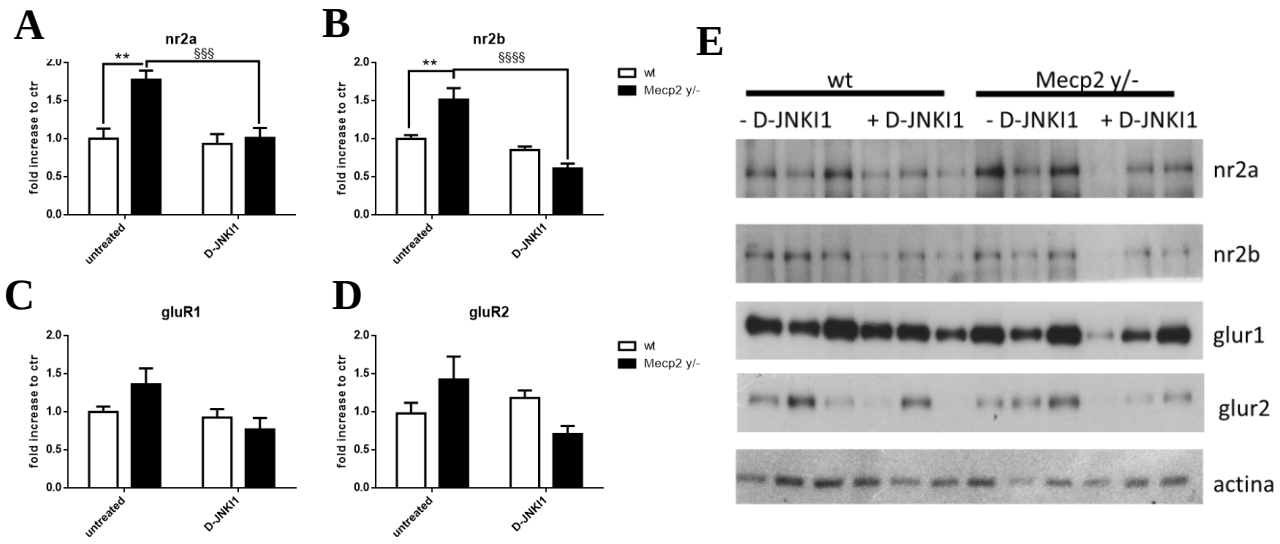

Figure 41-Analysis of JNK signalling and D-JNKI1 effect in MeCP2 mice. A-B) *Western blot and relative quantification of the TIF fraction of male MeCP2 ko and wt mice. The male MeCP2 -/y mice showed a significant increase of NR2A and NR2B subunits of NMDAr if compared with age-matched wt mice. The D-JNKI1 treated mice showed a significant reduction of NR2A and NR2B subunits of NMDAr to control level of wt mice (n=4 for each group). Statistical analysis: two-way ANOVA, post-hoc test: bonferroni's multiple comparison, significant relative to wt mice ** p>0.001, D-JNKI1 ko treated vs no treated §§§ p>0.001 §§§§ P<0,0001. Data were shown as mean ± SEM*

We then study the PSD-95 scaffold protein and its phosphorylation, PSD-95 is an important scaffold protein of the PSD region and its alteration is a symptom a dysfunction of the post-synaptic element. We found an increment of phosphorylated form of PSD95

in MeCP2 -/y mice, this may indicate a destabilization of mature to immature dendritic spines, that was reduced to a level comparable with wt by D-JNKI1 treatment. Instead the PSD95 total level decrease in MeCP2 -/y mice, the D-JNKI1 treatment seems to increase its level to control mice.

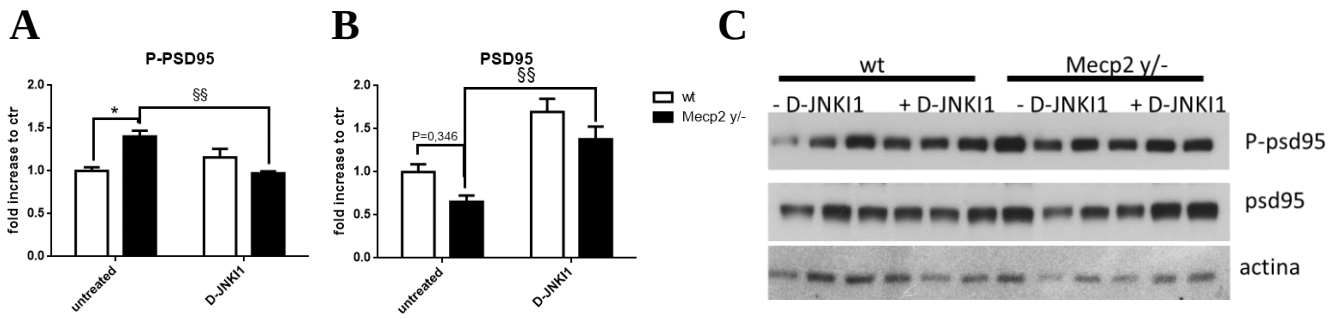

*Figure 42 -Analysis of D-JNKI1 effect on PSD95 scaffold protein in MeCP2 a significant increase of P-PSD-95 is visible in MeCP2 -/y compared to wt mice, D-JNKI1 decrease the P-PSD95 level (A, C). While MeCP2-/y mice present a decrease level of total PSD-95 compare to wt mice (B, C). The D-JNKI1 stabilizes PSD-95 level to wt mice. A significant increase of PSD-95 (**B**) in D-JNKI1 treated MECP2 compared to not treated MeCP2 -/y mice (n=4 for each group). Statistical analysis: two-way ANOVA, post-hoc test: Bonferroni's multiple comparison wt mice *p< 0.05 D-JNKI1 MeCP2 mice vs untreated MeCP2 mice §§ p< 0.01, *** p< 0.001. Data were shown as mean ± SEM.*

The second important scaffold protein for the organization of excitatory postsynaptic densities was Shank3. Levels of Shank3 protein was drastically reduced in MeCP2 -/y compare to wt mice (fig 43 A-B). Interestingly the D-JNKI1 treatment could rescue Shank3 level and reported it to control condition of wt mice. We detected also RNA expression (fig.46 C).

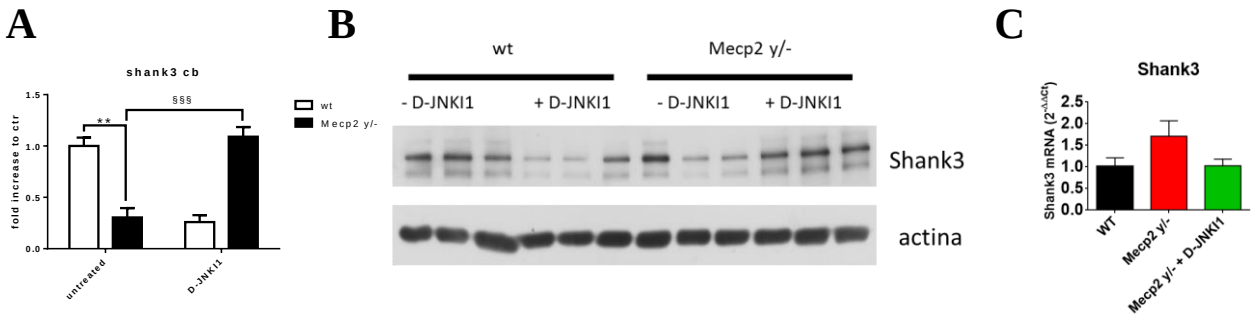

*Figure 43-Analysis of D-JNKI1 effect on SHANK3 scaffold protein in MeCP2. As seen before, a significant decrease of SHANK3 is visible in MeCP2 -/y compared to wt mice. D-JNKI1, we found a significant increase of shank3 (A, **B**) in D-JNKI1 treated MECP2 compared to untreated MeCP2 -/y mice*

*(n=4 for each group). Significant relative to wt mice **p< 0.01 D-JNKI1 MeCP2 mice vs untreated MeCP2 mice §§§ p< 0. 001. Data were shown as mean ± SEM.*

The expression analysis of Shank3 (fig. 41C) performed by real time PCR, showed a tendence to increase in MeCP2 ko. D-JNKI1 treatment restore the situation taking ko levels to the wt.

7.11 *D-JNKI1 in MeCP2 mouse model: immunohistochemical analysis*

The MeCP2 -/y mice exhibited a state of inflammation, hyperactivated microglia we here investigated if the D-JNKI1 treatment is able to prevent the inflammation state in the brain parenchyma of this RTT mouse model.

The D-JNKI1 treated mice showed a reduction of inflammation state (GFAP positive staining, panel A-B) as well as a reduction of microglia hyperactivation (CD11β positive staining, panel C-D), inducting a powerful effect on inflammation.

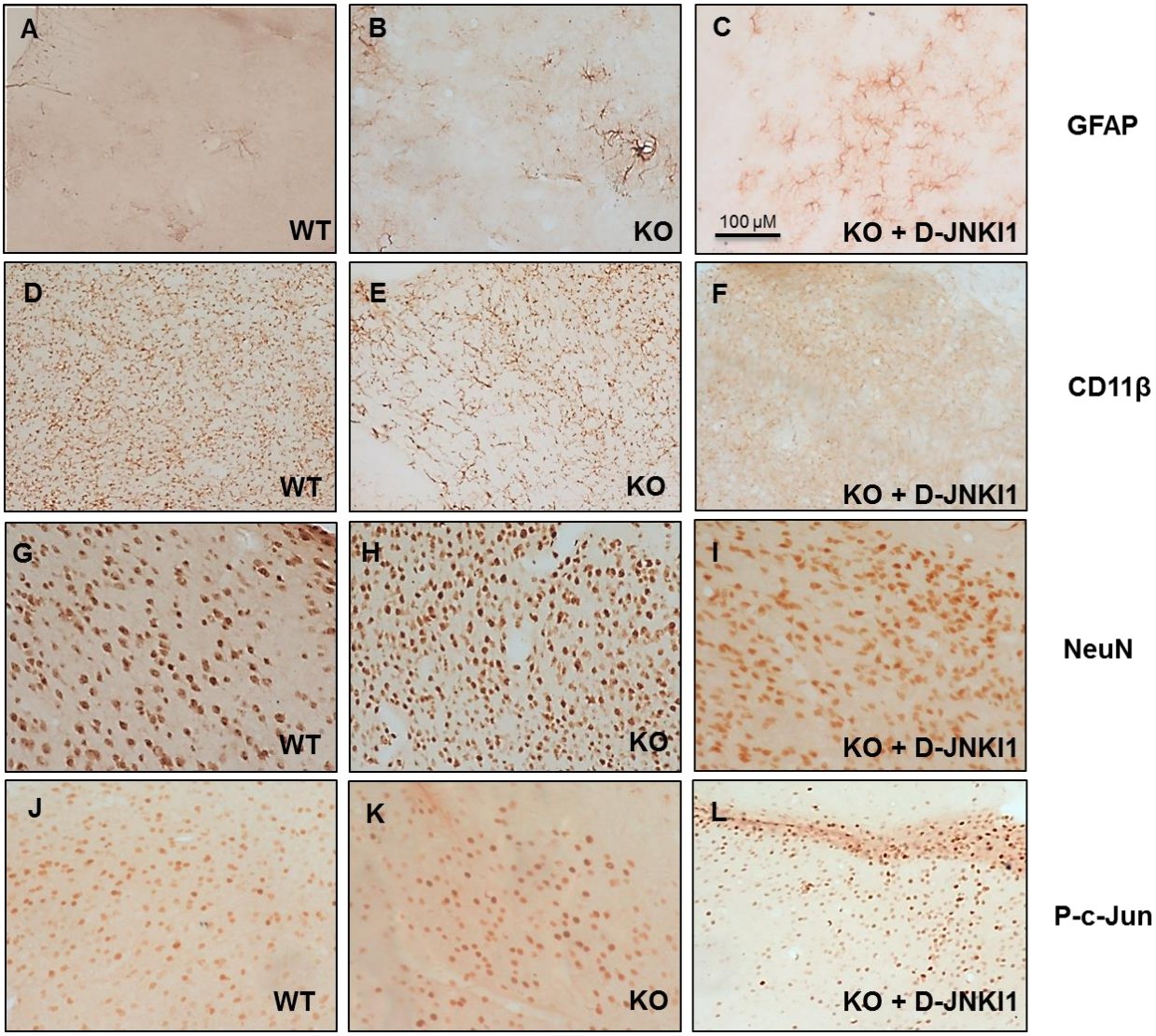

Figure 44 - Immunoistochemical analysis of D-JNKI1 effect in cerebellum of wild type, MeCP2 -/y and treated MeCP2 -/y mice. A-B-C) *GFAP staining revealed an advanced state of inflammation in D-JNKI treated ko compared to wt mice.* ***D-E-F)*** *CD11β staining revealed a microglial de-activation in ko compared to wt mice, resolved by D-JNKI1 treatment.* ***G-H-I)*** *NeuN staining revealed a similar situation for the three-considered group, with no reduction of neuronal population.* ***L-M-N)*** *P-c-Jun staining revealed an increase of c-Jun phosphorylation in ko compared to wt mice. Representative sections are shown of 4 animals used per each group. Scale bar: 100 µm.*

We also analysed the effect of D-JNKI1 on survival of the neuronal population in treated versus and the untreated mice: the inhibition of JNK prevents death and promote survival, in fact we showed an increasing in neuronal population (Neun positive staining, panel E-F) and this is directly correlated the decrease of P- c-Jun staining treated mice compared

to untreated (P-C-Jun positive staining, panel G-H), confirming the D-JNKI1 is inhibiting JNK action on its elective target, c-Jun.

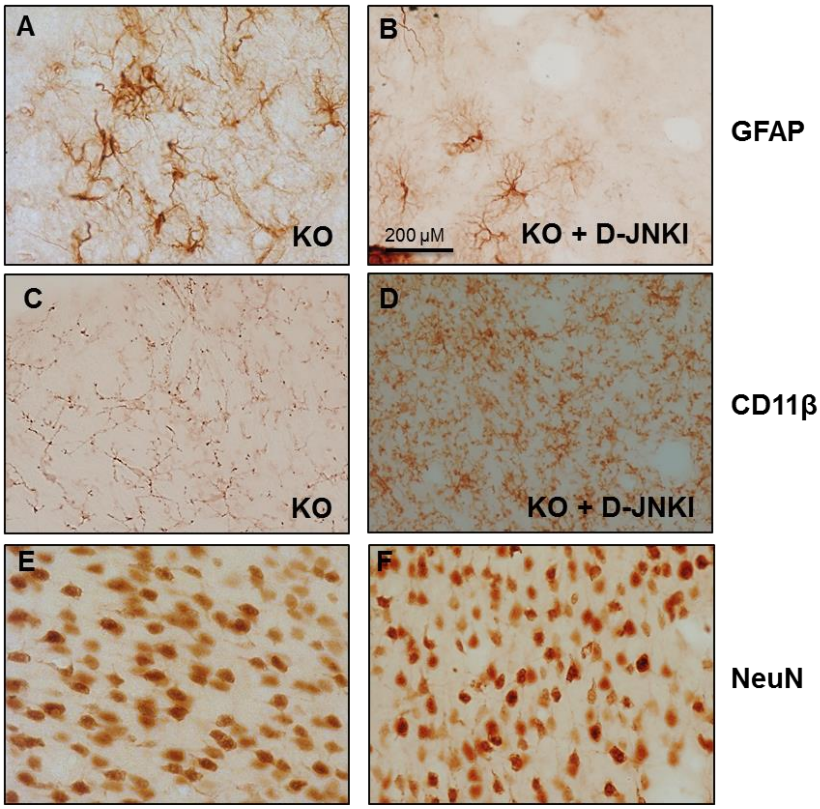

Figure 45- Magnification (40X) of immunohistochemical analysis of D-JNKI1 effect in cerebellum of MeCP2 -/ymice. A-B) *GFAP staining revealed a recovery of inflammation state in D-JNKI1treated mecp2 compared to mecp2 untreated mice .**C-D)** CD11β staining revealed a reduction of microglia activation in D-JNKI1 treated MeCP2 -/y compared to MeCP2 -/y untreated mice. **E-F)** NeuN staining revealed the same neuronal population in D-JNKI1 treated mecp2 compared to mecp2 untreated mice.*

7.12 Biochemical evaluation of D-JNKI1 effect on inflammation in MeCP2 mouse model.

Activation of c-Jun led to the transcription of molecules involved in inflammatory response and in neuronal toxicity. Many studies reported an accumulation of glutamate in synaptic region of RTT mouse model, that can overstimulate neurons to an inflammatory response. We investigated inflammatory state of these mice by analysing

astrocytes and microglia reactivity, studying GFAP (astroglial marker) and IBA-1 (microglial marker).

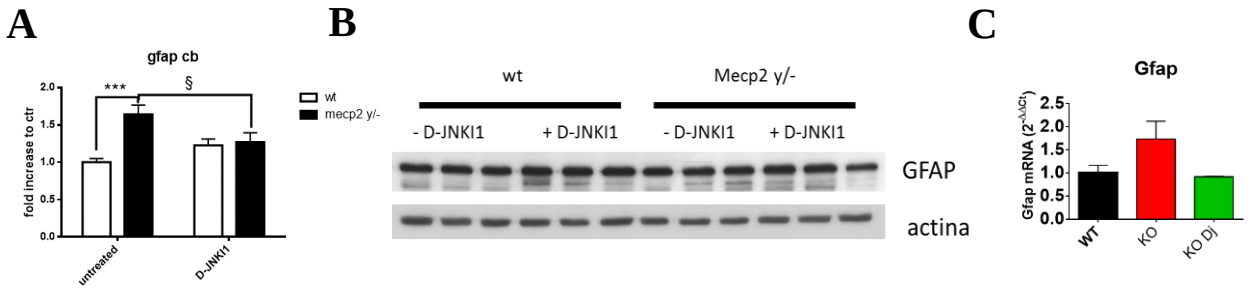

Figure 46-Analysis of D-JNKI1 effect on GFAP in MeCP2 mice. (A) densitometry of GFAP in MeCP2 mice. *We see a significant increment of the GFAP protein level in MeCP2 -/y compared to wt mice. D-JNKI1 treatment led GFAP level of MeCP2 -/y comparable to a wt condition (n=4 for each group) (C) real time of GFAP expression is in line with western blot results treated MECP2 increased GFAP expression and compared to wt and D-JNKI1 treatment of MeCP2 -/y mice powerfully reduce its level. (n=3 for each group). Statistical analisys: two-way ANOVA Significant relative to wt mice ***p< 0.001 D-JNKI1 MeCP2 mice vs untreated MeCP2 mice § p< 0.05. Data were shown as mean ± SEM.*

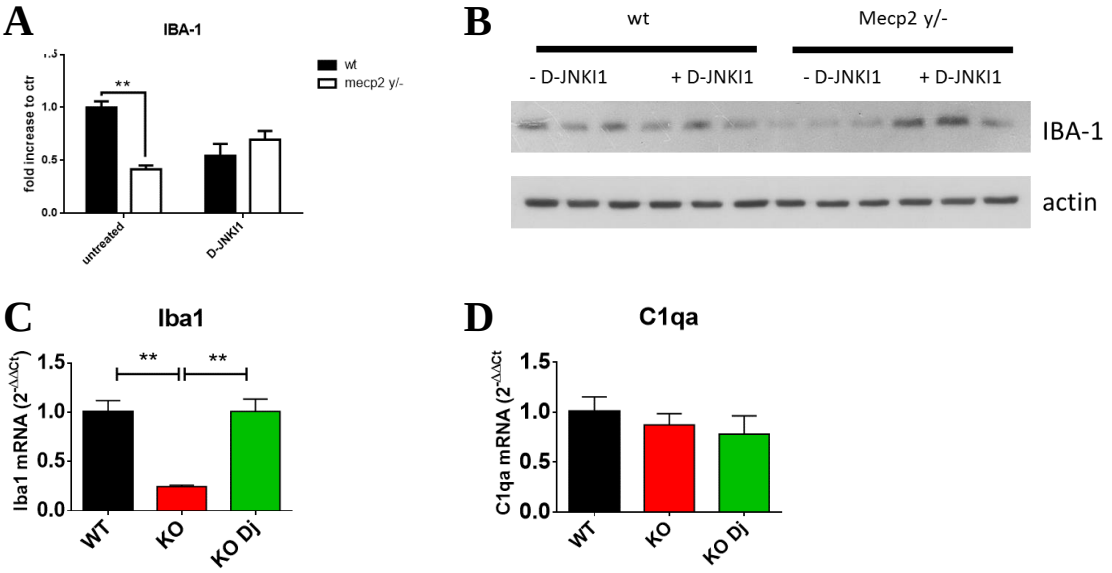

Figure 47 -Analysis of D-JNKI1 effect on microglyosis in MeCP2 mice. We see *a significant increment of the protein level in MeCP2 -/y compared to wt mice (A, B). D-JNKI1 Treatment led MeCP2 -/y to a wt condition (n=4 for each group) (C) real time of IBA-1 expression is in line with western blot results treated MECP2 compared to not treated MeCP2 -/y mice (n=3 for each group). (D) RNA expression of C1qa, a marker of whole microglia, activated or not. We didn't see differences in every analysed group, that correspond to the same cell number in every brain. Statistical analysis: two-way ANOVA Significant relative to wt mice ***p< 0.001 D-JNKI1 MeCP2 -/y mice vs untreated MeCP2 mice § p< 0.05. Data were shown as mean ± SEM.*

To highlight the microglia reactivity in MeCP2 -/y mice, we first analysed the most important microglial markers, IBA-1 with western blot and real time PCR. MeCP2 -/y mice had a significant decrement of IBA-1 protein level as well as expression level compared with wt mice. The D-JNKI1 treatment partially prevented the IBA-1 decrease while completely inhibited the expression level drop.

To be sure that IBA-1 level does not depend from the cell number, we evaluated the expression of C1qA gene, but we found an equal expression in wt, treated and untreated MeCP2 -/y; we thus are more confident that suggest that the changes of microglia are correlated with this pathological state.

7.13 JNK pathway in a translational model: IPSCS from RETT HUMAN girl deriving from fibroblasts.

In collaboration with the Prof. Renieri's laboratory (University of Siena), we analysed the JNK signalling in the IPSCs cell, that are induced pluripotent stem cells, derived from human fibroblast of Rett patience. After differentiation in pyramidal neurons (fig 49B), cells were treated with the D-JNKI1, and then were used for biochemical analysis. As shown in fig.49 C-D, the Rett allele of clone R301C of the patience that expressed the mutated MeCP2 presented an increased P-C-Jun/c-Jun ratio compared to the allele without mutation, expressing the normal MeCP2 of the same R301C of the patience that is expressing the normal gene. Importantly to our aim, the D-JNKI1 treatment strongly decrease c-Jun phosphorylation, indicated as a ratio (P-C-Jun/c-Jun). This experiments are still in progress. Moreover, we performed an LDH assay to evaluate cell well-being after treatment and we found a significant increment of LDH levels in mutated cells and a rescue in treated mutated cells.

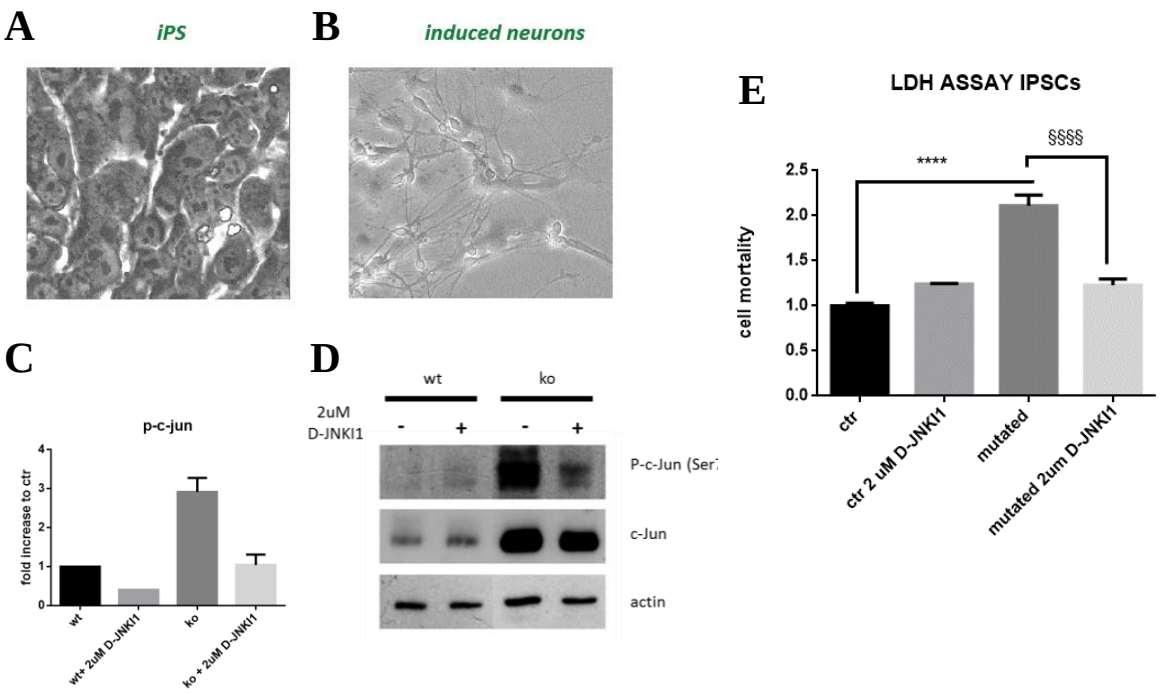

Figure 48-Analysis of D-JNKI1 effect on JNK pathway in MeCP2 mice. (A) *imaging of IPS cells take before the differentiation and induced neuron. Morphology is too different between these two kinds of cells (B-C) western blot analysis of cells confirmed what we saw in animals: we found an activation of c-Jun and in the same time comparing wt with ko, and a rescue with D-JNKI1 treatment comparing ko with treated ko. (n=1 for wt and treated wt; n=2 for ko and treated ko. Statistical analysis no possible. Data were shown as mean ± SEM.*

6. Discussion

Rett syndrome (RTT) is a severe neurological disease X-linked, with an incidence of 1:10000 children almost exclusively female. The syndrome is included in ASD, autistic spectre disorders. In more than 90% of the cases, Rett syndrome is caused by mutations of MECP2 gene, encoding the methyl-CpG binding protein 2. The clinical course of the Rett syndrome and the severity are different among girls affected by this disorder, ranging from a mild to a severe phenotype, because of random X-inactivation[54]. RTT onset is characterized by a normal development, followed by the appearance of cognitive impairment, autism-like bahaviour and the progressive loss of acquired skills, such as verbal communication, using purposive of the hands and ambulation. This phenotypic variability was reproduced in many different mouse models. In 2011, a workshop was organized to evaluate the variability in the genetic of MeCP2 mutant mice, the methodologies used by the laboratories to produce and to analyse data and to define the physiological and behavioural phenotypes of the different mouse models which were considered more or less closer to the clinical observations in Rett human individuals. The aim of the workshop was to define the aspects in different mouse models which were important for preclinical studies of the Rett syndrome. The participants observed that in particular,MeCP2 Bird and Jaenish (deficient mice), showed a marked reduction in brain size with alterations in neuronal morphology and a quite reproducible variation in respiratory and cardiac activities. Thus, in this project, we decided to use MeCP2 tm 1.1 Bird mice, the mouse model that presents the most significant alterations in brain weight, volumes of cortex and cerebellum than those observed, for example, in the Jaenisch strain[120,220]. In addition, these alterations in cortical morphology in MeCP2 mice are highly reproducible and closely resemble those observed in patients thus, they are considered strong evidence of face validity of these Rett mouse models[221].

MeCP2 is found in a wide variety of tissues, but is most abundant in the brain. A quantitative survey normalized against cytoplasmic proteins suggested that lung and spleen are also MeCP2-riched tissues[59]. Direct quantification in adult mouse brain has estimated 16 million molecules of MeCP2 per nucleus in neurons with almost an order of magnitude less in glial cells and 30-fold less in liver cells[222]. The neuronal MeCP2 level is relatively low at birth but, in the mouse, increases greatly during the first 3 weeks of life before reaching a plateau[115,222]. Because neurogenesis is largely complete before birth, the increase is due to the upregulation of MeCP2 expression within a constant number of neurons. These neurons are, however, developmentally active, undergoing synaptogenesis at this time.

In addition, MeCP2 has a role in post-mitotic neurons, where is involved in the maintenance processes. A Rett brain, in fact, is characterized by neurons with smaller dimensions and a high degree of packing without neuronal death, despite this, neurons show dysfunctionality. MeCP2 deficiency affects the brain and the mechanism of this alteration are poorly understood and are the subject of intense research. Progresses are being made on all these fronts[4,223–225], but as things stand, a definitive molecular pathology of RTT remains elusive.

In this project, we studied MeCP2 tm 1.1 bird male mice valuating general wellbeing conditions, biochemical alterations of spine, neuronal morphology, locomotor and exploratory functions; in this context, we analysed also the JNK's role in Rett syndrome because previous studies of our laboratory showed its involvement in disease characterized by synaptopathology.

Since today still there are no treatments to cure or slow RTT, we also evaluated the effects of JNK's inhibition with a well-characterized cell-permeable peptide, the JNK inhibitor peptide (D-JNKI1) and we found that this treatment significantly improved the general

health and rescued behavioural impairments as well as synaptic dysfunctions in this mouse model. The male mouse model, chosen for our evaluations, are hemizygous for MeCP2 and manifest the pathological symptoms already at 3 weeks of age and progressively until their deaths (9 -10 weeks). Whereas female mice (MeCP2 +/-) are heterozygous for the deletion and similarly to humans, have an X-random inactivation. This random inactivation mirrors the mosaicism and the great variability of symptoms; furthermore, they have a delayed onset and don't show a progressive pathology.

Despite the difficulties to amplify and to breed colony, we started our studies on male hemizygous mice (MeCP2 -/y) because of their homogenous phenotype and for the possibility to treat them for a shorter period of time in addition the proof of concept of the neuroprotective D-JNKI1 effect in a more severe phenotype is an add value to for the potential therapeutic approach. In fact, we think that if D-JNKI1 show to prevent or to slow down the most severe RTT phenotype of MeCP2 -/y mice, it will be powerful in a less severe phenotype (female MeCP2 +/-) and even more protective.

The intracellular pathways related to Rett-pathological mechanisms are largely unknown; we here investigated the c-Jun N-terminal protein kinase (JNK) pathway in this RTT mouse model. We showed that JNK plays an important role in MeCP2 -/y Bird model. These results represent *the proof-of-principle of JNK activation* in RTT. Importantly, RTT is a pathology involving neuronal dysfunctionality and JNK is strongly implicated in both synaptic injury as well as plasticity in the CNS. Furthermore, JNK is a pivotal player in mediating many different brain-stress signal pathways, in fact is implicated in apoptosis, oxidative stress, neuronal degeneration and inflammation, all conditions related to RTT. Our results proved the significant increment of the ratio of P-c-Jun/c-Jun in MeCP2 Bird mouse model in more affected brain areas as cerebellum, hippocampus and cerebral cortex (results not shown for hippocampus and cortex). Importantly, JNK

protein kinase is not just a well-known key player in response to acute and chronic stress in the CNS and is strongly involved in plasticity/synaptopathy in neurodegenerative diseases[126,226,216].

The over-phosphorylation of c-Jun underlines a strong activation of the JNK signalling pathway in the nucleus, which led to transcription of proteins involved in many different processes like for instance synaptopathology, axonal grow and dendrite branching, inflammation as well as neuronal death. Moreover, immunohistochemical studies effectuated on brain of MeCP2-/y mice by other groups, demonstrated that pyramidal neurons exhibit a reduction of the soma area, the diameter of the proximal dendrite on the first branch and the diameter of the distal dendrite at 100 μm from the soma. Sholl' analysis revealed also a reduction in the apical dendritic arborization in MeCP2-/y mice[115,116].

Anatomically, MeCP2 deficiency causes reduced brain size. This may be due to size decreases in major brain regions such as the frontal and temporal lobes, caudate nucleus, thalamus, midbrain, and cerebellum, all of which have been documented in RTT patients[121,227–229]. At cellular level, the neuronal soma is smaller in the absence of MeCP2, and cells are more densely packed[57,109,230]. More specific abnormalities have been observed at the synapses: post-mortem brain samples from RTT patients and MeCP2-deficient mice present postsynaptic morphological defects such as reduced dendritic spine density and alterations in spine morphology[57,104–106,115,116,120,229,231]. At pre-synaptic sites, the lack of MeCP2 is associated with an abnormal number of axons[120] and a defect in axonal targeting[120,232,233]. These results imply a decrease in the number of synapses in RTT brains, which has been confirmed for glutamatergic synapses in primary neuronal cultures[27]. Overall, the structural defects described at the synapse may suggest that the loss of MeCP2 triggers alterations in the functioning of the synapses and, consequently,

of the neuronal networks. However, morphological analyses have focused on neurons and specific cerebral regions, namely the hippocampus and various cortical regions. Therefore, even though it is tempting to assume that the morphological defects described are the same throughout the entire brain, all major brain regions have not been studied systematically. Analysis of neurotransmission associated with loss of MeCP2 provides further evidence for synapse dysfunction. Post-mortem analysis in RTT brains showed altered levels of neurotransmitters such as glutamate and biogenic amines as well as changes in the abundance of some neurotransmitter receptors. Several studies contradict these results, however[229,234]. These discrepancies may be due to technical issues associated with human post-mortem brain analysis. In mice, reduced levels of serotonin (5-hydroxytryptamine), adrenaline, and dopamine have been found in the *Mecp2*-null brain[235–238]. These are associated with regional defects in the expression of key rate-limiting enzymes tyrosine hydroxylase and tryptophan hydroxylase 2 in the brainstem, the substantia nigra, and the raphe nuclei [230,236,239]. Analysis of spontaneous miniature excitatory and inhibitory postsynaptic currents indicated a shift in the excitatory/inhibitory (E/I) balance, with increased excitatory and decreased inhibitory neurotransmission in the hippocampus and cortex[28,29,34,240,241]. This is supported by data showing pre- and post-synaptic defects of GABA-ergic, and therefore inhibitory, neurotransmission in the brainstem[242]. Consistent with the idea of disturbance of the E/I balance, long-term potentiation (LTP) is also altered in the hippocampus of symptomatic MeCP2-deficient mice[61,118,243]. These data, added to the morphological studies, imply that loss of MeCP2 causes malfunction of numerous synapses throughout the brain, which creates less efficient neuronal networks and gives rise to RTT-like phenotypes.

Unfortunately, the MeCP2 mutant mice behavioural phenotypes are far from Rett patients, for instance the typical human cognitive disability. In MeCP2 mice model, motor

impairments are described and in the Open field and elevated plus maze test revealed an anxiety behaviour in 4 week-old MeCP2-/y Bird mice[244].

In our study, performing Rotarod and Open field tests, we observed a strong reduction of locomotor performances in Mecp2 -/y compared to wt mice.

Taken together, latency time on rotarod, distance moved, velocity and immobility parameters, highlighted that motor impairment is severe and debilitating and get worst during time progression of the pathology. From these results, we showed that the major hallmark of this mouse model is locomotor impairment, but they showed also an anxiety behaviour, these results will probably become more consistent by increasing the number of mice analysed. In accordance with us, Bittolo et al. found that both in open field and elevated plus maze tests, MeCP2-/y mice had a reduced motility, a reduced rearing and grooming activity[245].

The brain areas most involved in locomotor activity are cortex and cerebellum. To detect a correlation between behavioural impairment and synaptic dysfunction, we investigate the JNK role in these regions.

We studied JNK activation at the spine level, by using the TIF fractionation, we detected a powerful JNK activation in the post-synaptic element. The JNK role at the spine level has been previously proved in AD synaptopathy[126,127,226]and we here confirmed the correlation between P-JNK increase and the biochemical alterations of the PSD.

To define JNK action at this level focusing on important post-synaptic receptors, AMPA and NMDA, and two important scaffold proteins PSD-95 and SHANK3 of the PSD region. While the nr2a and nr2b as well as glur1 and glur2 levels significate increased, the scaffold proteins decreased. Scaffold proteins link directly or indirectly the receptor and take them up at the membrane level of the PSD region, favouring plasticity. The NMDA and AMPA receptor level increment and the PSD95 and SHANK3 level

decrement can be related to the synaptic dysfunction phenomenon, in which receptors are in the right place without an efficacy link to the scaffold proteins that make them not normally functioning and JNK is strongly activated as well at the post-synaptic element. However, biochemical marker changes in the PSD region of Mecp2 -/y can reasonably be expected due to the impaired neuronal function of these mice. These data seem to be in agreement with a study that proved an altered dynamics of spine and dendritic filopodia during development, which hinders the correct formation and the plasticity of synapses in MeCP2 mice[113]. Moreover, the deficit in spine stabilization in MeCP2 mice was also confirmed by a reduction in levels of PSD95 expression compared to wild-type mice[113]. The short-time structural plasticity of dendritic spines is altered in a model of Rett syndrome. We confirmed with immunohistochemical analysis that c-Jun is strongly activated in MeCP2 -/y compared to wild type mice. The c-Jun staining is usually related to neuronal death pathway, we therefore checked using NeuN, a marker of neuronal vitality, to verify eventually differences in neuronal population between wt and ko. No signs of neuronal death have been detected in cerebellum. However, c-Jun is also implicated in the inflammatory pathway and we look for an inflammatory response in Rett brain analysing astroglial and microglial response/reaction. The astroglial activation was finally detected in Mecp2 -/y mice. Furthermore, individuals with RTT have increased expression of glial fibrillary acidic protein (GFAP)[246], an intermediate filament protein family that is predominantly expressed in astrocytes within the CNS[247,248] While it is well-defined that GFAP within astrocytes plays an important structural role, it is also becoming clear that GFAP is also important for synaptic plasticity, vesicular transport of neurochemicals and responses to injury[249]. More importantly, atypical expression of GFAP has been observed in numerous mental health diseases and increased expression of GFAP in mice causes a lethal astrocyte dysfunction[250]. Taken together, these data

suggest that tight control of GFAP expression may be necessary for normal brain development and function. In fact, the restoration of MeCP2 in glial cells can reverse some RTT symptoms in mice that have a mutation in MeCP2[35].

This strongly supports the idea that GLIA plays an important role in Rett Syndrome. Many evidences in literature had shown that astrogliosis is associated to microgliosis, thus we decided to investigate this correlation using the CD11β, a markers of activated microglia, and we found that Mecp2 -/y presented a strong activation compare to wt mice. Further investigations are needed to clarify this aspect. However, the role of microglia as sensors of pre- and post-natal environmental stimuli and its involvement in the regulation of synaptic connectivity, maturation of brain circuitry and neurogenesis has recently emerged[251,252]. The immune dysregulation has been found in children with Fragile X syndrome and an intrinsic microglia dysfunction has been recently reported in Rett syndrome[253].

At present, there is no cure for the Rett syndrome. Some approaches tried to reverse the symptoms of this disorder starting from the reactivation of MECP2 gene or through reactivation of the normal allele[58]. An alternative approach to rescue the Rett phenotype is to act on the factors that are downstream of MeCP2 function through a pharmacological treatment. These factors include neurotrophins (like BDNF or IGF-1) and neurotransmitters (like noradrenaline, serotonin and dopamine). A deficit in monoamine levels, including noradrenaline, serotonin and dopamine was reported in the brain and cerebrospinal fluid of both Rett patients and MeCP2-/y mice[235].

Previously studies of our laboratory widely showed that, D-JNKI1, by preventing JNK action, was able to inhibit neuronal degeneration in both acute and chronic brain damage. We here test the D-JNKI1 against Rett syndrome symptomatology. The treatment started at the 3rd week of life, in an asymptomatic state, in wild-type and Mecp2 -/y mice until

the 7rd week of life; then we evaluated the effect of the peptide on wellbeing conditions (body weight, food and water consumption, survival rate), motor and exploratory performance, synaptopathy and brain parenchyma inflammation.

The ability of D-JNKI1 to chronically inhibit c-Jun phosphorylation *in vivo* was assessed by Western Blotting and immunoreaction in Rett mouse model. As expected, D-JNKI1 strongly prevented c-Jun activation. Interestingly D-JNKI1 treatment reduces this c-Jun activation to a level comparable to the one observed in wt mice. These results underline that D-JNKI1 is able to prevents JNK's action on its elective target and the peptide is working as expected[133,159,219,226,216,254].

Our findings corroborate the concept that JNK plays a critical role in the Rett neurodegenerative process. The treatment with the peptide, by preventing JNK action, increase significantly the body weight, underling the protective effect on wellbeing of the severe phenotype of Mecp2 -/y. Importantly this is correlated to an improvement also in motor and cognitive performance of treated Mecp2 -/y.

Valuating the D-JNKI1 effect on behavioural performance of Mecp2 -/y mice, we observed the recovery of a locomotor performance in the rotarod test, and in the rescue of the exploratory behaviour in the open field test. The evident reduction of the time spent in immobile condition correlated to a rescue of locomotor and coordination abilities in the animals treated with D-JNKI1 could be due to a neuroprotective effect of the treatment.

The treatment underlines for the first time the therapeutic potential of JNK inhibitory treatment against Rett pathology. Indeed, we here show that D-JNKI specific JNK inhibition promotes functional recovery of Rett behavioural impairment, by inhibition of c-Jun and these changes are accompanied by an increase in motor and cognitive performances. Investigating more in detail the JNK pathway and the relationship among

MKK4 and MKK7, that play different functions in the JNK signal transduction pathway, we found a strong activation of P-MKK4/MKK4 ratio, while P-MKK7/MKK7 was unchanged this indicated that the upstream activator of JNK is just MKK4 and the treatment with the peptide prevented MKK4 activation as well as c-Jun phosphorylation. Consequently, D-JNKI1 acts downstream JNK by preventing its action on targets and in the same time, upstream inhibiting its upstream activator MKK4.

D-JNKI1 was administrated 3rd week after the first spine alteration and we used a "post-symptomatic" treatment since it is clinically more relevant. The fact that the treatment reverted the behavioural defects suggest, as previously demonstrated, that it acts at the spine level and rescue synapsis dysfunction. In AD synaptopathy the JNK inhibitor peptide prevented the biochemical alterations of the PSD[226,216]. Here the treatment increased the NMDA receptors as well as PSD95 levels while it is ineffective on AMPA receptor. D-JNKI1 counteracts partially the biochemical changes in the PSD regions of Mecp2 -/y. Since RTT is an autistic spectrum disorder (ASD), we decided to investigate also another SAP that would be implicated in synaptic function. SHANK3 (SH3 and multiple ankyrin repeat domain 3) is a member of the highly conserved Shank/ProSAP family of synaptic scaffolding proteins. In addition, SHANK3 is suggested as a strong candidate gene for the pathogenesis of Autism and its loss results in disruption of synaptic function[255]. In fact, shank is major components of the excitatory postsynaptic density[101,256]. It is probably implicated in synaptic abnormality during neuronal development. Dysregulation of Shank3 leads to alterations in spine morphogenesis, shape, and activity of the synapse via altering actin dynamics[257]. The Shank3 levels drastically drop in Mecp2 -/y mice, this collapse may be responsible for abnormal spine formation and plasticity. The rescue with D-JNKI1 treatment is important because it

determinate a restoration of Shank3 levels and its functionality at the PSD region, but further study in this direction will be necessary.

Different monogenic diseases included into ASD as Rett syndrome (RTT), Fragile X syndrome, and *SHANK3* gene deficiency (Phelan-Mc Dermic syndrome) are commonly related to synaptic and immune function[258]. These diseases although caused by different mechanisms share the same pathology at the cellular and molecular levels. Common pathological processes in central nervous system (CNS) disorders involve inflammation of the brain, abnormal microglial function and synaptic dysfunction,

Since we observed a c-Jun activation, astrogliosis and activated microglia in Mecp2 -/y mice, we analysed whether D-JNKI1 inhibition could have a protective effect on these two types of inflammatory responses.

The biochemical analysis had revealed a protective effect of D-JNKI1 on synaptic dysfunction, and the immunoistochemical analysis of cerebellum and brain parenchyma revealed that P-c-Jun staining link to astrogliosis and activated microglia both in cortex and cerebellum of Mecp2 -/y mice. In fact, the p-c-Jun, GFAP and CD11β staining was reduced in Mecp2 -/y treated compared to untreated mice, indicating a powerful effect of D-JNKI1 on in our experimental model. Many evidences in literature had reported altered microglial function in Rett syndrome [37,43,259,260]. In fact, neuron-only expression of normal MeCP2 was not sufficient to reverse the Rett phenotype in mice; instead brain-wide expression was needed suggesting the importance of glia cells, astrocytes or some other brain cell type[61]. According to our results, it was found also increased glia neurodensity in Rett syndrome suggesting inflammatory astrocytosis[234], underlying the importance of D-JNKI1 effect to counteract this important pathological aspect.

Biochemical data obtained with western blot analysis had confirmed D-JNKI1 protective effect both in cortex and cerebellum of Mecp2 -/y mice.

Since CD11β is a marker of whole microglia, it is not easily detectable with western blot, to investigate microglia, we checked its activation by study the IBA-1 protein level and relative RNA expression, and we found in both cases a reduction of levels in Mecp2 untreated mice. So microglia seem to be less reactivity in Mecp2 -/y compared to wild-type mice, assuming that it could be related to the microglial total cell number. Thus we decided to value the C1qa expression, a marker that detects all microglial population and we don't find any differences among experimental groups. Summarizing the data obtained from these analyses, we concluded that the number of microglial cells in the brain are similar in every case, so Mecp2 -/y cells are less reactive then the wild-type mice. Anyway, we observed a protective D-JNKI1 effect detected by a recovery of IBA-1levels in treated Mecp2 mice. However further experiment will be done to clarify this issue.

While concerning neuronal death, since valuating the neuronal population with NeuN, a marker of neuronal vitality, we didn't found differences between wt and Mecp2 -/y mice, consequently we decided to not investigate the D-JNKI1 effect against neuronal death.

CONCLUSIONS

Our work underlines the key role of JNK pathway never reported before in Rett syndrome, and the importance of D-JNKI1 treatment in MeCP2-/y mice to restore the main symptoms, in particular the general well-being, synaptic dysfunction and the correlated behavioural impairments as well as inflammation generated by astrogliosis and microgliosis. However, other studies are necessary to understand the role of JNK, firstly in heterozygous female MeCP2 mice that show a less severe symptomatology compared to male mice, but replicate exactly the genetic mutations as human female RTT patients. Subsequently, we will investigate the D-JNKI1 effect on female MeCP2 mice, performing also EM ultrastructural observations to better analyse the synaptic dysfunction and the recovery associated to the treatment. Moreover, our preliminary data on hIPS cells showed the same activated pathway detected in the used mice model and a rescue by D-JNKI1 treatment. Obviously, the unexpected enrolment of JNK pathway in RTT syndrome open a way for transnationality of this study, but we have to deepen the effective role of JNK's pathway in mutated human cells.

In conclusion, we believe that we provide the first proof of the key role of JNK in RTT and more importantly that the manipulation of JNK pathway may represent the development of an innovative strategy to tackle Rett Syndrome, providing a real chance of cure for patients being D-JNKI1 already in phase III clinical trials (see AM-111 (AurisMedical) and XG102 (Xigen) produced by two biopharmaceutical companies. Both AM-111 and XG102 are already in phase II & III clinical trials, http://www.xigenpharma.com/clinical-trials and http://www.aurismedical.com/product-candidates/pipeline).

BIBLIOGRAPHY

1. Rett, A. [On an until now unknown disease of a congenital metabolic disorder]. *Krankenschwester* **19,** 121–2 (1966).
2. Rett, A. [On a unusual brain atrophy syndrome in hyperammonemia in childhood]. *Wien. Med. Wochenschr.* **116,** 723–6 (1966).
3. Hagberg, B., Aicardi, J., Dias, K. & Ramos, O. A progressive syndrome of autism, dementia, ataxia, and loss of purposeful hand use in girls: Rett's syndrome: Report of 35 cases. *Ann. Neurol.* **14,** 471–479 (1983).
4. Zoghbi, H. Y. *et al.* Rett syndrome is caused by mutations in X-linked MECP2, encodingmethyl-CpG-binding protein 2. *Nat. Genet.* **23,** 185–188 (1999).
5. Archer, H. L. *et al.* CDKL5 mutations cause infantile spasms, early onset seizures, and severe mental retardation in female patients. *J. Med. Genet.* **43,** 729–34 (2006).
6. Ariani, F. *et al.* FOXG1 is responsible for the congenital variant of Rett syndrome. *Am. J. Hum. Genet.* **83,** 89–93 (2008).
7. Orrico, A. *et al.* MECP2 mutation in male patients with non-specific X-linked mental retardation. *FEBS Lett.* **481,** 285–288 (2000).
8. Masuyama, T. *et al. Classic Rett syndrome in a boy with R133C mutation of MECP2*. *Brain and Development* **27,** (2005).
9. Renieri, A. *et al.* Rett syndrome: the complex nature of a monogenic disease. *J. Mol. Med. (Berl).* **81,** 346–54 (2003).
10. Zahorakova, D. in *Chromatin Remodelling* (InTech, 2013). doi:10.5772/55020
11. Kerr, A. M. & Julu, P. O. O. Recent insights into hyperventilation from the study of Rett syndrome. *Arch. Dis. Child.* **80,** 384–387 (1999).
12. Kerr, A. Early Clinical Signs in the Rett Disorder. *Neuropediatrics* **26,** 67–71 (1995).
13. Khajuria, R. *et al.* Novel non-identical MECP2 mutations in Rett syndrome family: A rare presentation. *Brain Dev.* **34,** 28–31 (2012).
14. Neul, J. L. *et al.* Rett syndrome: revised diagnostic criteria and nomenclature. *Ann. Neurol.* **68,** 944–50 (2010).
15. Dragich, J., Houwink-Manville, I. & Schanen, C. Rett syndrome: a surprising result of mutation in MECP2. *Hum. Mol. Genet.* **9,** 2365–75 (2000).
16. Bühler, E. M., Malik, N. J. & Alkan, M. Rett syndrome and genetic drift. *Brain Dev.* **21,** 175–8 (1999).
17. Hagberg, B. Clinical manifestations and stages of Rett syndrome. *Ment. Retard. Dev. Disabil. Res. Rev.* **8,** 61–5 (2002).
18. Zappella, M. The Rett girls with preserved speech. *Brain Dev.* **14,** 98–101 (1992).
19. Ariani, F. *et al.* FOXG1 is responsible for the congenital variant of Rett syndrome. *Am. J. Hum. Genet.* **83,** 89–93 (2008).
20. Hanefeld, F. [Epileptic attacks in childhood--myopathies in childhood]. *Offentl. Gesundheitswes.* **47,** 357–60 (1985).

21. Tao, J. *et al. Mutations in the X-Linked Cyclin-Dependent Kinase–Like 5 (CDKL5/STK9) Gene Are Associated with Severe Neurodevelopmental Retardation*. *The American Journal of Human Genetics* **75,** (2004).
22. Hagberg, B. A. & Skjeldal, O. H. Rett variants: a suggested model for inclusion criteria. *Pediatr. Neurol.* **11,** 5–11 (1994).
23. Shahbazian, M. D. & Zoghbi, H. Y. Rett syndrome and MeCP2: linking epigenetics and neuronal function. *Am. J. Hum. Genet.* **71,** 1259–72 (2002).
24. Zhou, Z. *et al.* Brain-specific phosphorylation of MeCP2 regulates activity-dependent Bdnf transcription, dendritic growth, and spine maturation. *Neuron* **52,** 255–69 (2006).
25. Cohen, S. *et al.* Genome-wide activity-dependent MeCP2 phosphorylation regulates nervous system development and function. *Neuron* **72,** 72–85 (2011).
26. Na, E. S., Nelson, E. D., Kavalali, E. T. & Monteggia, L. M. The Impact of MeCP2 Loss- or Gain-of-Function on Synaptic Plasticity. *Neuropsychopharmacology* **38,** 212–219 (2013).
27. Chao, H.-T., Zoghbi, H. Y. & Rosenmund, C. MeCP2 controls excitatory synaptic strength by regulating glutamatergic synapse number. *Neuron* **56,** 58–65 (2007).
28. Dani, V. S. *et al.* Reduced cortical activity due to a shift in the balance between excitation and inhibition in a mouse model of Rett Syndrome. *Proc. Natl. Acad. Sci.* **102,** 12560–12565 (2005).
29. Nelson, E. D., Kavalali, E. T. & Monteggia, L. M. MeCP2-Dependent Transcriptional Repression Regulates Excitatory Neurotransmission. *Curr. Biol.* **16,** 710–716 (2006).
30. Tropea, D. *et al.* Partial reversal of Rett Syndrome-like symptoms in MeCP2 mutant mice. *Proc. Natl. Acad. Sci. U. S. A.* **106,** 2029–34 (2009).
31. Collins, A. L. *et al.* Mild overexpression of MeCP2 causes a progressive neurological disorder in mice. *Hum. Mol. Genet.* **13,** 2679–2689 (2004).
32. Nguyen, M. V. C. *et al.* MeCP2 is critical for maintaining mature neuronal networks and global brain anatomy during late stages of postnatal brain development and in the mature adult brain. *J. Neurosci.* **32,** 10021–34 (2012).
33. Gemelli, T. *et al.* Postnatal loss of methyl-CpG binding protein 2 in the forebrain is sufficient to mediate behavioral aspects of Rett syndrome in mice. *Biol. Psychiatry* **59,** 468–76 (2006).
34. Chao, H.-T. *et al.* Dysfunction in GABA signalling mediates autism-like stereotypies and Rett syndrome phenotypes. *Nature* **468,** 263–9 (2010).
35. Lioy, D. T. *et al.* A role for glia in the progression of Rett's syndrome. *Nature* **475,** 497–500 (2011).
36. Ballas, N., Lioy, D. T., Grunseich, C. & Mandel, G. Non-cell autonomous influence of MeCP2-deficient glia on neuronal dendritic morphology. *Nat. Neurosci.* **12,** 311–7 (2009).
37. Derecki, N. C. *et al.* Wild-type microglia arrest pathology in a mouse model of Rett syndrome. *Nature* **484,** 105–9 (2012).
38. Kriaucionis, S. & Bird, A. The major form of MeCP2 has a novel N-terminus generated by alternative splicing. *Nucleic Acids Res.* **32,** 1818–23 (2004).

39. Mnatzakanian, G. N. A previously unidentified *MECP2* open reading frame defines a new protein isoform relevant to Rett syndrome. *Nat. Genet.* **36,** (2004).
40. Dragich, J. M., Kim, Y.-H., Arnold, A. P. & Schanen, N. C. Differential distribution of the MeCP2 splice variants in the postnatal mouse brain. *J. Comp. Neurol.* **501,** 526–42 (2007).
41. Mnatzakanian, G. N. *et al.* A previously unidentified MECP2 open reading frame defines a new protein isoform relevant to Rett syndrome. *Nat. Genet.* **36,** 339–41 (2004).
42. Saxena, A. *et al.* Lost in translation: translational interference from a recurrent mutation in exon 1 of MECP2. *J. Med. Genet.* **43,** 470–7 (2006).
43. Zachariah, R. M. & Rastegar, M. Linking epigenetics to human disease and Rett syndrome: the emerging novel and challenging concepts in MeCP2 research. *Neural Plast.* **2012,** 415825 (2012).
44. Nan, X., Tate, P., Li, E. & Bird, A. DNA methylation specifies chromosomal localization of MeCP2. *Mol. Cell. Biol.* **16,** 414–21 (1996).
45. Galvão, T. C. & Thomas, J. O. Structure-specific binding of MeCP2 to four-way junction DNA through its methyl CpG-binding domain. *Nucleic Acids Res.* **33,** 6603–9 (2005).
46. Klose, R. J. *et al.* DNA binding selectivity of MeCP2 due to a requirement for A/T sequences adjacent to methyl-CpG. *Mol. Cell* **19,** 667–78 (2005).
47. Jones, P. L. *et al.* Methylated DNA and MeCP2 recruit histone deacetylase to repress transcription. *Nat. Genet.* **19,** 187–91 (1998).
48. Nan, X. *et al.* Transcriptional repression by the methyl-CpG-binding protein MeCP2 involves a histone deacetylase complex. *Nature* **393,** 386–9 (1998).
49. Kudo, S. Methyl-CpG-binding protein MeCP2 represses Sp1-activated transcription of the human leukosialin gene when the promoter is methylated. *Mol. Cell. Biol.* **18,** 5492–9 (1998).
50. Buschdorf, J. P. & Strätling, W. H. A WW domain binding region in methyl-CpG-binding protein MeCP2: impact on Rett syndrome. *J. Mol. Med. (Berl).* **82,** 135–43 (2004).
51. Chahrour, M. *et al.* MeCP2, a key contributor to neurological disease, activates and represses transcription. *Science* **320,** 1224–9 (2008).
52. Stancheva, I., Collins, A. L., Van den Veyver, I. B., Zoghbi, H. & Meehan, R. R. A mutant form of MeCP2 protein associated with human Rett syndrome cannot be displaced from methylated DNA by notch in Xenopus embryos. *Mol. Cell* **12,** 425–35 (2003).
53. Yusufzai, T. M. & Wolffe, A. P. Functional consequences of Rett syndrome mutations on human MeCP2. *Nucleic Acids Res.* **28,** 4172–9 (2000).
54. Chahrour, M. & Zoghbi, H. Y. The story of Rett syndrome: from clinic to neurobiology. *Neuron* **56,** 422–37 (2007).
55. Guy, J., Hendrich, B., Holmes, M., Martin, J. E. & Bird, A. A mouse Mecp2-null mutation causes neurological symptoms that mimic Rett syndrome. *Nat. Genet.* **27,** 322–326 (2001).
56. Braunschweig, D., Simcox, T., Samaco, R. C. & LaSalle, J. M. X-Chromosome

inactivation ratios affect wild-type MeCP2 expression within mosaic Rett syndrome and Mecp2-/+ mouse brain. *Hum. Mol. Genet.* **13,** 1275–86 (2004).
57. Chen, R. Z., Akbarian, S., Tudor, M. & Jaenisch, R. Deficiency of methyl-CpG binding protein-2 in CNS neurons results in a Rett-like phenotype in mice. *Nat. Genet.* **27,** 327–31 (2001).
58. Luikenhuis, S., Giacometti, E., Beard, C. F. & Jaenisch, R. Expression of MeCP2 in postmitotic neurons rescues Rett syndrome in mice. *Proc. Natl. Acad. Sci. U. S. A.* **101,** 6033–8 (2004).
59. Shahbazian, M. *et al.* Mice with truncated MeCP2 recapitulate many Rett syndrome features and display hyperacetylation of histone H3. *Neuron* **35,** 243–54 (2002).
60. Neul, J. L. *et al.* Specific mutations in methyl-CpG-binding protein 2 confer different severity in Rett syndrome. *Neurology* **70,** 1313–21 (2008).
61. Guy, J., Gan, J., Selfridge, J., Cobb, S. & Bird, A. Reversal of neurological defects in a mouse model of Rett syndrome. *Science* **315,** 1143–7 (2007).
62. Calfa, G., Percy, A. K. & Pozzo-Miller, L. Experimental models of Rett syndrome based on Mecp2 dysfunction. *Exp. Biol. Med. (Maywood).* **236,** 3–19 (2011).
63. Bernardinelli, Y., Nikonenko, I. & Muller, D. tructural plasticity: mechanisms and contribution to developmental psychiatric disorders. *Front. Neuroanat.* **8,** 123 (2014).
64. Volk, L., Chiu, S.-L., Sharma, K. & Huganir, R. L. Glutamate synapses in human cognitive disorders. *Annu. Rev. Neurosci.* **8,** (2015).
65. Tzschentke, T. M. Glutamatergic mechanisms in different disease states: overview and therapeutical implications - An introduction. *Amino Acids* **23,** 147–152 (2002).
66. Storey, E., Kowall, N. W., Finn, S. F., Mazurek, M. F. & Beal, M. F. The cortical lesion of Huntington's disease: Further neurochemical characterization, and reproduction of some of the histological and neurochemical features byN-methyl-D-aspartate lesions of rat cortex. *Ann. Neurol.* **32,** 526–534 (1992).
67. Daggett, A. & Yang, X. W. Huntington's disease: easing the NMDAR traffic jam. *Nat. Med.* **19,** 971–973 (2013).
68. Rattray, M. & Bendotti, C. Does excitotoxic cell death of motor neurons in ALS arise from glutamate transporter and glutamate receptor abnormalities? *Exp. Neurol.* **201,** 15–23 (2006).
69. Ferrarese, C. *et al.* Glutamate uptake is decreased in platelets from Alzheimer's disease patients. *Ann. Neurol.* **47,** 641–3 (2000).
70. Kline, D. D., Ogier, M., Kunze, D. L. & Katz, D. M. Exogenous brain-derived neurotrophic factor rescues synaptic dysfunction in Mecp2-null mice. *J. Neurosci.* **30,** 5303–10 (2010).
71. Gerrow, K. & Triller, A. Synaptic stability and plasticity in a floating world. *Curr. Opin. Neurobiol.* **20,** 631–9 (2010).
72. Luebke, J. I. *et al.* Dendritic vulnerability in neurodegenerative disease: insights from analyses of cortical pyramidal neurons in transgenic mouse models. *Brain Struct. Funct.* **214,** 181–99 (2010).
73. Trachtenberg, J. T. *et al.* Long-term in vivo imaging of experience-dependent

synaptic plasticity in adult cortex. *Nature* **420,** 788–94

74. Kasai, H., Matsuzaki, M., Noguchi, J., Yasumatsu, N. & Nakahara, H. Structure-stability-function relationships of dendritic spines. *Trends Neurosci.* **26,** 360–8 (2003).
75. Chapleau, C. A., Larimore, J. L., Theibert, A. & Pozzo-Miller, L. Modulation of dendritic spine development and plasticity by BDNF and vesicular trafficking: fundamental roles in neurodevelopmental disorders associated with mental retardation and autism. *J. Neurodev. Disord.* **1,** 185–96 (2009).
76. Rochefort, N. L. & Konnerth, A. Dendritic spines: from structure to in vivo function. *EMBO Rep.* **13,** 699–708 (2012).
77. Grutzendler, J., Kasthuri, N. & Gan, W.-B. Long-term dendritic spine stability in the adult cortex. *Nature* **420,** 812–6
78. Holtmaat, A. J. G. D. *et al.* Transient and persistent dendritic spines in the neocortex in vivo. *Neuron* **45,** 279–91 (2005).
79. Fiala, J. C., Feinberg, M., Popov, V. & Harris, K. M. Synaptogenesis via dendritic filopodia in developing hippocampal area CA1. *J. Neurosci.* **18,** 8900–11 (1998).
80. Blanpied, T. A. & Ehlers, M. D. Microanatomy of dendritic spines: emerging principles of synaptic pathology in psychiatric and neurological disease. *Biol. Psychiatry* **55,** 1121–1127 (2004).
81. Snyder, E. M. *et al.* Regulation of NMDA receptor trafficking by amyloid-β. *Nat. Neurosci.* **8,** 1051–1058 (2005).
82. Hsieh, H. *et al.* AMPAR removal underlies Abeta-induced synaptic depression and dendritic spine loss. *Neuron* **52,** 831–43 (2006).
83. Shankar, G. M. *et al.* Amyloid-beta protein dimers isolated directly from Alzheimer's brains impair synaptic plasticity and memory. *Nat. Med.* **14,** 837–42 (2008).
84. Sun, B. *et al.* Imbalance between GABAergic and Glutamatergic Transmission Impairs Adult Neurogenesis in an Animal Model of Alzheimer's Disease. *Cell Stem Cell* **5,** 624–33 (2009).
85. Horn, D., Levy, N. & Ruppin, E. Neuronal-based synaptic compensation: a computational study in Alzheimer's disease. *Neural Comput.* **8,** 1227–43 (1996).
86. Hasselmo, M. E. A computational model of the progression of Alzheimer's disease. *MD. Comput.* **14,** 181–91
87. Okabe, S. Molecular anatomy of the postsynaptic density. *Mol. Cell. Neurosci.* **34,** 503–518 (2007).
88. Sheng, M. & Hoogenraad, C. C. The postsynaptic architecture of excitatory synapses: a more quantitative view. *Annu. Rev. Biochem.* **76,** 823–47 (2007).
89. Oliva, C., Escobedo, P., Astorga, C., Molina, C. & Sierralta, J. Role of the MAGUK protein family in synapse formation and function. *Dev. Neurobiol.* **72,** 57–72 (2012).
90. Cheng, D. *et al.* Relative and absolute quantification of postsynaptic density proteome isolated from rat forebrain and cerebellum. *Mol. Cell. Proteomics* **5,** 1158–70 (2006).
91. Ehrlich, I. & Malinow, R. Postsynaptic density 95 controls AMPA receptor

incorporation during long-term potentiation and experience-driven synaptic plasticity. *J. Neurosci.* **24,** 916–27 (2004).
92. Zhang, P. & Lisman, J. E. Activity-dependent regulation of synaptic strength by PSD-95 in CA1 neurons. *J. Neurophysiol.* **107,** (2012).
93. Pawson, T. & Scott, J. D. Signaling through scaffold, anchoring, and adaptor proteins. *Science* **278,** 2075–80 (1997).
94. Ziff, E. B. Enlightening the postsynaptic density. *Neuron* **19,** 1163–74 (1997).
95. Cho, K.-O., Hunt, C. A. & Kennedy, M. B. The rat brain postsynaptic density fraction contains a homolog of the drosophila discs-large tumor suppressor protein. *Neuron* **9,** 929–942 (1992).
96. Kornau, H.-C., Schenker, L.T., Kennedy, M.B., Seeburg, P. . Domain interaction between NMDA receptor subunits and the postsynaptic density protein PSD-95. *Science (80-.).* **269,** 1737–1740 (1995).
97. Niethammer, M. *et al.* CRIPT, a Novel Postsynaptic Protein that Binds to the Third PDZ Domain of PSD-95/SAP90. *Neuron* **20,** 693–707 (1998).
98. Sheng, M. & Kim, E. The Shank family of scaffold proteins. *J. Cell Sci.* 1851–6 (2000).
99. Naisbitt, S. *et al.* Shank, a novel family of postsynaptic density proteins that binds to the NMDA receptor/PSD-95/GKAP complex and cortactin. *Neuron* **23,** 569–82 (1999).
100. Tu, J. C. *et al.* Coupling of mGluR/Homer and PSD-95 complexes by the Shank family of postsynaptic density proteins. *Neuron* **23,** 583–92 (1999).
101. Blanpied, T. A., Scott, D. B. & Ehlers, M. D. Dynamics and regulation of clathrin coats at specialized endocytic zones of dendrites and spines. *Neuron* **36,** 435–49 (2002).
102. Hara, M. *et al.* De novo *SHANK3* mutation causes Rett syndrome-like phenotype in a female patient. *Am. J. Med. Genet. Part A* **167,** 1593–1596 (2015).
103. Sala, C. *et al.* Regulation of dendritic spine morphology and synaptic function by Shank and Homer. *Neuron* **31,** 115–30 (2001).
104. Armstrong, D., Dunn, J. K., Antalffy, B. & Trivedi, R. Selective dendritic alterations in the cortex of Rett syndrome. *J. Neuropathol. Exp. Neurol.* **54,** 195–201 (1995).
105. Belichenko, P. V, Oldfors, A., Hagberg, B. & Dahlström, A. Rett syndrome: 3-D confocal microscopy of cortical pyramidal dendrites and afferents. *Neuroreport* **5,** 1509–13 (1994).
106. Chapleau, C. A. *et al.* Dendritic spine pathologies in hippocampal pyramidal neurons from Rett syndrome brain and after expression of Rett-associated MECP2 mutations. *Neurobiol. Dis.* **35,** 219–33 (2009).
107. Bauman, M. L., Kemper, T. L. & Arin, D. M. Pervasive neuroanatomic abnormalities of the brain in three cases of Rett's syndrome. *Neurology* **45,** 1581–6 (1995).
108. Bauman, M. L., Kemper, T. L. & Arin, D. M. Microscopic observations of the brain in Rett syndrome. *Neuropediatrics* **26,** 105–8 (1995).
109. Kaufmann, W. E. & Moser, H. W. Dendritic anomalies in disorders associated with

mental retardation. *Cereb. Cortex* **10,** 981–91 (2000).
110. Xu, X., Miller, E. C. & Pozzo-Miller, L. Dendritic spine dysgenesis in Rett syndrome. *Front. Neuroanat.* **8,** 97 (2014).
111. Li, W. & and Pozzo-Miller, L. Beyond Widespread Deletions to Model Rett Syndrome: Conditional Spatio-Temporal Knockout, Single-Point Mutations and Transgenic Rescue Mice. . *Autism Open Access* **5,** (2012).
112. Chapleau, C. A. *et al.* Hippocampal CA1 pyramidal neurons of Mecp2 mutant mice show a dendritic spine phenotype only in the presymptomatic stage. *Neural Plast.* **2012,** 976164 (2012).
113. Landi, S. *et al.* The short-time structural plasticity of dendritic spines is altered in a model of Rett syndrome. *Sci. Rep.* **1,** 45 (2011).
114. Castro, J. *et al.* Functional recovery with recombinant human IGF1 treatment in a mouse model of Rett Syndrome. *Proc. Natl. Acad. Sci. U. S. A.* **111,** 9941–6 (2014).
115. Kishi, N. & Macklis, J. D. MECP2 is progressively expressed in post-migratory neurons and is involved in neuronal maturation rather than cell fate decisions. *Mol. Cell. Neurosci.* **27,** 306–21 (2004).
116. Fukuda, T., Itoh, M., Ichikawa, T., Washiyama, K. & Goto, Y. Delayed maturation of neuronal architecture and synaptogenesis in cerebral cortex of Mecp2-deficient mice. *J. Neuropathol. Exp. Neurol.* **64,** 537–44 (2005).
117. Moretti, P. *et al.* Learning and memory and synaptic plasticity are impaired in a mouse model of Rett syndrome. *J. Neurosci.* **26,** 319–27 (2006).
118. Asaka, Y., Jugloff, D. G. M., Zhang, L., Eubanks, J. H. & Fitzsimonds, R. M. Hippocampal synaptic plasticity is impaired in the Mecp2-null mouse model of Rett syndrome. *Neurobiol. Dis.* **21,** 217–27 (2006).
119. Purpura, D. P. Dendritic spine "dysgenesis" and mental retardation. *Science* **186,** 1126–8 (1974).
120. Belichenko, N. P., Belichenko, P. V & Mobley, W. C. Evidence for both neuronal cell autonomous and nonautonomous effects of methyl-CpG-binding protein 2 in the cerebral cortex of female mice with Mecp2 mutation. *Neurobiol. Dis.* **34,** 71–7 (2009).
121. Saywell, V. *et al.* Brain magnetic resonance study of Mecp2 deletion effects on anatomy and metabolism. *Biochem. Biophys. Res. Commun.* **340,** 776–83 (2006).
122. Metcalf, B. M., Mullaney, B. C., Johnston, M. V & Blue, M. E. Temporal shift in methyl-CpG binding protein 2 expression in a mouse model of Rett syndrome. *Neuroscience* **139,** 1449–60 (2006).
123. Murakami, J. W., Courchesne, E., Haas, R. H., Press, G. A. & Yeung-Courchesne, R. Cerebellar and cerebral abnormalities in Rett syndrome: a quantitative MR analysis. *Am. J. Roentgenol.* **159,** 177–183 (1992).
124. Oldfors, A., Hagberg, B., Nordgren, H., Sourander, P. & Witt-Engerström, I. Rett syndrome: spinal cord neuropathology. *Pediatr. Neurol.* **4,** 172–4
125. Schaeffer, H. J. & Weber, M. J. Mitogen-activated protein kinases: specific messages from ubiquitous messengers. *Mol. Cell. Biol.* **19,** 2435–44 (1999).
126. Sclip, A. *et al.* c-Jun N-terminal kinase has a key role in Alzheimer disease synaptic

dysfunction in vivo. *Cell Death Dis.* **5,** e1019 (2014).
127. Sclip, A. *et al.* JNK mediates synaptic dysfunction caused by Aß oligomers in Alzheimer disease.
128. Hibi, M., Lin, A., Smeal, T., Minden, A. & Karin, M. Identification of an oncoprotein- and UV-responsive protein kinase that binds and potentiates the c-Jun activation domain. *Genes Dev.* **7,** 2135–48 (1993).
129. Adler, V., Polotskaya, A., Wagner, F. & Kraft, A. S. Affinity-purified c-Jun amino-terminal protein kinase requires serine/threonine phosphorylation for activity. *J. Biol. Chem.* **267,** 17001–5 (1992).
130. Pulverer, B. J., Kyriakis, J. M., Avruch, J., Nikolakaki, E. & Woodgett, J. R. Phosphorylation of c-jun mediated by MAP kinases. *Nature* **353,** 670–4 (1991).
131. Davis, R. J. Signal transduction by the JNK group of MAP kinases. *Cell* **103,** 239–52 (2000).
132. Gupta, S. *et al.* Selective interaction of JNK protein kinase isoforms with transcription factors. *EMBO J.* **15,** 2760–70 (1996).
133. Borsello, T. *et al.* A peptide inhibitor of c-Jun N-terminal kinase protects against excitotoxicity and cerebral ischemia. *Nat. Med.* **9,** 1180–6 (2003).
134. Coffey, E. T. *et al.* c-Jun N-terminal protein kinase (JNK) 2/3 is specifically activated by stress, mediating c-Jun activation, in the presence of constitutive JNK1 activity in cerebellar neurons. *J. Neurosci.* **22,** 4335–45 (2002).
135. Kuan, C.-Y. & Burke, R. E. Targeting the JNK signaling pathway for stroke and Parkinson's diseases therapy. *Curr. Drug Targets. CNS Neurol. Disord.* **4,** 63–7 (2005).
136. Morishima, Y. *et al.* Beta-amyloid induces neuronal apoptosis via a mechanism that involves the c-Jun N-terminal kinase pathway and the induction of Fas ligand. *J. Neurosci.* **21,** 7551–60 (2001).
137. Schmit, T. L., Dowell, J. A., Maes, M. E. & Wilhelm, M. c-Jun N-terminal kinase regulates mGluR-dependent expression of post-synaptic FMRP target proteins. *J. Neurochem.* **127,** 772–81 (2013).
138. Kuan, C. Y. *et al.* The Jnk1 and Jnk2 protein kinases are required for regional specific apoptosis during early brain development. *Neuron* **22,** 667–76 (1999).
139. Gdalyahu, A. *et al.* DCX, a new mediator of the JNK pathway. *EMBO J.* **23,** 823–32 (2004).
140. Antoniou, X. & Borsello, T. The JNK signalling transduction pathway in the brain. *Front. Biosci. (Elite Ed).* **4,** 2110–20 (2012).
141. Dajas-Bailador, F., Jones, E. V & Whitmarsh, A. J. The JIP1 scaffold protein regulates axonal development in cortical neurons. *Curr. Biol.* **18,** 221–6 (2008).
142. Sato, S., Ito, M., Ito, T. & Yoshioka, K. Scaffold protein JSAP1 is transported to growth cones of neurites independent of JNK signaling pathways in PC12h cells. *Gene* **329,** 51–60 (2004).
143. Bjorkblom, B. Constitutively Active Cytoplasmic c-Jun N-Terminal Kinase 1 Is a Dominant Regulator of Dendritic Architecture: Role of Microtubule-Associated Protein 2 as an Effector. *J. Neurosci.* **25,** 6350–6361 (2005).
144. Chang, L., Jones, Y., Ellisman, M. H., Goldstein, L. S. B. & Karin, M. JNK1 is

required for maintenance of neuronal microtubules and controls phosphorylation of microtubule-associated proteins. *Dev. Cell* **4,** 521–33 (2003).
145. Thomas, G. M., Lin, D.-T., Nuriya, M. & Huganir, R. L. Rapid and bi-directional regulation of AMPA receptor phosphorylation and trafficking by JNK. *EMBO J.* **27,** 361–72 (2008).
146. Zhu, Y. *et al.* Rap2-JNK Removes Synaptic AMPA Receptors during Depotentiation. *Neuron* **46,** 905–916 (2005).
147. Mori, Y., Higuchi, M., Hirabayashi, Y., Fukuda, M. & Gotoh, Y. JNK phosphorylates synaptotagmin-4 and enhances Ca2+-evoked release. *EMBO J.* **27,** 76–87 (2008).
148. Bogoyevitch, M. A. & Kobe, B. Uses for JNK: the Many and Varied Substrates of the c-Jun N-Terminal Kinases. *Microbiol. Mol. Biol. Rev.* **70,** 1061–1095 (2006).
149. Whitmarsh, A. J., Cavanagh, J., Tournier, C., Yasuda, J. & Davis, R. J. A mammalian scaffold complex that selectively mediates MAP kinase activation. *Science* **281,** 1671–4 (1998).
150. Li, L., Feng, Z. & Porter, A. G. JNK-dependent Phosphorylation of c-Jun on Serine 63 Mediates Nitric Oxide-induced Apoptosis of Neuroblastoma Cells. *J. Biol. Chem.* **279,** 4058–4065 (2003).
151. Choi, W. S., Chun, S. Y., Markelonis, G. J., Oh, T. H. & Oh, Y. J. Overexpression of calbindin-D28K induces neurite outgrowth in dopaminergic neuronal cells via activation of p38 MAPK. *Biochem. Biophys. Res. Commun.* **287,** 656–61 (2001).
152. Centeno, C. *et al.* Role of the JNK pathway in NMDA-mediated excitotoxicity of cortical neurons. *Cell Death Differ.* **14,** 240–53 (2007).
153. Antoniou, X. & Borsello, T. Cell Permeable Peptides: A Promising Tool to Deliver Neuroprotective Agents in the Brain. *Pharmaceuticals (Basel).* **3,** 379–392 (2010).
154. Song, J. J. & Lee, Y. J. Dissociation of Akt1 from its negative regulator JIP1 is mediated through the ASK1–MEK–JNK signal transduction pathway during metabolic oxidative stress. *J. Cell Biol.* **170,** 61–72 (2005).
155. Repici, M., Wehrlé, R., Antoniou, X., Borsello, T. & Dusart, I. c-Jun N-terminal kinase (JNK) and p38 play different roles in age-related Purkinje cell death in murine organotypic culture. *Cerebellum* **10,** 281–90 (2011).
156. Hong, M.-Y. *et al.* Effect of c-Jun NH_2-terminal kinase-mediated p53 expression on neuron autophagy following traumatic brain injury in rats. *Chin. Med. J. (Engl).* **125,** 2019–24 (2012).
157. Byun, J.-Y. *et al.* Reactive Oxygen Species-Dependent Activation of Bax and Poly(ADP-ribose) Polymerase-1 Is Required for Mitochondrial Cell Death Induced by Triterpenoid Pristimerin in Human Cervical Cancer Cells. *Mol. Pharmacol.* **76,** 734–744 (2009).
158. Weston, C. R. & Davis, R. J. The JNK signal transduction pathway. *Curr. Opin. Cell Biol.* **19,** 142–9 (2007).
159. Sclip, A. *et al.* c-Jun N-terminal kinase has a key role in Alzheimer disease synaptic dysfunction in vivo. *Cell Death Dis.* **5,** e1019 (2014).
160. Widmann, C., Gibson, S., Jarpe, M. B. & Johnson, G. L. Mitogen-activated protein kinase: conservation of a three-kinase module from yeast to human. *Physiol. Rev.*

79, 143–80 (1999).
161. Kishimoto, H. *et al.* Different properties of SEK1 and MKK7 in dual phosphorylation of stress-induced activated protein kinase SAPK/JNK in embryonic stem cells. *J. Biol. Chem.* **278,** 16595–601 (2003).
162. Tournier, C. *et al.* MKK7 is an essential component of the JNK signal transduction pathway activated by proinflammatory cytokines. *Genes Dev.* **15,** 1419–26 (2001).
163. Zhang, Q., Tian, H., Fu, X. & Zhang, G. Delayed activation and regulation of MKK7 in hippocampal CA1 region following global cerebral ischemia in rats. *Life Sci.* **74,** 37–45 (2003).
164. Tu, Z., Mooney, S. M. & Lee, F. S. A subdomain of MEKK1 that is critical for binding to MKK4. *Cell. Signal.* **15,** 65–77 (2003).
165. Hammaker, D. R., Boyle, D. L., Inoue, T. & Firestein, G. S. Regulation of the JNK pathway by TGF-beta activated kinase 1 in rheumatoid arthritis synoviocytes. *Arthritis Res. Ther.* **9,** R57 (2007).
166. Takekawa, M., Tatebayashi, K. & Saito, H. Conserved Docking Site Is Essential for Activation of Mammalian MAP Kinase Kinases by Specific MAP Kinase Kinase Kinases. *Mol. Cell* **18,** 295–306 (2005).
167. Mooney, L. M. & Whitmarsh, A. J. Docking interactions in the c-Jun N-terminal kinase pathway. *J. Biol. Chem.* **279,** 11843–52 (2004).
168. Tanoue, T. & Nishida, E. Molecular recognitions in the MAP kinase cascades. *Cell. Signal.* **15,** 455–62 (2003).
169. Haeusgen, W., Herdegen, T. & Waetzig, V. The bottleneck of JNK signaling: Molecular and functional characteristics of MKK4 and MKK7. *Eur. J. Cell Biol.* **90,** 536–544 (2011).
170. Borsello, T. The cell permeable peptide strategy is a promising new tool for the prevention of neurodegeneration. *Discov. Med.* **4,** 319–24 (2004).
171. Morrison, D. K. & Davis, R. J. Regulation of MAP Kinase Signaling Modules by Scaffold Proteins in Mammals*. *Annu. Rev. Cell Dev. Biol.* **19,** 91–118 (2003).
172. Raivich, G. *et al.* The AP-1 Transcription Factor c-Jun Is Required for Efficient Axonal Regeneration. *Neuron* **43,** 57–67 (2004).
173. Ameyar, M., Wisniewska, M. & Weitzman, J. B. A role for AP-1 in apoptosis: the case for and against. *Biochimie* **85,** 747–52 (2003).
174. Shaulian, E. & Karin, M. AP-1 as a regulator of cell life and death. *Nat. Cell Biol.* **4,** E131-6 (2002).
175. Han, T. H. & Prywes, R. Regulatory role of MEF2D in serum induction of the c-jun promoter. *Mol. Cell. Biol.* **15,** 2907–15 (1995).
176. Han, T. H., Lamph, W. W. & Prywes, R. Mapping of epidermal growth factor-, serum-, and phorbol ester-responsive sequence elements in the c-jun promoter. *Mol. Cell. Biol.* **12,** 4472–7 (1992).
177. Kato, Y. *et al.* BMK1/ERK5 regulates serum-induced early gene expression through transcription factor MEF2C. *EMBO J.* **16,** 7054–66 (1997).
178. Marinissen, M. J., Chiariello, M., Pallante, M. & Gutkind, J. S. A network of mitogen-activated protein kinases links G protein-coupled receptors to the c-jun promoter: a role for c-Jun NH2-terminal kinase, p38s, and extracellular signal-

regulated kinase 5. *Mol. Cell. Biol.* **19,** 4289–301 (1999).
179. Nateri, A. S., Spencer-Dene, B. & Behrens, A. Interaction of phosphorylated c-Jun with TCF4 regulates intestinal cancer development. *Nature* **437,** 281–285 (2005).
180. Behrens, A., Sibilia, M. & Wagner, E. F. Amino-terminal phosphorylation of c-Jun regulates stress-induced apoptosis and cellular proliferation. *Nat. Genet.* **21,** 326–9 (1999).
181. Kallunki, T., Deng, T., Hibi, M. & Karin, M. c-Jun can recruit JNK to phosphorylate dimerization partners via specific docking interactions. *Cell* **87,** 929–39 (1996).
182. Herdegen, T. & Leah, J. D. Inducible and constitutive transcription factors in the mammalian nervous system: control of gene expression by Jun, Fos and Krox, and CREB/ATF proteins. *Brain Res. Brain Res. Rev.* **28,** 370–490 (1998).
183. Kolbus, A. *et al.* c-Jun-dependent CD95-L expression is a rate-limiting step in the induction of apoptosis by alkylating agents. *Mol. Cell. Biol.* **20,** 575–82 (2000).
184. Falvo, J. V *et al.* Stimulus-specific assembly of enhancer complexes on the tumor necrosis factor alpha gene promoter. *Mol. Cell. Biol.* **20,** 2239–47 (2000).
185. Bakiri, L., Lallemand, D., Bossy-Wetzel, E. & Yaniv, M. Cell cycle-dependent variations in c-Jun and JunB phosphorylation: a role in the control of cyclin D1 expression. *EMBO J.* **19,** 2056–68 (2000).
186. Timsit, S. *et al.* Increased cyclin D1 in vulnerable neurons in the hippocampus after ischaemia and epilepsy: a modulator of in vivo programmed cell death? *Eur. J. Neurosci.* **11,** 263–78 (1999).
187. Kirch, H. C., Flaswinkel, S., Rumpf, H., Brockmann, D. & Esche, H. Expression of human p53 requires synergistic activation of transcription from the p53 promoter by AP-1, NF-kappaB and Myc/Max. *Oncogene* **18,** 2728–38 (1999).
188. Low, W., Smith, A., Ashworth, A. & Collins, M. JNK activation is not required for Fas-mediated apoptosis. *Oncogene* **18,** 3737–41 (1999).
189. Napieralski, J. A., Raghupathi, R. & McIntosh, T. K. The tumor-suppressor gene, p53, is induced in injured brain regions following experimental traumatic brain injury. *Brain Res. Mol. Brain Res.* **71,** 78–86 (1999).
190. Yang, H., Courtney, M. J., Martinsson, P. & Manahan-Vaughan, D. Hippocampal long-term depression is enhanced, depotentiation is inhibited and long-term potentiation is unaffected by the application of a selective c-Jun N-terminal kinase inhibitor to freely behaving rats. *Eur. J. Neurosci.* **33,** 1647–55 (2011).
191. Bonny, C., Oberson, A., Negri, S., Sauser, C. & Schorderet, D. F. Cell-permeable peptide inhibitors of JNK: novel blockers of beta-cell death. *Diabetes* **50,** 77–82 (2001).
192. Borsello, T. & Bonny, C. Use of cell-permeable peptides to prevent neuronal degeneration. *Trends Mol. Med.* **10,** 239–44 (2004).
193. Borsello, T. *et al.* A peptide inhibitor of c-Jun N-terminal kinase protects against excitotoxicity and cerebral ischemia. **9,** (2003).
194. Repici M1, Mare L, Colombo A, Ploia C, Sclip A, Bonny C, Nicod P, Salmona M, B. T. c-Jun N-terminal kinase binding domain-dependent phosphorylation of mitogen-activated protein kinase kinase 4 and mitogen-activated protein kinase

kinase 7 and balancing cross-talk between c-Jun N-terminal kinase and extracellular signal-regulated kinase . *Neuroscience.* (2009). doi:10.1016/j.neuroscience.2008.11.049

195. Repici, M., Mariani, J. & Borsello, T. Neuronal death and neuroprotection: a review. *Methods Mol. Biol.* **399,** 1–14 (2007).
196. Wang, W. *et al.* SP600125, a new JNK inhibitor, protects dopaminergic neurons in the MPTP model of Parkinson's disease. *Neurosci. Res.* **48,** 195–202 (2004).
197. Tezel, G., Chauhan, B. C., LeBlanc, R. P. & Wax, M. B. Immunohistochemical assessment of the glial mitogen-activated protein kinase activation in glaucoma. *Invest. Ophthalmol. Vis. Sci.* **44,** 3025–33 (2003).
198. Repici, M. *et al.* Specific inhibition of the JNK pathway promotes locomotor recovery and neuroprotection after mouse spinal cord injury. *Neurobiol. Dis.* **46,** 710–721 (2012).
199. Fischer, R., Fotin-Mleczek, M., Hufnagel, H. & Brock, R. Break on through to the other side-biophysics and cell biology shed light on cell-penetrating peptides. *Chembiochem* **6,** 2126–42 (2005).
200. Maroney, A. C. *et al.* Cep-1347 (KT7515), a semisynthetic inhibitor of the mixed lineage kinase family. *J. Biol. Chem.* **276,** 25302–8 (2001).
201. Borasio, G. D., Horstmann, S., Anneser, J. M., Neff, N. T. & Glicksman, M. A. CEP-1347/KT7515, a JNK pathway inhibitor, supports the in vitro survival of chick embryonic neurons. *Neuroreport* **9,** 1435–9 (1998).
202. Bennett, B. L. *et al.* SP600125, an anthrapyrazolone inhibitor of Jun N-terminal kinase. *Proc. Natl. Acad. Sci. U. S. A.* **98,** 13681–6 (2001).
203. Marques, C. A. *et al.* Neurotoxic mechanisms caused by the Alzheimer's disease-linked Swedish amyloid precursor protein mutation: oxidative stress, caspases, and the JNK pathway. *J. Biol. Chem.* **278,** 28294–302 (2003).
204. WATZMAN, N., BARRY, H., BUCKLEY, J. P. & KINNARD, W. J. SEMIAUTOMATIC SYSTEM FOR TIMING ROTAROD PERFORMANCE. *J. Pharm. Sci.* **53,** 1429–30 (1964).
205. Jones, B. J. & Roberts, D. J. A rotarod suitable for quantitative measurements of motor incoordination in naive mice. *Naunyn. Schmiedebergs. Arch. Exp. Pathol. Pharmakol.* **259,** 211 (1968).
206. Buitrago, M. M., Schulz, J. B., Dichgans, J. & Luft, A. R. Short and long-term motor skill learning in an accelerated rotarod training paradigm. *Neurobiol. Learn. Mem.* **81,** 211–6 (2004).
207. Seibenhener, M. L. & Wooten, M. C. Use of the Open Field Maze to measure locomotor and anxiety-like behavior in mice. *J. Vis. Exp.* e52434 (2015). doi:10.3791/52434
208. Crawley, J. N. Mouse behavioral assays relevant to the symptoms of autism. *Brain Pathol.* **17,** 448–59 (2007).
209. Kalueff, A. V. *et al.* Neurobiology of rodent self-grooming and its value for translational neuroscience. *Nat. Rev. Neurosci.* **17,** 45–59 (2015).
210. Gardoni, F. *et al.* Hippocampal synaptic plasticity involves competition between Ca2+/calmodulin-dependent protein kinase II and postsynaptic density 95 for

binding to the NR2A subunit of the NMDA receptor. *J. Neurosci.* **21,** 1501–9 (2001).
211. Gardoni, F. *et al.* The NMDA receptor complex is altered in an animal model of human cerebral heterotopia. *J. Neuropathol. Exp. Neurol.* **62,** 662–75 (2003).
212. Kaminska, B. in *Methods in molecular biology (Clifton, N.J.)* **512,** 249–264 (2009).
213. Leoncini, S. *et al.* Cytokine Dysregulation in *MECP2* - and *CDKL5* -Related Rett Syndrome: Relationships with Aberrant Redox Homeostasis, Inflammation, and ω -3 PUFAs. *Oxid. Med. Cell. Longev.* **2015,** 1–18 (2015).
214. Cortelazzo, A. *et al.* Subclinical Inflammatory Status in Rett Syndrome. *Mediators Inflamm.* **2014,** 1–13 (2014).
215. Davoli, E. *et al.* Determination of tissue levels of a neuroprotectant drug: the cell permeable JNK inhibitor peptide. *J. Pharmacol. Toxicol. Methods* **70,** 55–61 (2014).
216. Sclip, A. *et al.* Soluble A oligomer-induced synaptopathy: c-Jun N-terminal kinase's role. *J. Mol. Cell Biol.* **5,** 277–279 (2013).
217. Lin, W., Ding, M., Xue, J. & Leng, W. The role of TLR2/JNK/NF-κB pathway in amyloid β peptide-induced inflammatory response in mouse NG108-15 neural cells. *Int. Immunopharmacol.* **17,** 880–4 (2013).
218. Vukic, V. *et al.* Expression of inflammatory genes induced by beta-amyloid peptides in human brain endothelial cells and in Alzheimer's brain is mediated by the JNK-AP1 signaling pathway. *Neurobiol. Dis.* **34,** 95–106 (2009).
219. Borsello, T. & Bonny, C. Use of cell-permeable peptides to prevent neuronal degeneration. *Trends Mol. Med.* **10,** 239–244 (2004).
220. Belichenko, N. P., Belichenko, P. V, Li, H. H., Mobley, W. C. & Francke, U. Comparative study of brain morphology in Mecp2 mutant mouse models of Rett syndrome. *J. Comp. Neurol.* **508,** 184–95 (2008).
221. Katz, D. M. *et al.* Preclinical research in Rett syndrome: setting the foundation for translational success. *Dis. Model. Mech.* **5,** 733–45 (2012).
222. Skene, P. J. *et al.* Neuronal MeCP2 is expressed at near histone-octamer levels and globally alters the chromatin state. *Mol. Cell* **37,** 457–68 (2010).
223. Monteggia, L. M. & Kavalali, E. T. Rett syndrome and the impact of MeCP2 associated transcriptional mechanisms on neurotransmission. *Biol. Psychiatry* **65,** 204–10 (2009).
224. Hite, K. C., Adams, V. H. & Hansen, J. C. Recent advances in MeCP2 structure and function. *Biochem. Cell Biol.* **87,** 219–27 (2009).
225. Gonzales, M. L. & LaSalle, J. M. The Role of MeCP2 in Brain Development and Neurodevelopmental Disorders. *Curr. Psychiatry Rep.* **12,** 127–134 (2010).
226. Sclip, A. *et al.* c-Jun N-terminal Kinase Regulates Soluble A Oligomers and Cognitive Impairment in AD Mouse Model. *J. Biol. Chem.* **286,** 43871–43880 (2011).
227. Subramaniam, B., Naidu, S. & Reiss, A. L. Neuroanatomy in Rett syndrome: cerebral cortex and posterior fossa. *Neurology* **48,** 399–407 (1997).
228. Reiss, A. L. *et al.* Neuroanatomy of Rett syndrome: a volumetric imaging study.

Ann. Neurol. **34,** 227–34 (1993).
229. Armstrong, D. D. Rett syndrome neuropathology review 2000. *Brain Dev.* **23 Suppl 1,** S72-6 (2001).
230. Taneja, P. *et al.* Pathophysiology of locus ceruleus neurons in a mouse model of Rett syndrome. *J. Neurosci.* **29,** 12187–95 (2009).
231. Smrt, R. D. *et al.* Mecp2 deficiency leads to delayed maturation and altered gene expression in hippocampal neurons. *Neurobiol. Dis.* **27,** 77–89 (2007).
232. Matarazzo, V. *et al.* The transcriptional repressor Mecp2 regulates terminal neuronal differentiation. *Mol. Cell. Neurosci.* **27,** 44–58 (2004).
233. Palmer, A., Qayumi, J. & Ronnett, G. MeCP2 mutation causes distinguishable phases of acute and chronic defects in synaptogenesis and maintenance, respectively. *Mol. Cell. Neurosci.* **37,** 794–807 (2008).
234. Armstrong, D. D. Can we relate MeCP2 deficiency to the structural and chemical abnormalities in the Rett brain? *Brain Dev.* **27,** S72–S76 (2005).
235. Santos, M. *et al.* Monoamine deficits in the brain of methyl-CpG binding protein 2 null mice suggest the involvement of the cerebral cortex in early stages of Rett syndrome. *Neuroscience* **170,** 453–67 (2010).
236. Samaco, R. C. *et al.* Loss of MeCP2 in aminergic neurons causes cell-autonomous defects in neurotransmitter synthesis and specific behavioral abnormalities. *Proc. Natl. Acad. Sci. U. S. A.* **106,** 21966–71 (2009).
237. Isoda, K. *et al.* Postnatal changes in serotonergic innervation to the hippocampus of methyl-CpG-binding protein 2-null mice. *Neuroscience* **165,** 1254–60 (2010).
238. Ide, S., Itoh, M. & Goto, Y. Defect in normal developmental increase of the brain biogenic amine concentrations in the mecp2-null mouse. *Neurosci. Lett.* **386,** 14–7 (2005).
239. Viemari, J.-C. *et al.* Mecp2 Deficiency Disrupts Norepinephrine and Respiratory Systems in Mice. *J. Neurosci.* **25,** 11521–11530 (2005).
240. Wood, L. & Shepherd, G. M. G. Synaptic circuit abnormalities of motor-frontal layer 2/3 pyramidal neurons in a mutant mouse model of Rett syndrome. *Neurobiol. Dis.* **38,** 281–287 (2010).
241. Zhang, L., He, J., Jugloff, D. G. M. & Eubanks, J. H. The MeCP2-null mouse hippocampus displays altered basal inhibitory rhythms and is prone to hyperexcitability. *Hippocampus* **18,** 294–309 (2008).
242. Medrihan, L. *et al.* Early defects of GABAergic synapses in the brain stem of a MeCP2 mouse model of Rett syndrome. *J. Neurophysiol.* **99,** 112–21 (2008).
243. Weng, S.-M., McLeod, F., Bailey, M. E. S. & Cobb, S. R. Synaptic plasticity deficits in an experimental model of rett syndrome: long-term potentiation saturation and its pharmacological reversal. *Neuroscience* **180,** 314–321 (2011).
244. Santos, M., Silva-Fernandes, A., Oliveira, P., Sousa, N. & Maciel, P. Evidence for abnormal early development in a mouse model of Rett syndrome. *Genes. Brain. Behav.* **6,** 277–86 (2007).
245. Bittolo, T. *et al.* Pharmacological treatment with mirtazapine rescues cortical atrophy and respiratory deficits in MeCP2 null mice. *Sci. Rep.* **6,** 19796 (2016).
246. Colantuoni, C. *et al.* Gene expression profiling in postmortem Rett Syndrome

brain: differential gene expression and patient classification. *Neurobiol. Dis.* **8,** 847–65 (2001).
247. Eng, L. F. Glial fibrillary acidic protein (GFAP): the major protein of glial intermediate filaments in differentiated astrocytes. *J. Neuroimmunol.* **8,** 203–14 (1985).
248. Eng, L. F., Vanderhaeghen, J. J., Bignami, A. & Gerstl, B. An acidic protein isolated from fibrous astrocytes. *Brain Res.* **28,** 351–4 (1971).
249. Middeldorp, J. & Hol, E. M. GFAP in health and disease. *Prog. Neurobiol.* **93,** 421–43 (2011).
250. Messing, A. *et al.* Fatal encephalopathy with astrocyte inclusions in GFAP transgenic mice. *Am. J. Pathol.* **152,** 391–8 (1998).
251. Kuijlaars, J. *et al.* Sustained synchronized neuronal network activity in a human astrocyte co-culture system. *Sci. Rep.* **6,** 36529 (2016).
252. Macht, V. A. Neuro-immune interactions across development: A look at glutamate in the prefrontal cortex. *Neurosci. Biobehav. Rev.* **71,** 267–280 (2016).
253. Di Marco, B., Bonaccorso, C. M., Aloisi, E., D'Antoni, S. & Catania, M. V. Neuro-Inflammatory Mechanisms in Developmental Disorders Associated with Intellectual Disability and Autism Spectrum Disorder: A Neuro- Immune Perspective. *CNS Neurol. Disord. Drug Targets* **15,** 448–63 (2016).
254. Zhuang, Z.-Y. *et al.* A Peptide c-Jun N-Terminal Kinase (JNK) Inhibitor Blocks Mechanical Allodynia after Spinal Nerve Ligation: Respective Roles of JNK Activation in Primary Sensory Neurons and Spinal Astrocytes for Neuropathic Pain Development and Maintenance. *J. Neurosci.* **26,** 3551–3560 (2006).
255. Mashayekhi, F., Mizban, N., Bidabadi, E. & Salehi, Z. The association of SHANK3 gene polymorphism and autism. *Minerva Pediatr.* (2016).
256. Sheng, M. & Kim, E. The postsynaptic organization of synapses. *Cold Spring Harb. Perspect. Biol.* **3,** (2011).
257. Sarowar, T. & Grabrucker, A. M. Actin-Dependent Alterations of Dendritic Spine Morphology in Shankopathies. *Neural Plast.* **2016,** 8051861 (2016).
258. Voineagu, I. *et al.* Transcriptomic analysis of autistic brain reveals convergent molecular pathology. *Nature* **474,** 380–4 (2011).
259. Derecki, N. C., Cronk, J. C. & Kipnis, J. The role of microglia in brain maintenance: implications for Rett syndrome. *Trends Immunol.* **34,** 144–150 (2013).
260. Maezawa, I., Calafiore, M., Wulff, H. & Jin, L.-W. Does microglial dysfunction play a role in autism and Rett syndrome? *Neuron Glia Biol.* **7,** 85–97 (2011).